MISCELLANEOUS PAPER GL-81-2

SITE EFFECTS ON POWER SPECTRAL DENSITIES AND SCALING FACTORS

by

Frank K. Chang

Geotechnical Laboratory
U. S. Army Engineer Waterways Experiment Station
P. O. Box 631, Vicksburg, Miss. 39180

July 1981
Final Report

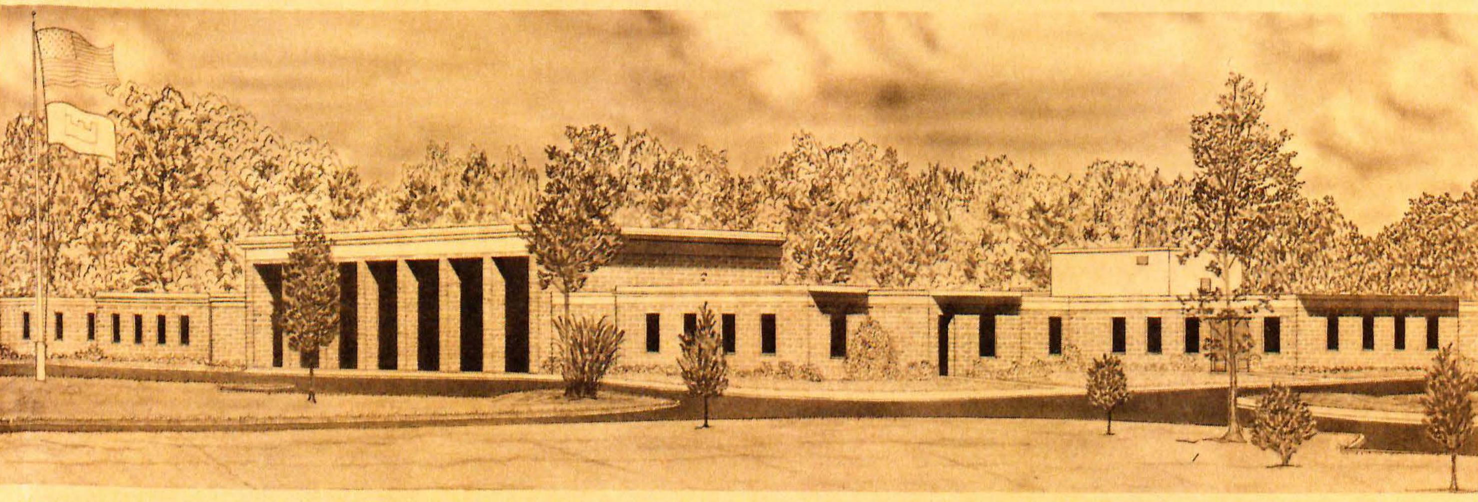

Prepared for Office, Chief of Engineers, U. S. Army
Washington, D. C. 20314

Under Project 4A161102AT22, Work Unit 00296

DEPARTMENT OF THE ARMY
WATERWAYS EXPERIMENT STATION, CORPS OF ENGINEERS
P. O. BOX 631
VICKSBURG, MISSISSIPPI 39180

IN REPLY REFER TO: WESGH

30 November 1981

Errata Sheet

No. 1

SITE EFFECTS ON POWER SPECTRAL DENSITIES

AND

SCALING FACTORS

Miscellaneous Paper GL-81-2

July 1981

1. Page 29, Figure 9: Change the horizontal scale of 0.1, 1, and 10 to 1, 10, and 100.

2. Page 31, Figure 11: Change the horizontal scale of 1, 10, and 100 to 0.1, 1, and 10.

3. Page 55, References: Line 16, change Keon County to Kern County.

Unclassified

SECURITY CLASSIFICATION OF THIS PAGE (When Data Entered)

REPORT DOCUMENTATION PAGE		READ INSTRUCTIONS BEFORE COMPLETING FORM
1. REPORT NUMBER Miscellaneous Paper GL-81-2	2. GOVT ACCESSION NO.	3. RECIPIENT'S CATALOG NUMBER
4. TITLE (and Subtitle) SITE EFFECTS ON POWER SPECTRAL DENSITIES AND SCALING FACTORS		5. TYPE OF REPORT & PERIOD COVERED Final report 6. PERFORMING ORG. REPORT NUMBER
7. AUTHOR(s) Frank K. Chang		8. CONTRACT OR GRANT NUMBER(s)
9. PERFORMING ORGANIZATION NAME AND ADDRESS U. S. Army Engineer Waterways Experiment Station Geotechnical Laboratory P. O. Box 631, Vicksburg, Miss. 39180		10. PROGRAM ELEMENT, PROJECT, TASK AREA & WORK UNIT NUMBERS Project 4A161102AT22, Work Unit 00296
11. CONTROLLING OFFICE NAME AND ADDRESS Office, Chief of Engineers, U. S. Army Washington, D. C. 20314		12. REPORT DATE July 1981 13. NUMBER OF PAGES 72
14. MONITORING AGENCY NAME & ADDRESS(if different from Controlling Office)		15. SECURITY CLASS. (of this report) Unclassified 15a. DECLASSIFICATION/DOWNGRADING SCHEDULE

16. DISTRIBUTION STATEMENT (of this Report)

Approved for public release; distribution unlimited.

17. DISTRIBUTION STATEMENT (of the abstract entered in Block 20, if different from Report)

18. SUPPLEMENTARY NOTES

Available from National Technical Information Service, 5285 Port Royal Road, Springfield, Va. 22151.

19. KEY WORDS (Continue on reverse side if necessary and identify by block number)

Accelerograms
Earthquake engineering
Power spectra
Spectrum analysis
Statistical analysis

20. ABSTRACT (Continue on reverse side if necessary and identify by block number)

This study presents the results of a statistical analysis of the spectral shapes of power spectral density (PSD) functions, $G(\omega)$, in the 0.006- to 10-Hz range for 421 horizontal ground accelerograms (all records processed to the same duration of 163.83 sec, i.e., 1/163.82 = 0.006 Hz) from 89 earthquakes, mostly in the western United States and Japan. The analysis shows clear differences in spectral shapes for different soil and geological conditions. Within the high-frequency range of 2.5 to 10 Hz, the spectrum for the rock sites contains the
(Continued)

DD FORM 1 JAN 73 1473 EDITION OF 1 NOV 65 IS OBSOLETE

Unclassified

SECURITY CLASSIFICATION OF THIS PAGE (When Data Entered)

20. ABSTRACT (Continued).

highest energy or intensity; the spectrum of the stiff soil sites is slightly less than for the rock sites; and the spectra of the soft clay and sand sites and the deep cohesionless soil sites are almost the same and are lower than those for stiff soils. However, in the low-frequency range of 0.006 to 2.5 Hz, the reverse exists: the soft sites indicate the highest energy, the deep cohesionless soil sites are next, the stiff soil sites are third, and finally, the rock sites.

A qualitative comparison was made of the spectral shapes of the PSD calculated in this study with the acceleration response spectra (ARS) of Kiremidjian and Shah (1978), Seed and Idriss (1971), and Seed, Ugas, and Lysmer (1976). There is general agreement in the shapes of both types of spectra, except the relative amplitudes for the rock sites for the ARS were less than those of the PSD in the high-frequency range. The difference in relative amplitudes for the rock PSD and ARS is due principally to the lesser number of records used in the data analysis for the latter. The number of records for the rock sites was 28 for the ARS and 56 for the PSD. Another difference is that the spectral shapes of PSD functions show more peaks than do the ARS, i.e., ARS are smoother. Above all, both differences could be affected by the frequency increment and the smoothing technique.

The average and average plus one standard deviation power density spectra functions for different site conditions have been normalized to a unit area. Based on these normalized PSD standard spectra and amplification scaling curves, which are derived from the average power λ^2, the area under $G(\omega)$, or its square root, the rms (root-mean-square) value (λ) developed in this study, a design earthquake PSD spectrum for any earthquake magnitude and distance can be generated. These scaling curves, i.e., the correlation curves of peak ground acceleration or peak velocity versus rms value, and rms value versus Modified Mercalli Intensity, can also serve as earthquake engineering intensity scales in a quantitative manner.

PREFACE

This study was conducted as a part of the work at the U. S. Army Engineer Waterways Experiment Station (WES) in the Military Works Program, Project 4A161102AT22, Work Unit 00296, which was monitored for the Office, Chief of Engineers, U. S. Army, by Mr. A. F. Muller.

This report was prepared by Mr. Frank K. Chang of the Earthquake Engineering and Geophysics Division (EE&GD), Geotechnical Laboratory (GL), under the general direction of Dr. A. G. Franklin, Principal Investigator; Dr. P. F. Hadala, Assistant Chief, GL; and Mr. C. L. McAnear, Acting Chief, GL.

The author would like to make special acknowledgements to Mr. Mike Landau, Assistant Analyst, Potomac Research, Consultants to the WES ADP Center, for his help in the data processing; Mr. Tatsuo Uwabe, visiting Research Engineer from the Port and Harbour Research Institute (PHRI), Japan, who provided the digitized Japanese strong-motion accelerograms of 1963 to 1975 recorded by the PHRI and the geological site conditions associated with each record; Professor M. Shinozuka, Columbia University, who provided the computer program used to calculate the one-sided PSD functions; Professor O. W. Nuttli, Saint Louis University, who made some comments for the first draft of this report; Professor E. H. Vanmarcke and Dr. Shih-Sheng (Paul) Lai, Massachusetts Institute of Technology; Professor H. C. Shah, Stanford University; Dr. S. C. Liu, National Science Foundation; and Drs. P. F. Hadala, W. F. Marcuson, and A. G. Franklin, WES, who made the critical reviews for this final report.

Commanders and Directors of WES during the period of this study were COL John L. Cannon, CE, and COL Nelson P. Conover, CE. Technical Director was Mr. F. R. Brown.

CONTENTS

Page

PREFACE 1

PART I: INTRODUCTION 3

Background 3
Purpose and Scope 5

PART II: POWER SPECTRAL DENSITY 6

Fourier Transform 6
Total Intensity, Average Power, and PSD 7
Strong-Motion Duration and Normalized PSD 8
Summary of Mathematical Relations 10

PART III: DATA SELECTION AND DATA PROCESSING 12

Data Selection 12
Definition of Average Power and Average Acceleration 12
Spectral Smoothing 12
Statistical Errors 13
Record Length, Increment Frequency, and NPSD Function 14
Spectral Frequency Range 18
Computer Procedures for Generating PSD 18

PART IV: DATA PRESENTATION 20

PART V: DATA ANALYSES 23

Analysis of Site-Dependent PSD Spectral Shape 23
Statistical Characteristics of the Earthquake Ground Motions 27
Maximum Ground Acceleration and Average Acceleration 28
Peak Factor 28
Comparison of Average Acceleration and Peak Ground Acceleration Versus Distance 37
Potential Uses of Site-Dependent Standard NPSD Spectral Curves 40
Peak Velocity Versus Average Acceleration 43
Correlation of Average Acceleration and Modified Mercalli Intensity 45
Correlation of I_o and MMI 45

PART VI: SUMMARY, CONCLUSIONS, AND RECOMMENDATIONS 51

Summary 51
Conclusions 53
Recommendations 54

REFERENCES 55

TABLES 1-8

SITE EFFECTS ON POWER SPECTRAL DENSITIES AND SCALING FACTORS

PART I: INTRODUCTION

Background

1. Three ways of expressing the characteristics of earthquake ground motion in the frequency domain are to compute the peak response spectrum, Fourier spectra, and power spectral density (PSD). The response spectrum represents the peak response of a linear 1-degree-of-freedom system to the ground motion and provides a convenient method of obtaining a preliminary analysis of certain structural dynamics problems. The PSD is related to the Fourier amplitude spectrum of the ground motion. In fact, the three are closely related.

2. Both response spectrum and PSD functions have been widely used to describe earthquake ground motions in the frequency domain. Pereira, Oliveira, and Duarte (1977), Vanmarcke and Cornell (1972), and Vanmarcke and Gasparini (1977) have shown that the PSD function, the acceleration-time plots, and the response spectra are all interrelated. Thus, if a design level response spectrum is specified, then an equivalent PSD function and a set of corresponding acceleration-time curves that are consistent with the response spectrum can be generated. However, neither the PSD nor the response spectrum can uniquely determine the acceleration-time curve, because both are incomplete representations of the ground motion, lacking phase information.

3. Seed and Idriss (1971), Tezcan (1971), and many others have confirmed that damage to buildings during past earthquakes has been closely associated with the vibrational characteristics of the underlying soils. Duke and Hradilek (1977) and Berrill (1977) utilized Fourier spectra to study the effects of local site conditions on ground motions recorded in the 9 February 1971 San Fernando earthquake and its aftershocks. However, no positive correlations were found. Hudson (1972)

and Hudson and Udwadia (1974) made a comparison of measured strong ground motions in the form of plots of Fourier spectra at selected sites and found that various governing factors could be individually studied; and in this way, it was shown that local variations are largely governed by (a) source mechanisms, (b) propagation path, and (c) local geology.

4. Seed, Ugas, and Lysmer (1976) presented the results of a statistical analysis of the response spectral shapes of 104 ground-motion accelerograms obtained from 23 earthquakes, mostly in the western United States. The analysis shows clear differences in spectral shapes for different soil and geological conditions. Chang and Krinitzsky (1977) studied the duration and spectral content of strong-motion records from the western United States according to site conditions and found that the predominant frequencies are in the range of 0.1 to 6.67 Hz and the spectral shape depends on the source spectrum function (magnitude), distance, and geological conditions.

5. An extensive study was made at the strong-motion station sites in Ferndale and El Centro, California, by Shannon and Wilson, Inc./ Agbabian Associates (1976). Both sites are located in a highly seismic region and have many ground-motion records. The subsurface conditions at these sites were defined by geotechnical investigations that included boring and sampling of the subsurface soil materials followed by field and laboratory tests to define the index properties and the dynamic properties of the soil needed for one-dimensional wave propagation analyses by numerical methods. The site-response analysis (SHAKE code), site-matched records, Seed-Ugas-Lysmer site dependent spectrum, Nuclear Commission Regulatory Guide 1.60 spectrum, and spectra from the measured records that correspond to the "design" earthquake event for the site were studied. No single method yielded the best vibratory motion criteria for both sites. The methods described above have limitations that either are related to the simplified models used for site-response wave propagation analyses or are a direct result of the limitations in the current library of strong-motion records.

6. Considering the earthquake ground motion to be random in

nature, Arnold (1975) and Arnold and Vanmarcke (1977) studied the influence of site azimuth relative to source fault orientation and local soil conditions on earthquake ground-motion spectra for the San Fernando, California, earthquake of 9 February 1971 using PSD functions. The result showed that local soil conditions and site azimuth, as well as epicentral distance, can have a significant effect on both the intensity and the frequency content of ground motions. This study demonstrated the potential value of PSD functions as a tool for comparing and studying variations in ground-motion characteristics and also showed the great utility of PSD functions as input to random vibration analyses of structural response.

Purpose and Scope

7. The main purpose of this study is to analyze the site dependence of PSD shapes in the frequency range of 0 to 10 Hz and to consider the application of PSD shapes in seismic design. Knowledge of the influence of site conditions on the characteristics of earthquake ground motions and their spectral shapes is necessary for earthquake-resistant design and analysis of structures such as earth, rockfill, or concrete dams, large buildings, nuclear power plants, and other military or civil facilities.

8. Factors affecting the ground motion at a particular site include the source mechanism (nature of fault movement and magnitude of energy release), propagation path characteristics, the direction of the site relative to the fault rupture, and local geological and soil conditions. This study, however, deals only with the influence of local geological and soil conditions on ground motion.

PART II: POWER SPECTRAL DENSITY

9. In the application of the random vibration theory of linear systems for evaluation of the effects of variations in ground-motion characteristics on structural response to earthquake excitation, the ground motion may be described in the form of a PSD function. The PSD function $G(\omega)$ is defined as a measure of the ground-motion power or energy per unit time as a function of frequency ω (Figure 1). Usually, estimates of the PSD are obtained from the squared amplitudes of the Fourier transform, or the squared Fourier amplitude spectrum. In Figure 1, A_i is the amplitude of sinusoidal waves.

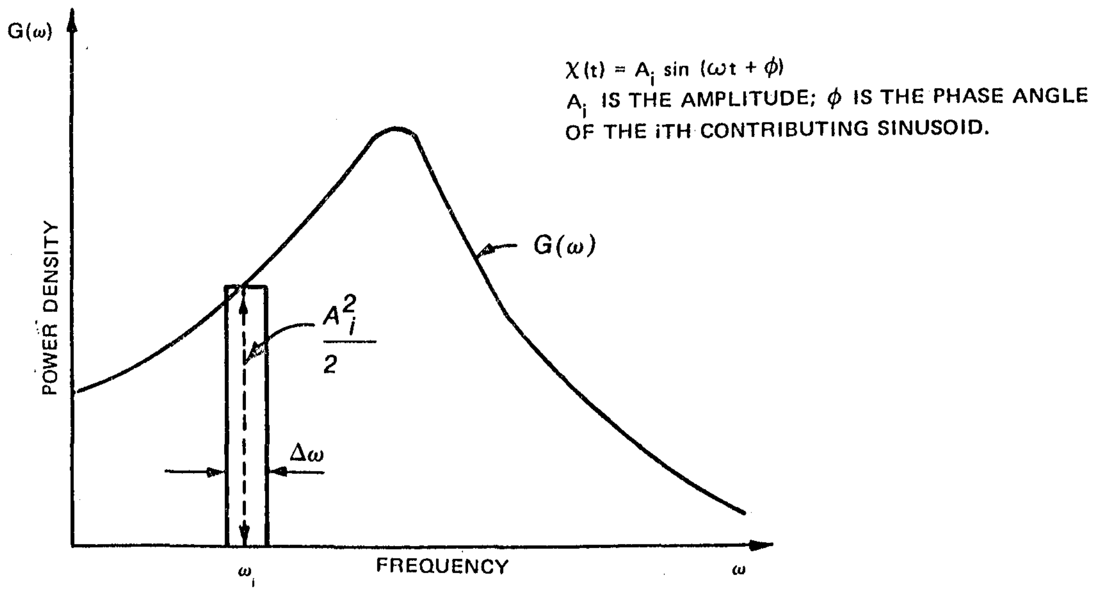

Figure 1. The PSD function $G(\omega)$

Fourier Transform

10. Generally, the given earthquake ground-motion function, such as an acceleration versus time plot, can be represented in the time domain as $a(t)$ and in the frequency domain as $F(\omega)$:

$$F(\omega) = \int_0^{t_o} a(t) e^{-i\omega t} \, dt \ , \quad i = \sqrt{-1} \tag{1}$$

and

$$a(t) = \frac{1}{\pi} \int_{\omega_1}^{\omega_o} F(\omega) e^{i\omega t} \, d\omega \ , \quad i = \sqrt{-1} \tag{2}$$

Equations 1 and 2 are called the Fourier transform pair; i.e., $F(\omega)$ is the Fourier integral or Fourier transform of $a(t)$, and $a(t)$ is the inverse Fourier transform of $F(\omega)$. The symbols t and t_o denote the instant in time and total duration, and ω, ω_1, and ω_o represent the frequency, lower frequency bound $\omega_1 = 2\pi/t_o$, and maximum frequency (in radians per second), respectively. For practical purposes, ω_1 can usually be taken as zero.

Total Intensity, Average Power, and PSD

11. By Parseval's theorem, the relation between the energy of the motion as expressed in the time domain and in the frequency domain can be represented in the following equations. For a nonperiodic function, the total energy or intensity I_o delivered by the source is given by

$$I_o = \int_0^{t_o} |a(t)|^2 \, dt = \frac{1}{\pi} \int_0^{\omega_o} |F(\omega)|^2 \, d\omega \tag{3}$$

The mean-square average value is expressed

$$\frac{1}{t_o} \int_0^{t_o} |a(t)|^2 \, dt = \frac{1}{\pi} \frac{1}{t_o} \int_0^{\omega_o} |F(\omega)|^2 \, d\omega = \int_0^{\omega_o} G(\omega) \, d\omega \tag{4}$$

in which $G(\omega)$ is the energy per unit time (power), or the power spectral density of the function $a(t)$. The integrand on the right side of Equation 4 can be written as

$$G(\omega) = \frac{1}{\pi}\frac{1}{S_o} |F(\omega)|^2 \tag{5}$$

if S_o (duration of strong motion) is substituted for t_o , and

$$\frac{1}{\pi}\int_o^{\omega_o} |F(\omega)|^2 \, d\omega = S_o \int_o^{\omega_o} G(\omega) \, d\omega$$

The quantity $|F(\omega)|^2$ is called the energy spectrum or energy spectral density function of $a(t)$ (Hsu 1967). The left side of Equation 4 gives the statistical average power λ_o^2 of the function $a(t)$ over the total duration of the motion t_o . From Equation 4, also note that λ_o^2 is equal to the area under the curve of $G(\omega)$ in Figure 1. Therefore, the average power can be written as

$$\lambda_o^2 = \int_o^{\omega_o} G(\omega) \, d\omega \tag{6}$$

Strong-Motion Duration and Normalized PSD

12. From the relation of Equations 3, 4, 5, and 6, the total intensity I_o can be expressed as

$$I_o = S_o \lambda_o^2 \tag{7a}$$

or

$$S_o = \frac{I_o}{\lambda_o^2} \tag{7b}$$

A peak factor r may be defined as

$$r = \frac{a_{max}}{\lambda_o} \tag{8a}$$

or

$$\lambda_o = \frac{a_{max}}{r} \tag{8b}$$

Therefore, by substitution

$$S_o = r^2 \frac{I_o}{a_{max}^2} \tag{9}$$

where r, which is a dimensionless parameter, can be determined empirically. This equation gives the strong-motion duration S_o, defined by Vanmarcke and Lai (1977), which is necessarily smaller than the total duration t_o. The PSD values in this report are computed in terms of t_o, which yields smaller PSD values.

13. A more effective way for dealing with the frequency content of ground motion is through the normalized spectral density function $G^*(\omega)$:

$$G^*(\omega) = \frac{1}{\lambda_o^2} G(\omega) \tag{10}$$

If $G_i^*(\omega)$ is an individual normalized PSD function, the statistical mean PSD curve will be

$$\overline{G}^*(\omega) = \frac{1}{n} \sum_{i=1}^{n} G_i^*(\omega) \quad , \quad i = 1,2,\ldots n \tag{11}$$

In practice, curves of $\overline{G}^*(\omega)$ computed from suites of actual earthquake records show large and irregular fluctuations. To isolate the systematic component from the random variations, frequency smoothing with a "Hanning" window (Blackman and Tukey 1958) should be used. A detailed procedure for the frequency smoothing will be presented in Part III.

Summary of Mathematical Relations

14. The above mathematical and logical presentations can be outlined as follows:

Time domain	Frequency domain	

Fourier transform pair:

$$a(t) = \frac{1}{\pi}\int_0^{\omega_o} F(\omega)e^{i\omega t}\, d\omega \; ; \qquad F(\omega) = \int_0^{t_o} a(t)e^{-i\omega t}\, dt \qquad (12a, b)$$

ω_o = maximum frequency $\qquad$ t_o = total duration

Total intensity:

$$I_o = \int_0^{t_o} |a(t)|^2\, dt \; ; \qquad I_o = \frac{1}{\pi}\int_0^{\omega_o} |F(\omega)|^2\, d\omega \qquad (13a, b)$$

Average power:

$$\lambda_o^2 = \frac{1}{t_o}\int_0^{t_o} |a(t)|^2\, dt \; ; \qquad \lambda_o^2 = \int_0^{\omega_o} G(\omega)\, d\omega \qquad (14a, b)$$

Power spectral density:

$$G(\omega) = \frac{1}{\pi}\frac{1}{S_o}|F(\omega)|^2 , \quad S_o \rightarrow t_o{}^*$$

---

* Either total duration t_o or strong-motion duration S_o (Vanmarcke and Lai 1977) may be used. In this study, t_o is generally used.

Average acceleration:

$$\lambda_o = \left[\frac{1}{t_o} \int_o^{t_o} |a(t)|^2 \, dt \right]^{1/2} \qquad \lambda_o = \left[\int_o^{\omega_o} G(\omega) \, d\omega \right]^{1/2} \qquad (15a, b)$$

Strong-motion duration:

$$S_o = \frac{I_o}{\lambda_o^2} \qquad S_o = \frac{I_o}{\lambda_o^2} \qquad (16)$$

15. This study includes investigation of (a) the site dependence of the PSD's or the power spectral shapes in the frequency range of 0 to 10 Hz for four general types of site conditions, which are classified as rock, stiff soil, deep cohesionless soil, and soft soil; (b) the statistical characteristics of the ground motions; (c) the relations between the power spectrum, average acceleration, average power (scaling factor), duration, and total intensity (Arias); and (d) the development of average acceleration as an alternative earthquake engineering intensity scale. The average acceleration not only describes the intensity of ground motion for input to structural design but also serves as the scaling factor (λ_o^2) of the normalized standard PSD spectra. In this report, duration will be considered in a general sense; the strong-motion duration will not be defined.

PART III: DATA SELECTION AND DATA PROCESSING

Data Selection

16. A total of 421 horizontal ground accelerograms from 89 earthquakes, mostly in the western United States and Japan (with a few records from Russia, Rumania, and India), were selected for this analysis. Based on the site classifications of Seed and Idriss (1971) and Seed, Ugas, and Lysmer (1976), these records have been divided into four groups: (a) 56 records for rock sites, (b) 131 records for stiff soil sites (depth <150 ft), (c) 120 records for deep cohesionless soil sites (depth >250 ft), and (d) 114 records for soft to medium clays with associated strata of sands or gravels. One hundred seventy-three of the 421 records were obtained from California Institute of Technology (CIT) Volume II-Corrected Accelerograms (1971-75), and 220 uncorrected records were provided by the Port and Harbour Research Institute (PHRI), Japan. The digitized Gazli (USSR) and Bucharest (Rumania) records were provided by Dr. A. G. Brady, U. S. Geological Survey. All 421 corrected and uncorrected records were adjusted to zero mean before processing the PSD.

Definition of Average Power and Average Acceleration

17. The main approach used in this study was to determine the normalized mean and the mean plus one standard deviation PSD shape (NPSD) for each group, and the average acceleration λ_o using Equation 15b, for each raw record. Figure 1 shows $G(\omega)$, whose value at ω_i is equal to $A_i^2/2\Delta\omega$, so that λ_o^2 is actually the power or energy density in an accelerogram for a finite frequency band ($0 \leq f \leq 10$ Hz in this study), and A_i is the amplitude of the ith wave component in centimetres per second squared. The total or average power will become equal to the area under the continuous curve $G(\omega)$.

Spectral Smoothing

18. The statistical (mean and mean plus one standard deviation)

NPSD function shapes for each group appear very irregular. Therefore, a spectral or frequency smoothing technique has to be employed to eliminate random, or nonsystematic, fluctuations of the NPSD curve. A final smooth estimate of the NPSD may now be formed by further frequency smoothing with a procedure called the "Hanning window" by Blackman and Tukey (1958) and Bendat and Piersol (1971). Let $\tilde{G}_K$ and $\hat{G}_K$ denote a raw and smooth estimate at harmonic K, where $K = 0,1,2,\ldots m$; then

$$\begin{aligned}
\hat{G}_o &= 0.5\tilde{G}_o + 0.5\tilde{G}_1 \\
\hat{G}_K &= 0.25\tilde{G}_{K-1} + 0.5\tilde{G}_K + 0.25\tilde{G}_{K+1} \qquad K = 1,2,\ldots m + 1 \\
\hat{G}_m &= 0.5\tilde{G}_{m-1} + 0.5\tilde{G}_m
\end{aligned} \tag{17}$$

Statistical Errors

19. The descriptive properties of a random variable cannot be precisely determined from sample data. Only estimates of the parameters of interest can be obtained from a finite sample of observations. The accuracy of parameter estimates based upon sample values can be described by a mean square error defined as

$$E\left[(\hat{\Phi} - \Phi)^2\right] = E\left\{\left[\hat{\Phi} - E(\hat{\Phi})\right]^2\right\} + E\left\{\left[E(\hat{\Phi}) - \Phi\right]^2\right\} \tag{18}$$

where $\hat{\Phi}$ is an estimator for Φ. The first term on the right side of Equation 18 is the variance $\mathrm{Var}\,(\hat{\Phi})$, which describes the random portion of the error; the second term is the square of a bias $b^2(\hat{\Phi})$, which describes the systematic portion of error. Therefore, the mean square error is the sum of two terms:

$$E\left[(\hat{\Phi} - \Phi)^2\right] = \mathrm{Var}\,(\hat{\Phi}) + b^2(\hat{\Phi}) \tag{19}$$

and the rms error is

$$\sqrt{E\left[(\hat{\Phi} - \Phi)^2\right]} = \sqrt{\sigma^2(\hat{\Phi}) + b^2(\hat{\Phi})} \tag{20}$$

where Var $(\hat{\Phi}) = \sigma^2(\hat{\Phi})$ and $\sigma(\hat{\Phi})$ equals the standard error or random error. Bendat and Piersol (1971) give the simple relationship between the random error E_r and the smoothing times N_d as $E_r = 1/\sqrt{N_d}$. Thus, for increasing numbers of smoothing times, the corresponding values of E_r are as follows:

N_d	E_r
25	0.20
100	0.10
500	0.045
10,000	0.01

The four normalized mean and mean plus one standard deviation PSD curves in this study have been smoothed 500 times, so the random error E_r should be less than 5 percent. Figure 2 shows the effect of the smoothing process on a typical PSD.

Record Length, Increment Frequency, and NPSD Function

20. The record length and spectral content (spectral amplitude and frequency range) are two basic elements for controlling the spectral intensity. The incremental frequency Δf, used in the PSD computer program, depends on the total record length. Since it is necessary to use the same value for Δf throughout, all accelerograms have been processed to give them a duration of 163.82 sec or 8192 (2^{13}) digital points with an equal time interval Δt of 0.02 sec, which gives $\Delta f = 0.006104$ Hz. Outside the time of the actual record, the amplitudes at extended times were set to zero. In this study, the PSD function $G(f)$ has been defined to include only the frequency range of 0 to 10 Hz so that

$$\lambda^2 = \int_0^{10\text{ Hz}} G(f)\,df \qquad (21)$$

Since Δf is 0.006104 Hz, there are 1640 points in the raw PSD function for each accelerogram. The NPSD function is defined as the PSD amplitude

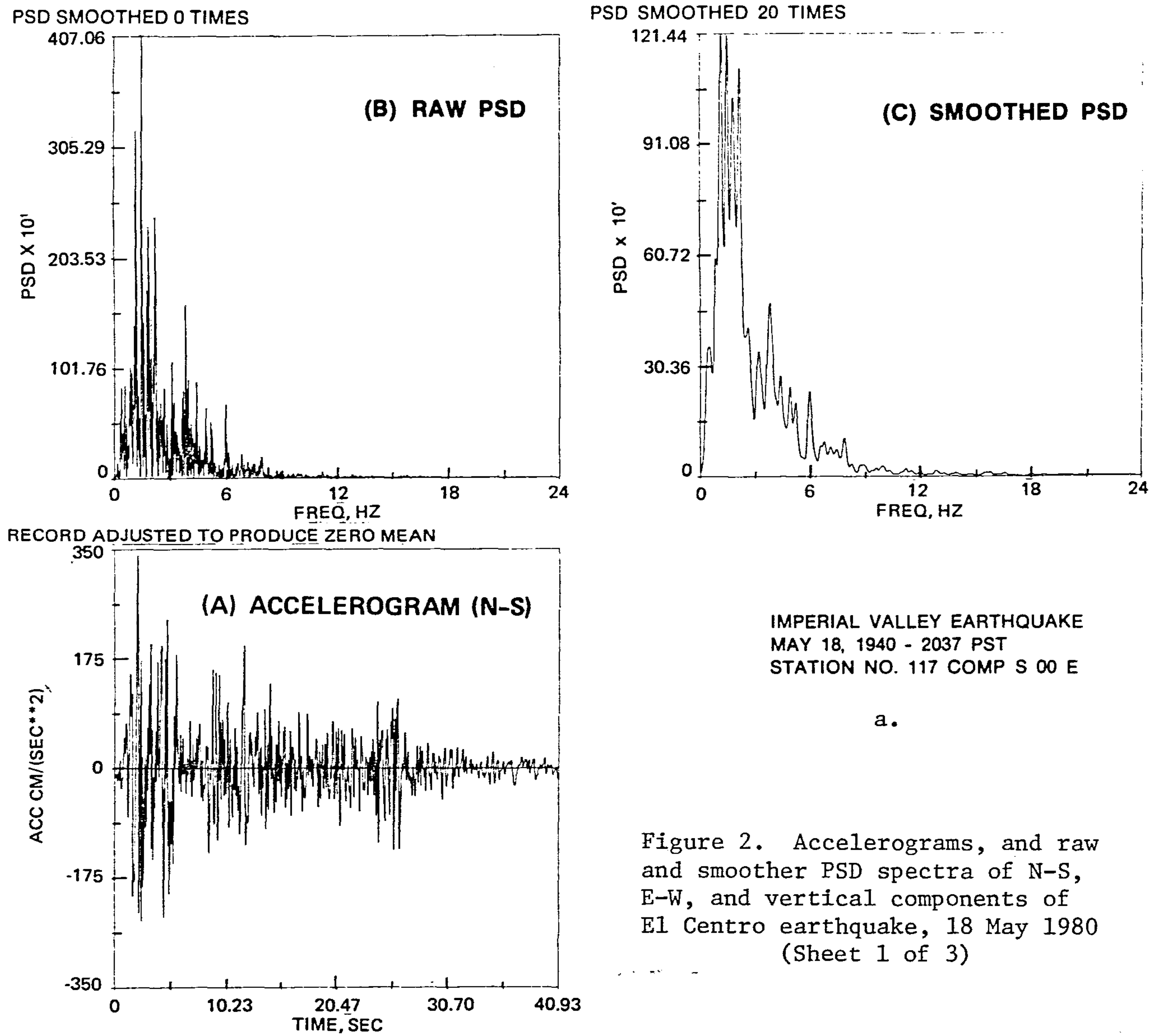

Figure 2. Accelerograms, and raw and smoother PSD spectra of N-S, E-W, and vertical components of El Centro earthquake, 18 May 1980 (Sheet 1 of 3)

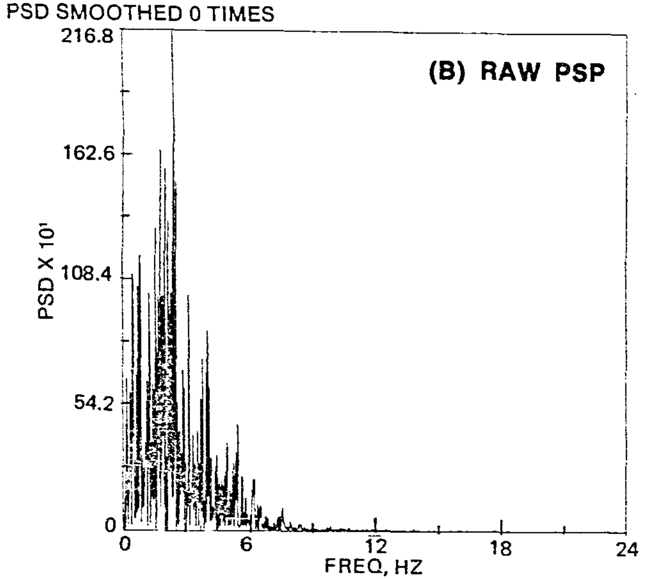

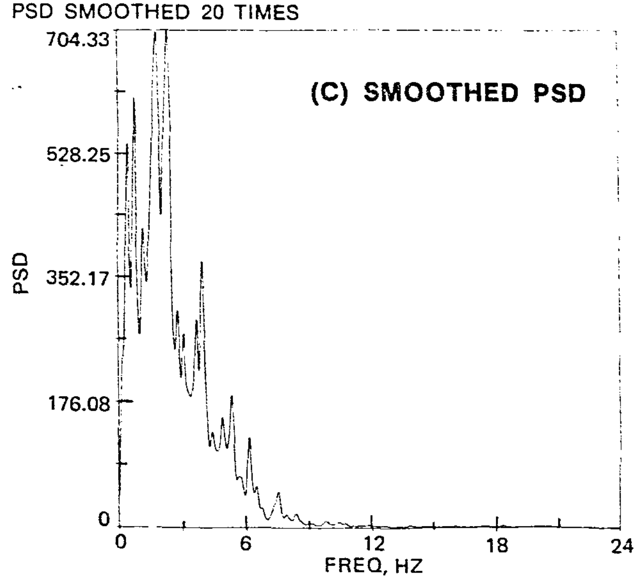

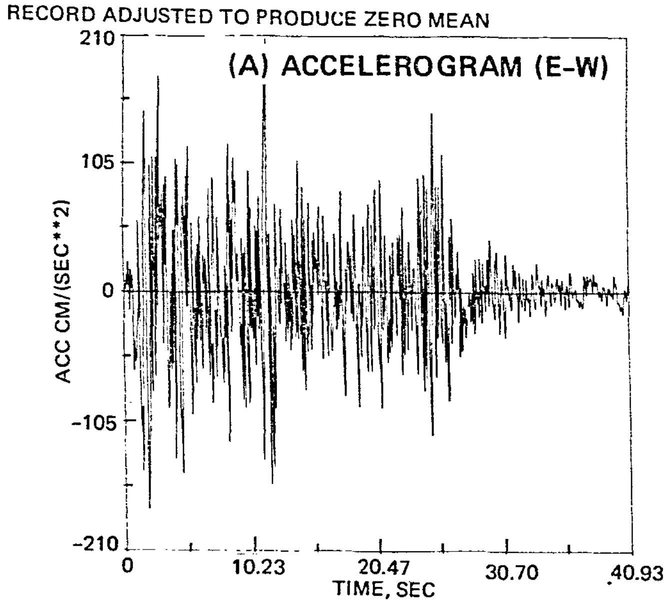

IMPERIAL VALLEY EARTHQUAKE
MAY 18, 1940 - 2037 PST
STATION NO. 117 COMP S 90 W

b.

Figure 2. (Sheet 2 of 3)

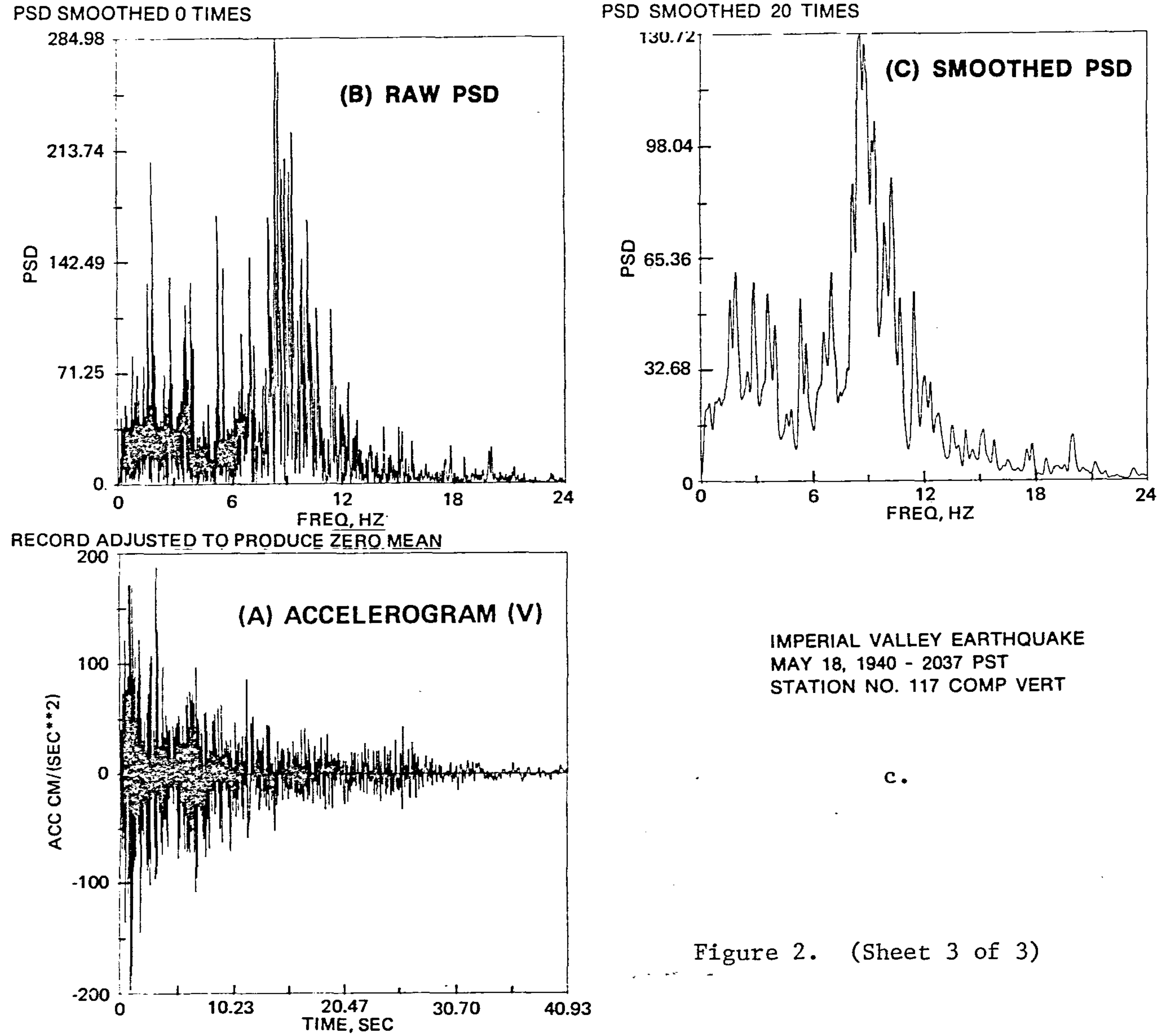

c.

Figure 2. (Sheet 3 of 3)

divided by the area λ^2 under the power density versus frequency curve. This area may also be called the spectral intensity.

Spectral Frequency Range

21. Figures 2a, b, and c show the PSD spectra of N-S, E-W, and vertical components, respectively, of the El Centro earthquake of 18 May 1940. The frequency range shown is between 0 and 24 Hz. While the energy of the PSD in the vertical component spreads between 0 and 22 Hz, the energy of the PSD for the two horizontal components is concentrated in the range of 0 to 10 Hz. For this record, the PSD frequency range of 0 to 10 Hz is adequate for the description of the spectra of the horizontal components.

Computer Procedures for Generating PSD

22. The computer program used to calculate one-sided PSD function was provided by Professor M. Shinozuka, Columbia University, and modified for the Honeywell 635 Computer by the U. S. Army Engineer Waterways Experiment Station Automatic Data Processing (WES ADP) Center. The procedures for generating PSD are as follows:

- a. Read in accelerogram.
- b. Scale accelerogram* so that accelerations are in centimetres per second squared.
- c. Adjust accelerogram* by interpolation so that the Δt between time points is 0.02 sec.
- d. Extend accelerogram to $(2^{13} - 1) \times 0.02 = 163.82$ sec by adding trailing zeros to the acceleration record (so far, no accelerogram is longer than 163.82 sec).
- e. Calculate the statistics (mean, standard deviation, etc.) for the extended accelerogram and adjust it to a zero mean.
- f. Calculate the PSD of the extended, zero-mean accelerogram (up to a frequency of 10 Hz).

---

* If necessary.

g. Calculate the area under the PSD curve and normalize the curve (NPSD) (i.e., divide each point of the PSD by the area under the PSD curve).

h. Smooth the PSD curve or NPSD curve using the "Hanning" process.

PART IV: DATA PRESENTATION

23. A total of 421 horizontal accelerograms were used to estimate the raw power spectral density (RPSD) function and its variance or RPSD intensity. These calculated PSD functions, normalized to unit area, will be used to represent the frequency content and characteristics of ground motions. The final mean normalized PSD (MNPSD) and MNPSD plus one standard deviation curves for four site groups were plotted.

24. Depending on their recording site conditions, the 421 horizontal records were grouped in Tables 1 to 4:

Table 1 - 56 records for rock sites

Table 2 - 131 records for stiff soil sites

Table 3 - 120 records for deep cohesionless soil sites

Table 4 - 114 records for soft to medium clay and sand

The headings for Columns 1-9 in each table are self-explanatory. The duration in Column 10 is arbitrarily estimated. Column 11 gives the base PSD average power λ^2 (note that $\lambda^2 = I_o/164$), which is the area under the RPSD function curve for an extended record length of 163.82 sec, or 164 sec for simplicity. Column 12 gives λ, the average acceleration, or the square root of the corresponding value in Column 11. Column 13 is the factor for conversion of λ^2 (Column 11) to λ_o^2, the area under the PSD function for the actual record length (Column 14). This conversion factor in Column 13 is the ratio of the extended time of 163.82 sec to the time of the total record length t_o or the arbitrarily selected duration (Column 10); i.e., Column 11 × Column 13 = Column 14, which is the raw average power λ_o^2. Column 15 gives λ_o, the average acceleration for the corresponding Column 14. Column 16 equals Column 14 multiplied by 0.875 and is the final corrected area, or average power λ_s^2 under the RPSD function curve. The constant 0.875 is the amount by which the power spectrum estimates should be multiplied so as to obtain the correct scale factor. An explanation for this correction is presented by Bendat and Piersol (1971, p. 323). Column 17 gives the average acceleration λ_s or the square root of the area under the estimated PSD function curve. Actually, the difference between λ_o and

λ_s is very small, so it can be considered that $\lambda_o \cong \lambda_s$. For practical purposes, the raw average power λ_o^2 may be accepted as the scaling factor for the standard (mean or mean plus one standard deviation) NPSD spectrum.

25. Most of the records used in this study were obtained at sites in the western part of the United States or Japan. A few other significant strong-motion records, such as those of the Koyna, India (1967), Gazli, USSR (1976), and Bucharest, Rumania (1977) earthquakes, were also included.

26. The RPSD average power values of the horizontal components for the earthquake accelerograms of El Centro (1934 and 1940), Taft (1952), and Olympia (1949) have been calculated for durations of 25 or 30 sec as indicated in Table 5. The average power of uncorrected versions of these records (for the same durations) was calculated by Ravara (1965) and should be different from that calculated in this study. For the purpose of comparison and evaluation of accuracy, Ravara's values are also listed in Row 1. The numerical values in Row 2 are directly calculated from the CIT corrected records. Average power values adjusted from these calculations for a duration of 163.82 sec to the lengths of the particular records are shown in Row 3. In comparing the average power in Row 2 and Row 4 of Table 5, there is a close agreement. The average power values in Row 3 estimated from the base average power λ^2 are higher than those in Row 2, which were directly calculated from the actual (shorter) duration records. Thus, the amount of increased average power (~ a constant factor) caused by adding zeros indicates that the final correction is needed.

27. Table 5 also shows that the average power estimated from the baseline uncorrected accelerograms by Ravara (1965) could have 18 to 66 percent error in comparison with CIT corrected data. The error for the extended 163.82-sec record duration in this study is in the range of 8 to 16 percent. The average error is about 12 percent, which is in agreement with the correction factor of 0.875 (Bendat and Piersol 1971). After the correction factor of 0.875 is applied, the error is reduced from 0.3 to 5.5 percent.

28. In conclusion, the base average power λ^2 of 421 records grouped in Column 11 of Tables 1-4, which are presented in a convenient way, can be employed to estimate the average power for any strong-motion duration of an individual accelerogram in the lists of all four tables as long as the selected duration is less than 163.82 seconds. Fortunately, not one of the 421 records exceeds the duration of 163.82 seconds.

29. Table 6 is a comparison of average power calculated by the method of Vanmarcke and Lai (1977) and Vanmarcke (1979) and the method of this study with the same strong-motion durations corresponding to the same records. By comparison of the average power λ_o^2 and the average acceleration λ_o for the same record in Table 6, it follows that the values calculated by Vanmarcke and Lai (1977) and in this study are in excellent agreement, even though Vanmarcke and Lai's values of λ_o^2 were directly derived from the time domain and the values in this study are calculated in the frequency domain. This comparison is verifying not only the processing techniques but also the theoretical background.

PART V: DATA ANALYSES

Analysis of Site-Dependent PSD Spectral Shape

30. The NPSD functions for the horizontal accelerograms in each group (Table 1-4) were first determined and then were analyzed statistically to obtain the average NPSD spectra and the average plus one standard deviation NPSD spectra (about 84 percentile). Figures 3-6 present these mean and mean plus one standard deviation NPSD spectra for the four different site conditions. The mean NPSD spectra for the different site conditions are compared in Figure 7, and the mean plus one standard deviation NPSD spectra are compared in Figure 8. Both NPSD spectra in Figures 7 and 8 are smoothed 500 times.

31. It is clear that the differences in PSD spectral shapes depend on the site conditions. In particular, two categories can be distinguished: sites having soft to medium clays and sands or deep cohesionless soils (>250 ft) are similar and form one category, the soft group; stiff soil and rock sites form another category, the hard group. A dividing line on the frequency axis appears at 2.5 Hz (0.4-sec period). In the frequency range below 2.5 Hz, spectral amplifications for the soft group are much higher than those for the hard group; in the frequency range above 2.5 Hz, spectral amplifications for the hard group are higher than those for the soft group. In the soft group, the energy peaks for the soft to medium clays and sands and the deep cohesionless soils both occur at about the same frequency of 1 Hz, but the amplifications are slightly different (0.4 and 0.35, respectively).

32. The average NPSD spectrum of the deep cohesionless soil sites has a large hump at 2.8 Hz (0.36-sec period), but the spectrum of the soft to medium clay and sand sites does not. The large amplitude at 0 Hz is believed to be caused by a digitization error, particularly that due to the uncorrected Japanese strong-motion data in the soil site group. For the hard site group, in the frequency range below 2.5 Hz, the spectral amplitude for the stiff soil is higher than that for the rock; but in the frequency range above 2.5 Hz, the spectral amplitude

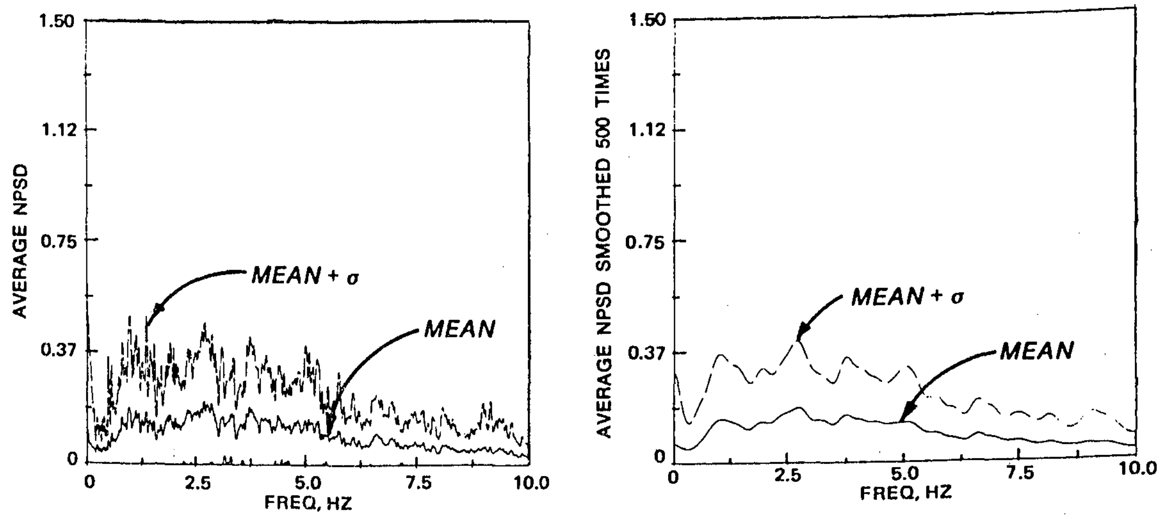

Figure 3. Mean and mean plus one standard deviation (σ) NPSD curves of rock sites, raw (left) and smoothed 500 times (right)

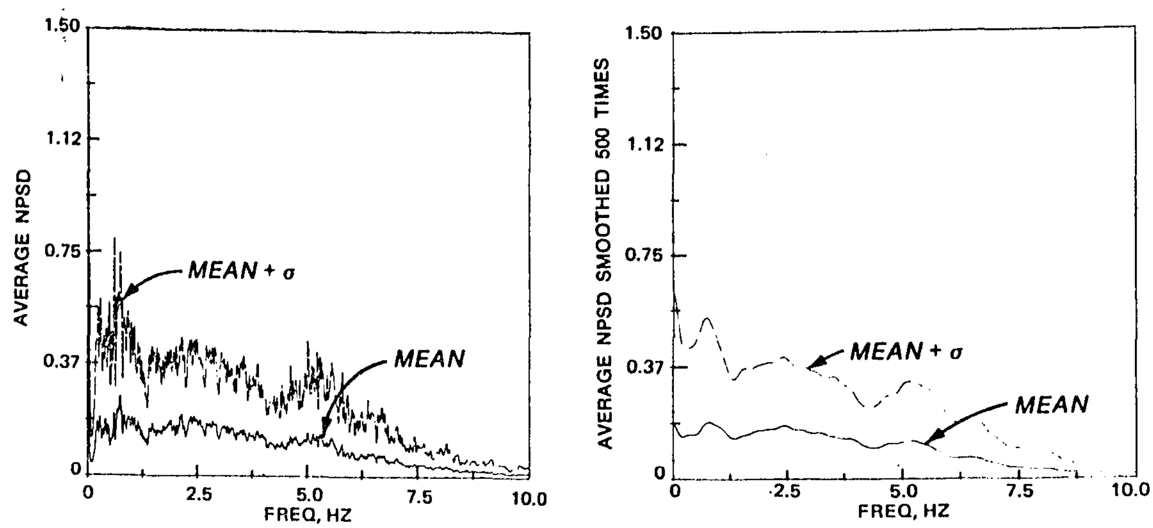

Figure 4. Mean and mean plus one standard deviation (σ) NPSD curves of stiff soil sites, raw (left) and smoothed 500 times (right)

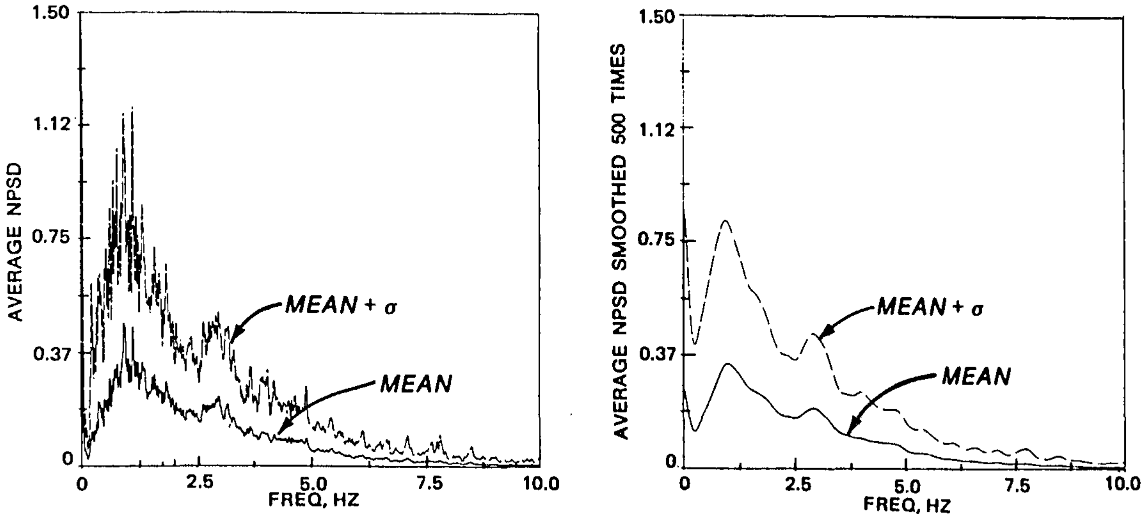

Figure 5. Mean and mean plus one standard deviation (σ) NPSD curves of deep cohesionless soil sites, raw (left) and smoothed 500 times (right)

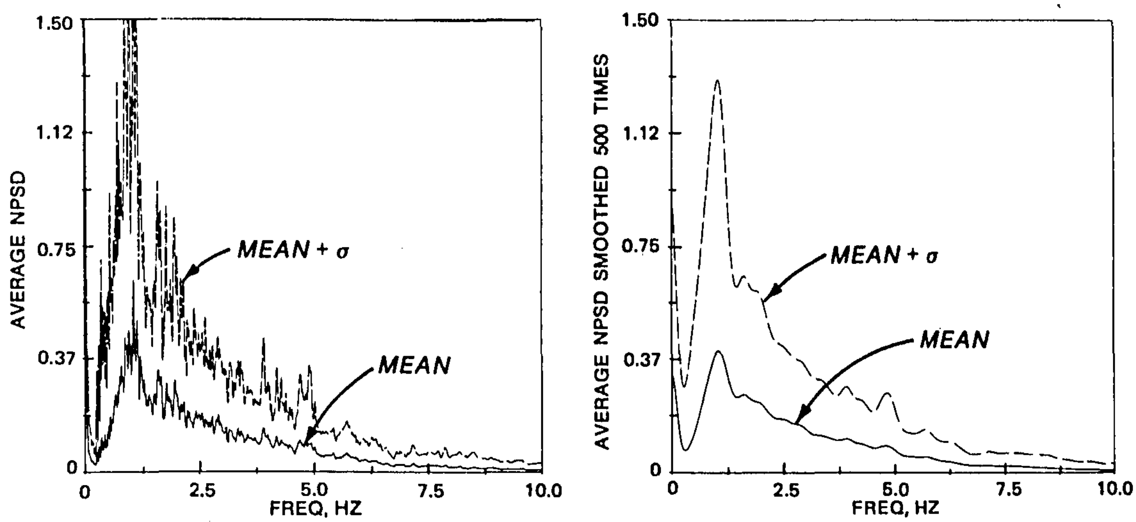

Figure 6. Mean and mean plus one standard deviation (σ) NPSD curves of soft to medium clay and sand sites, raw (left) and smoothed 500 times (right)

LEGEND

GROUP 1 ROCK SITES (56 RECORDS; 11 EARTHQUAKES)
GROUP 2 STIFF SOIL SITES (131 RECORDS; 39 EARTHQUAKES)
GROUP 3 DEEP COHESIONLESS SOIL SITES (120 RECORDS; 47 EARTHQUAKES)
GROUP 4 SOFT TO MEDIUM CLAY AND SAND SITES (114 RECORDS; 28 EARTHQUAKES)

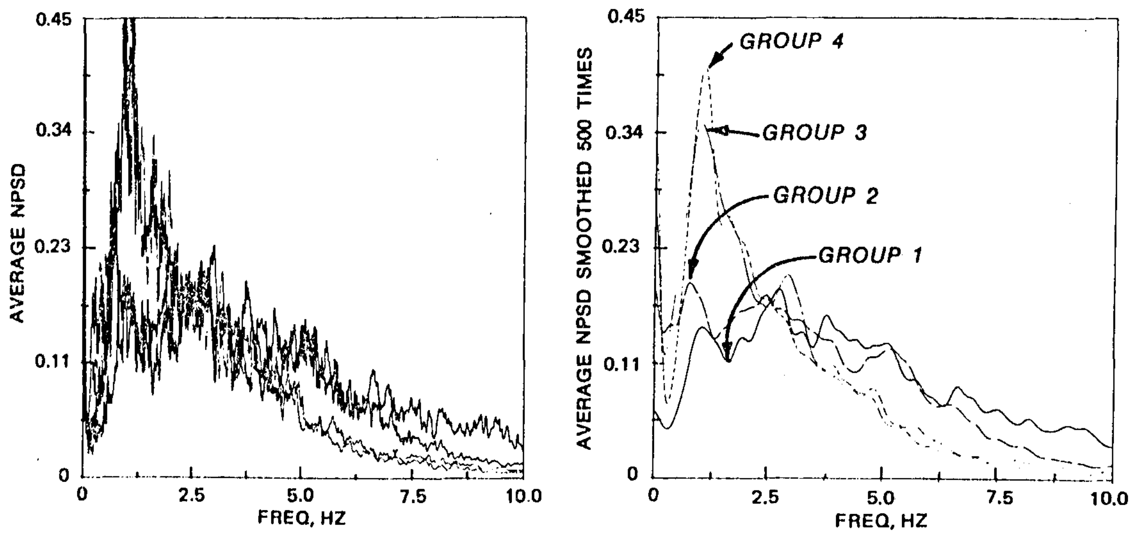

Figure 7. Comparison of mean NPSD curves of four soil groups, raw (left) and smoothed 500 times (right)

LEGEND

GROUP 1 ROCK SITES (56 RECORDS; 11 EARTHQUAKES)
GROUP 2 STIFF SOIL SITES (131 RECORDS; 39 EARTHQUAKES)
GROUP 3 DEEP COHESIONLESS SOIL SITES (120 RECORDS; 47 EARTHQUAKES)
GROUP 4 SOFT TO MEDIUM CLAY AND SAND SITES (114 RECORDS; 28 EARTHQUAKES)

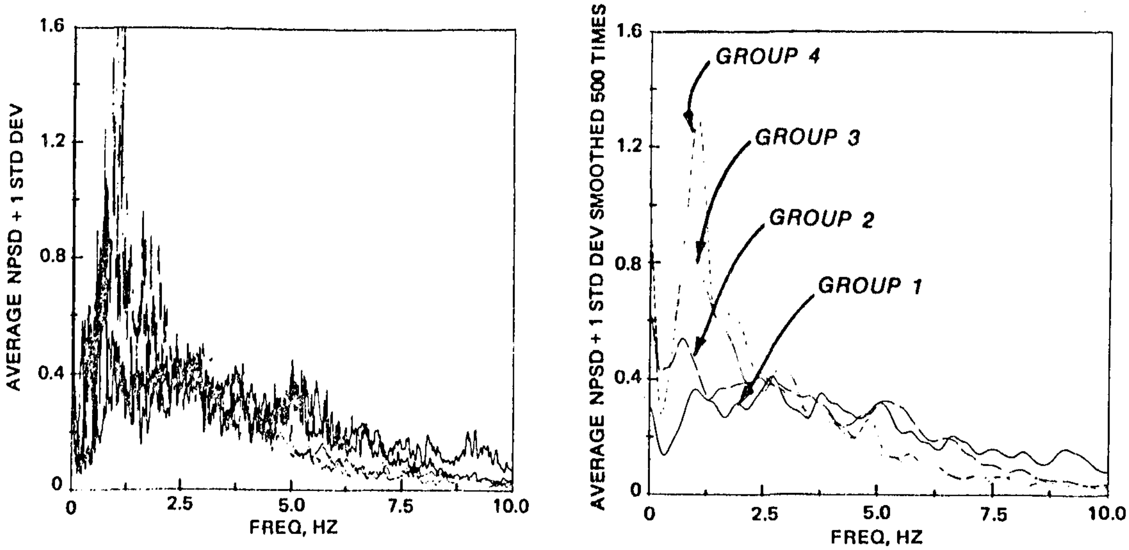

Figure 8. Comparison of mean plus one standard deviation NPSD curves of four soil groups, raw (left) and smoothed 500 times (right)

for the rock is slightly higher than that for the stiff soil. The largest energy peaks for the rock sites and the stiff soil sites are at 2.75 Hz (0.36 sec) and 0.8 Hz (1.25 sec), respectively.

Statistical Characteristics of the Earthquake Ground Motions

33. Based on the maximum ground accelerations and average accelerations (PSD intensities) in Tables 1-4, and the average NPSD function estimates for the four site conditions (Figures 7 and 8), Table 7 lists the statistical characteristics of the earthquake ground motions.

34. It is apparent from Table 7 that statistical characteristics of the ground motions are strongly site dependent. The rock sites produce an average maximum ground acceleration of about 0.20 g for the entire suite of 56 records. The rock site group shows the highest maximum acceleration and average acceleration of the four site groups. The PSD function estimates are almost uniform over the peak frequencies of 1.06, 2.75, 3.80, and 5.17 Hz.

35. The average maximum ground accelerations and PSD spectral intensities (or average accelerations) for the other three site groups--stiff soils, deep cohesionless soils, and soft to medium clays and sands--are relatively close together. However, the spreads of the standard deviation of maximum accelerations for the stiff soil and cohesionless soil groups are wider than for the soft to medium clays and sands group. This large spread is believed to be caused by the different magnitudes of earthquakes and the different epicentral distances. The group of accelerograms for soft to medium clays and sands shows relatively low ground acceleration but the highest PSD function estimates at the frequency of 1 Hz among the four groups. One second (1 Hz) is probably near the predominant natural period of sites on soft to medium clays and sands. It seems that the acceleration and the PSD spectral intensity at 1 Hz are roughly in proportion and inverse proportion, respectively, to the degree of stiffness of the site material. In conclusion, the average acceleration or the mean spectral intensity is site dependent.

Maximum Ground Acceleration and Average Acceleration

36. Figures 9-16 show plots of maximum ground accelerations a_{max} against base average accelerations λ (i.e., the rms value of the average power for extended durations of 163.82 sec) and against the average acceleration λ_s (for selected or actual record durations) for each of the four site condition groups. These figures indicate a common linear trend for all four groups. This approximately linear relationship may provide a basis for predicting strong earthquake ground motions for engineering design. The data points show greater scatter on the plots of a_{max} versus λ than on the plots of a_{max} versus λ_s. However, mean lines for both kinds of plot are parallel, probably because of the close relationship between λ and λ_s. Also, the data points for soft sites show a wider spread than those for hard sites.

36. It is worthwhile to note that there is a strong correlation (Figures 17 and 18) between a_{max} and λ_o, which were derived from the values of $I_o = S_o\lambda_o^2$ of 140 strong-motion records in Vanmarcke and Lai (1977, 1980). The quantity I_o is the total motion energy at constant power λ_o^2 over the strong-motion duration S_o. Twenty-two of the 140 records are for rock sites, and the rest are for soil sites. At the same time, the two mean lines for rock sites and soil sites are almost identical, thus indicating that the linear relationship between a_{max} and λ_o is independent of the site conditions. The mean lines of a_{max} versus λ_o calculated from the strong-motion data of Vanmarcke and Lai (1977) are also plotted in Figures 10, 12, 14, and 16 and lie to the right of the data for this study. Since λ_o is inversely proportional to S_o, λ_o is minimum when the whole record length is considered. The durations selected in this study were close to the whole record lengths; thus, the calculated average accelerations are lower than the rms accelerations of Vanmarke and Lai (1977).

Peak Factor

38. The peak factor r is defined as the ratio of the peak

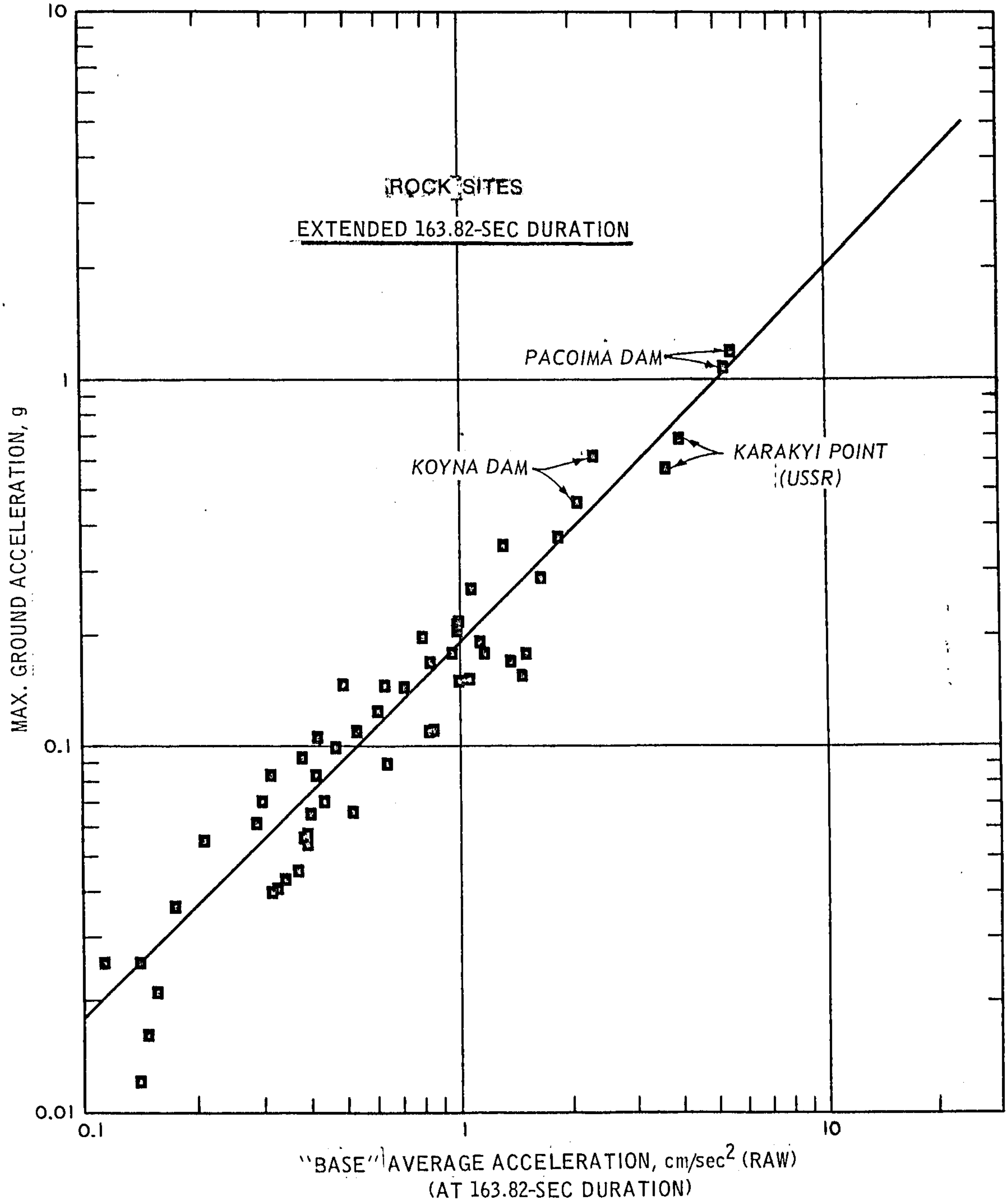

Figure 9. Correlation of maximum ground acceleration (g) versus "base" average acceleration calculated based on extended 163.82-sec duration for rock sites

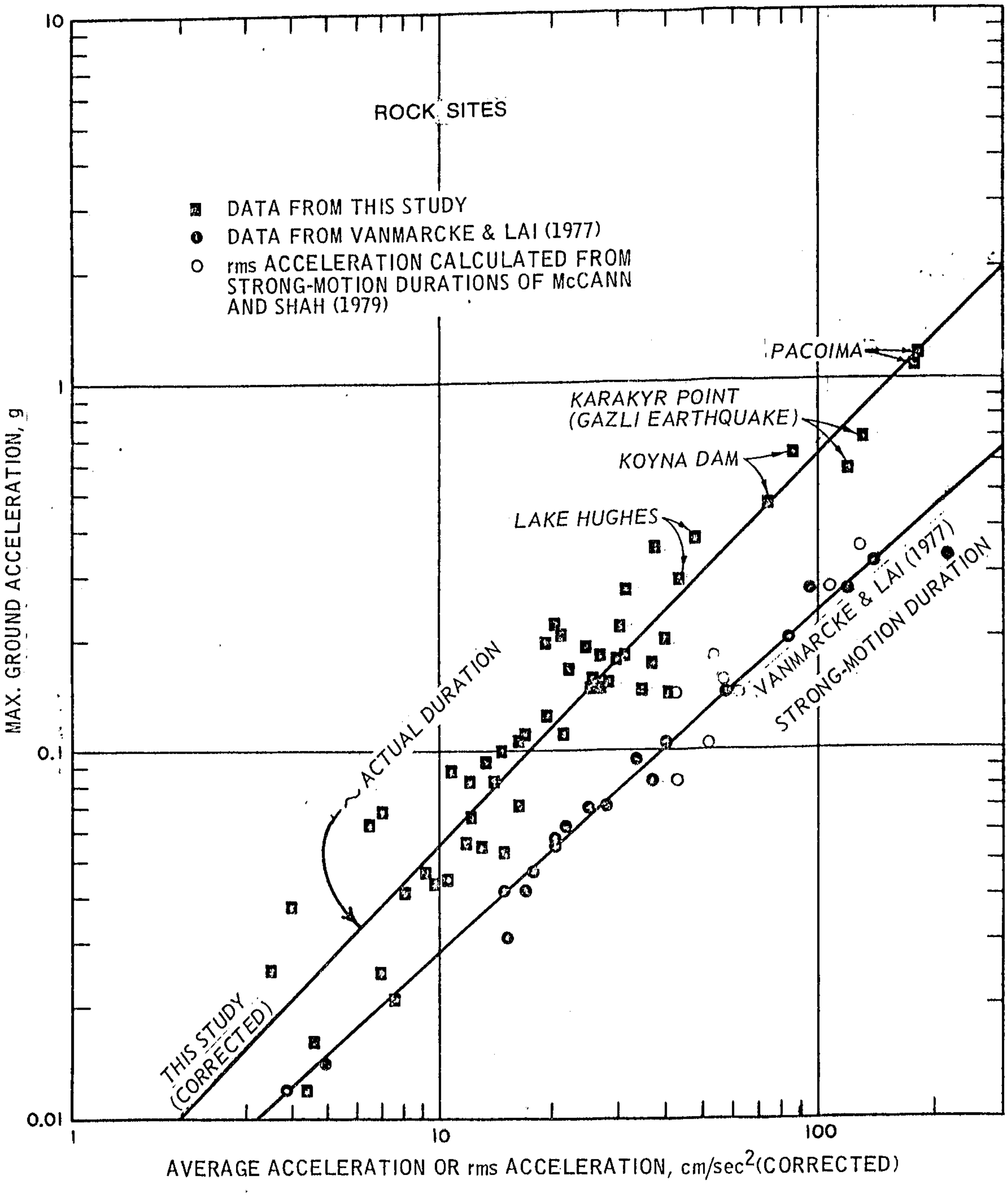

Figure 10. Correlation of maximum ground acceleration (g) versus average acceleration and rms acceleration based on actual durations and strong-motion durations for rock sites

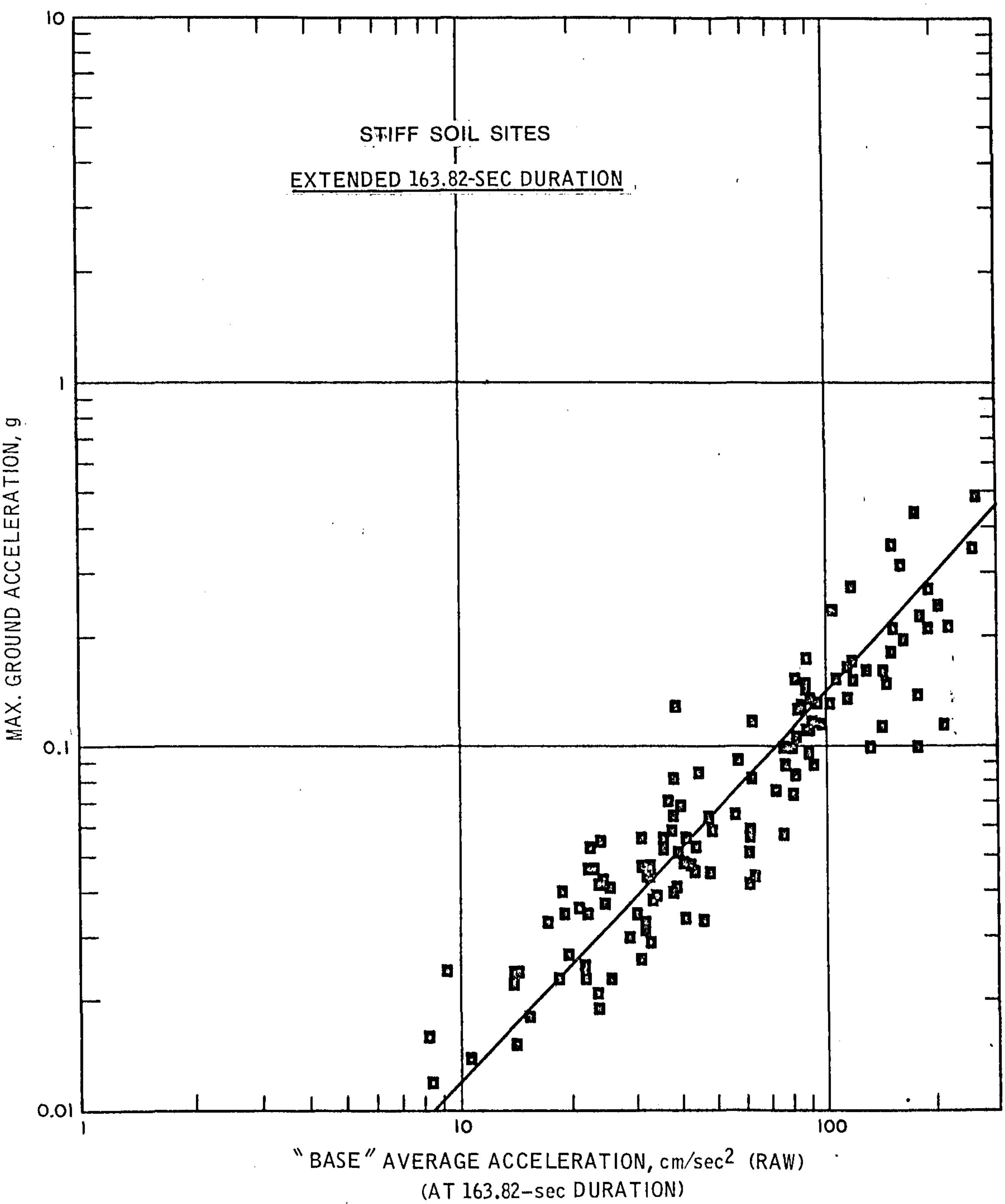

Figure 11. Correlation of maximum ground acceleration (g) versus "base" average acceleration based on extended 163.82-sec duration for stiff soil sites

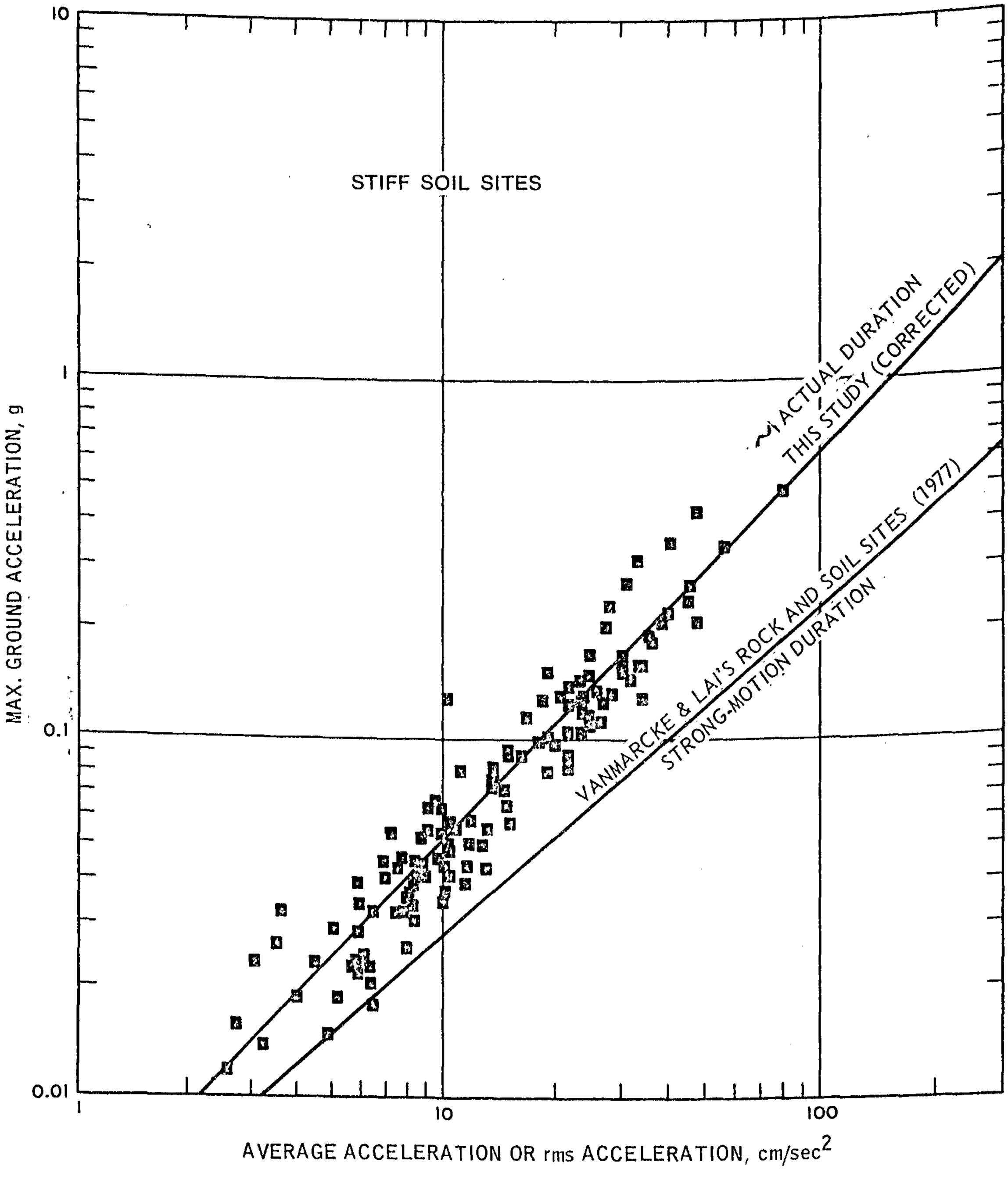

Figure 12. Correlation of maximum ground acceleration (g) versus average accelerations and rms accelerations based on actual durations and strong-motion durations for stiff soil sites

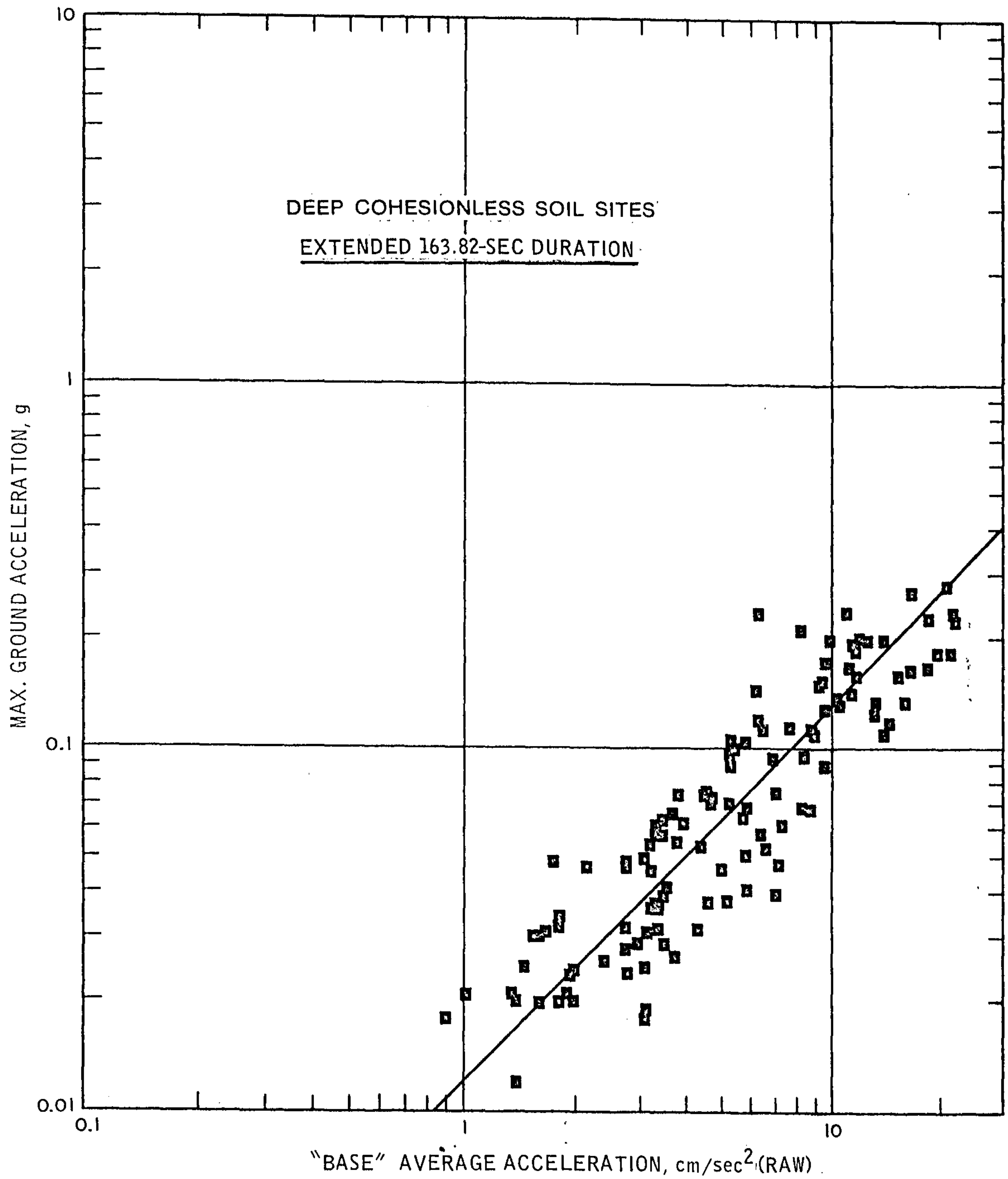

Figure 13. Correlation of maximum ground acceleration (g) versus "base" average acceleration based on extended 163.82-sec duration for deep cohesionless soil sites

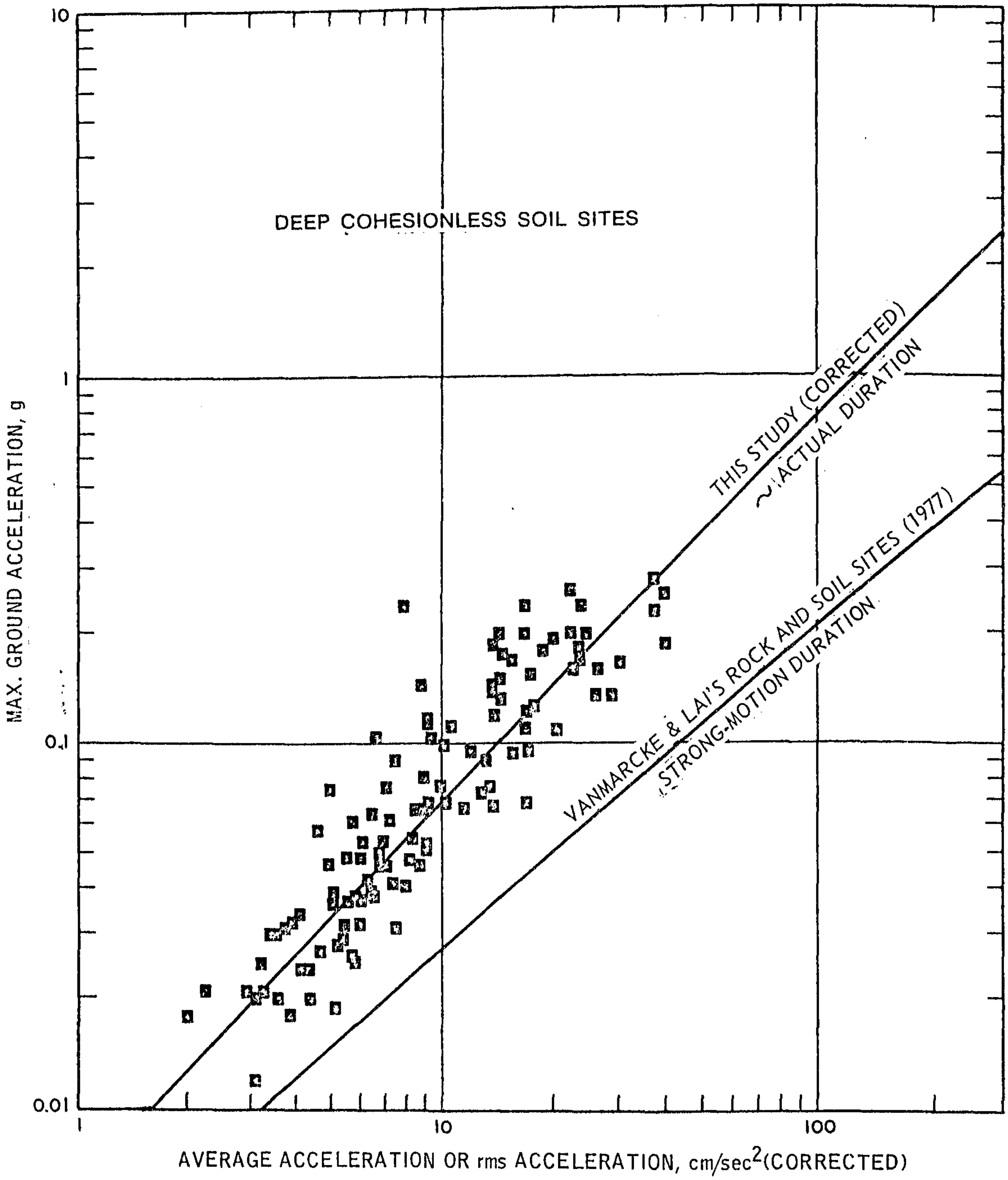

Figure 14. Correlation of maximum ground acceleration (g) versus average acceleration and rms acceleration based on selected actual durations and strong-motion durations for deep cohesionless soil sites

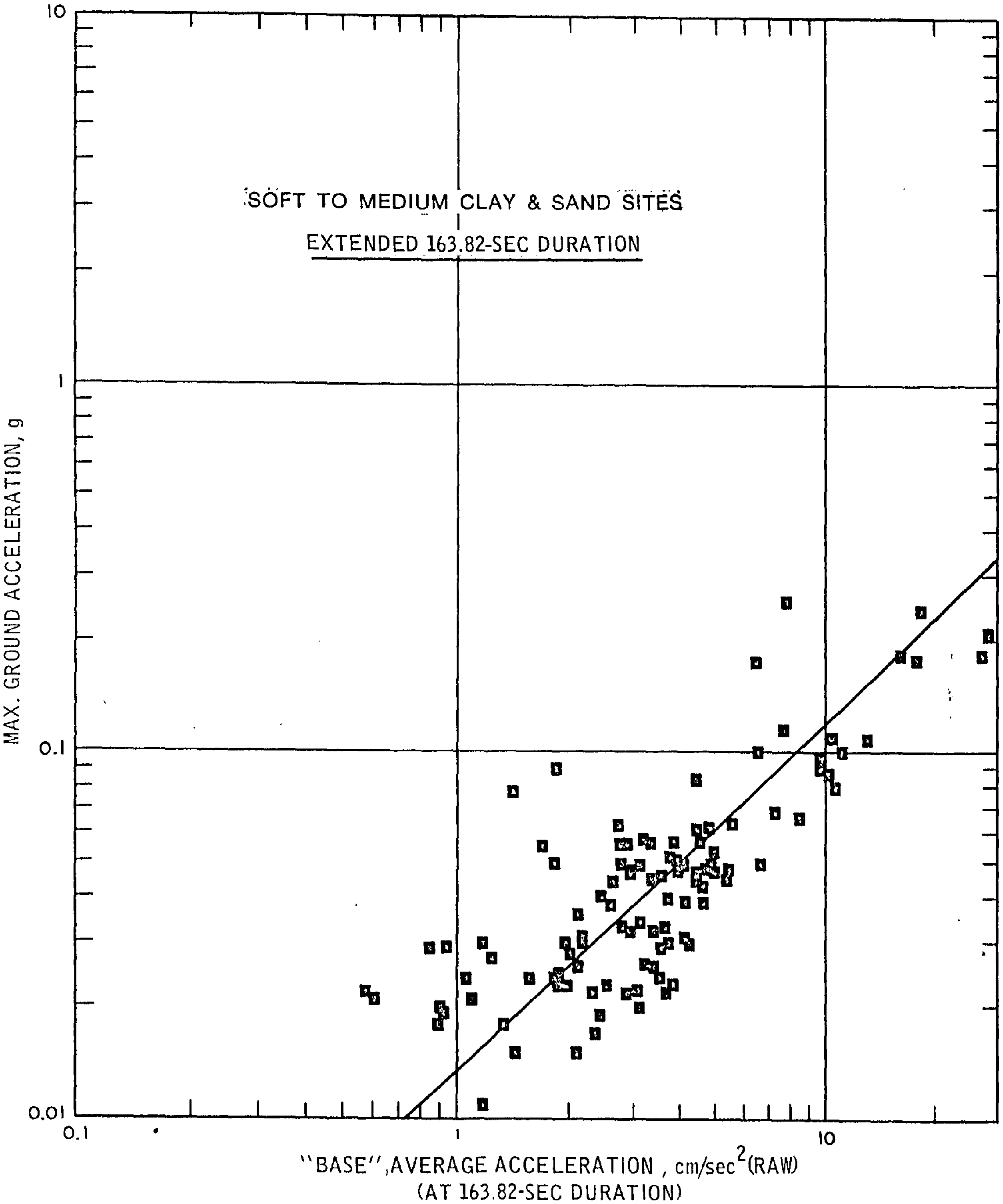

Figure 15. Correlation of maximum ground acceleration (g) versus "base" average acceleration based on extended 163.82-sec duration for soft to medium clay and sand sites

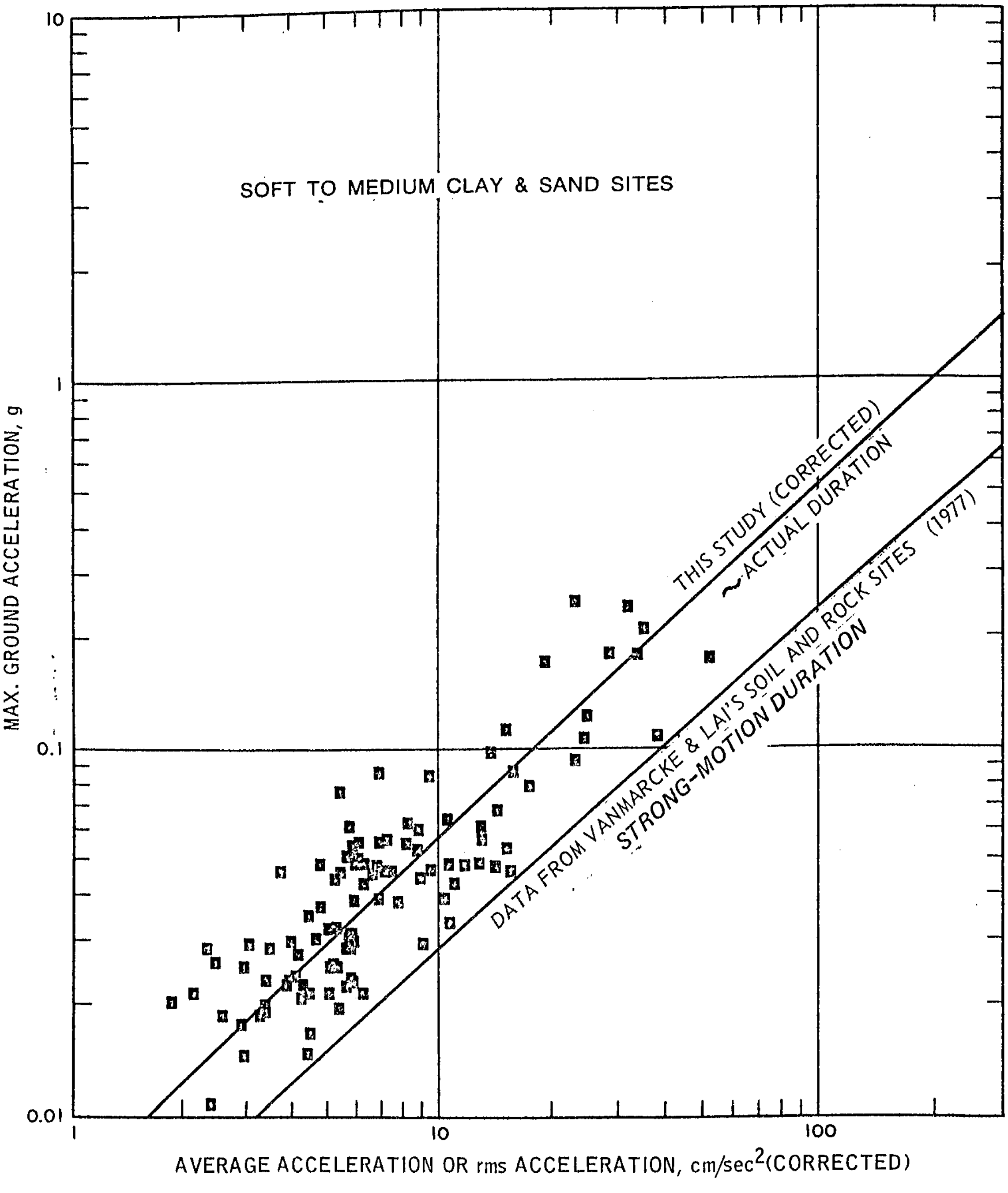

Figure 16. Correlation of maximum ground acceleration (g) versus average acceleration and rms acceleration calculated based on selected actual durations and strong-motion durations for soft to medium clay and sand sites

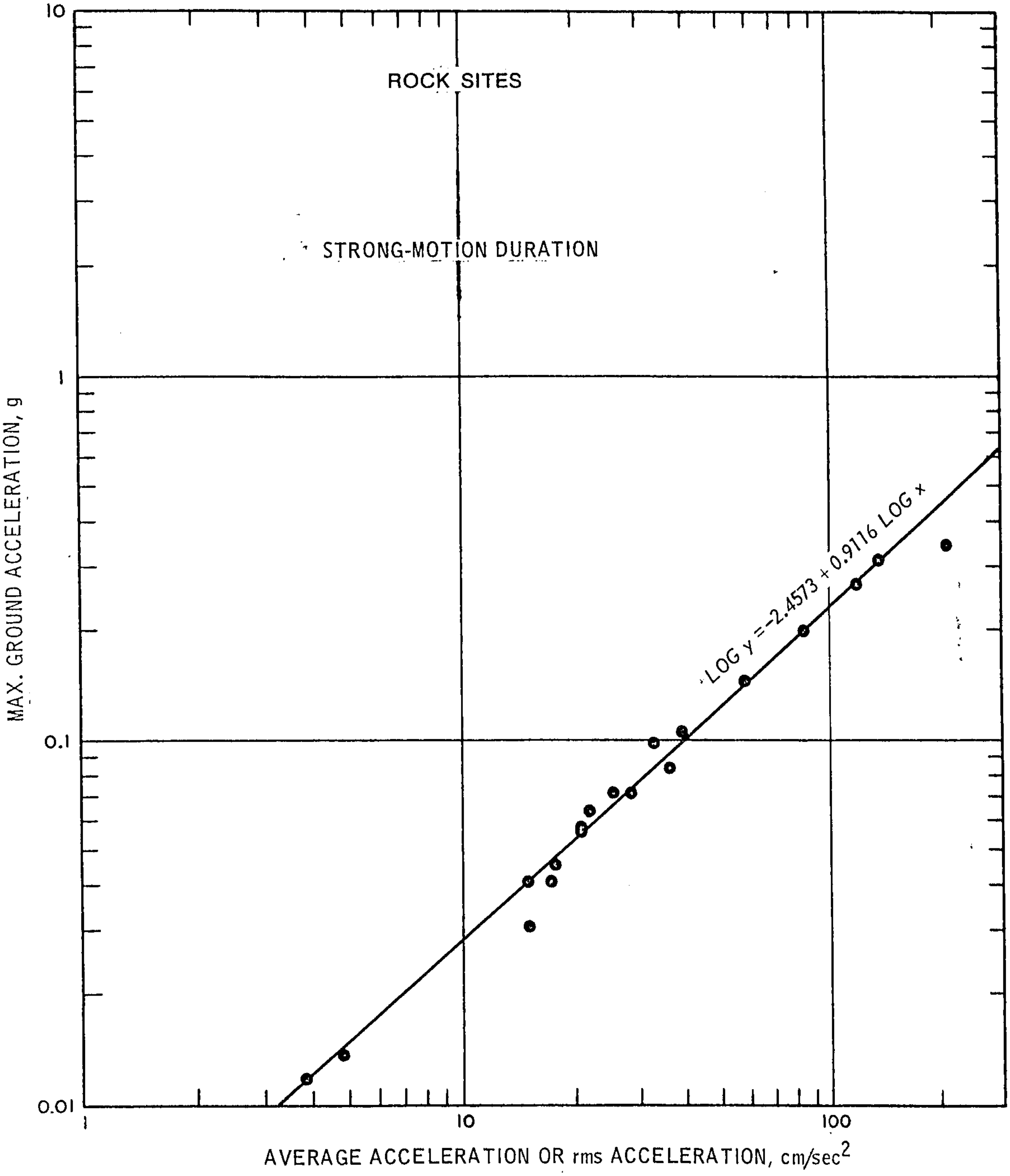

Figure 17. Maximum ground acceleration (g) versus rms or average acceleration for strong-motion duration case - rock sites

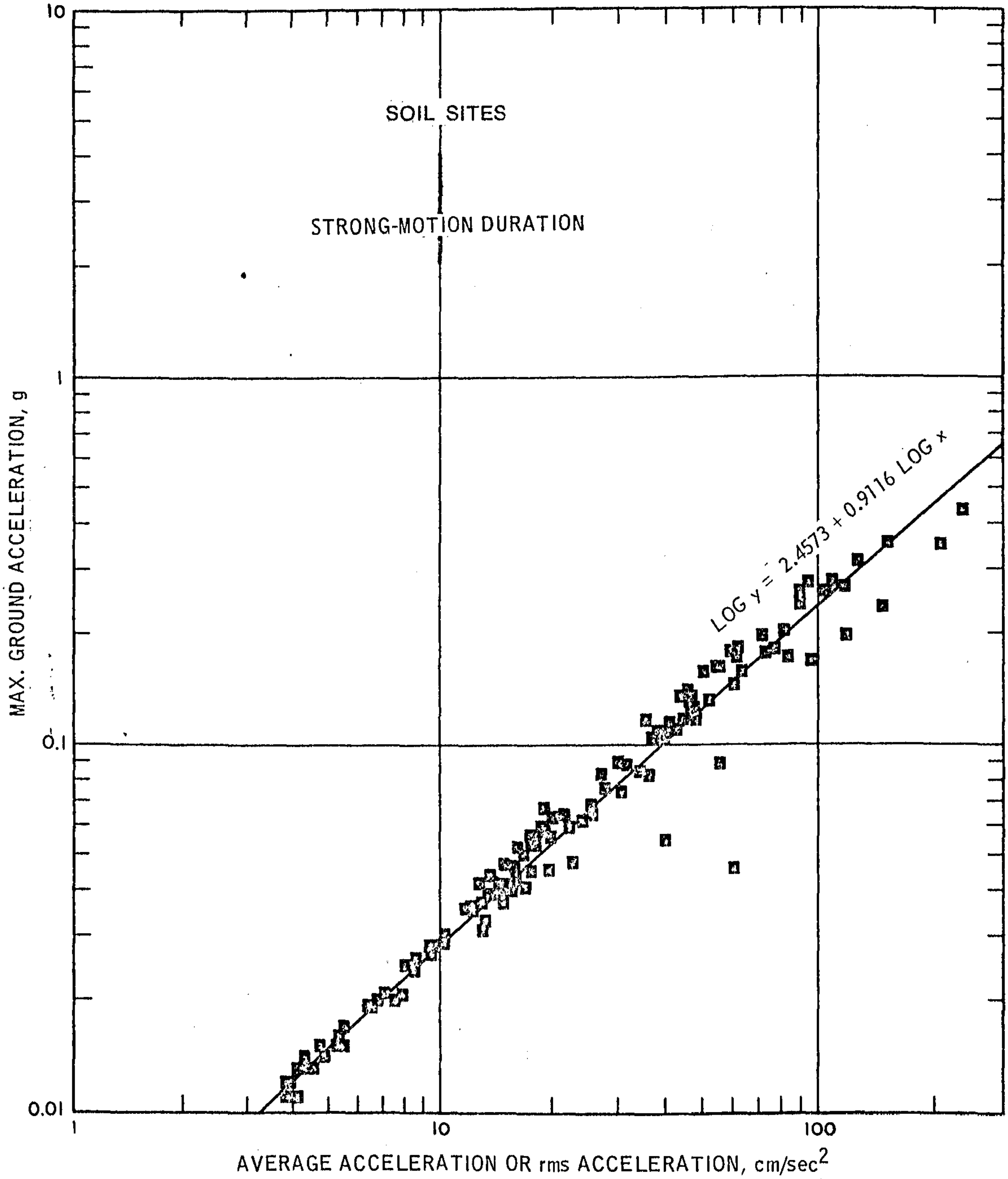

Figure 18. Maximum ground accelerations (g) versus rms or average acceleration for strong-motion duration case - soil sites

ground acceleration a_{max} to the average acceleration λ_o, or

$$r = \frac{a_{max}}{\lambda_o} \tag{22}$$

The physical meaning of r is the slope of the lines plotted in Figures 9-18. Equation 22 may be written as

$$\lambda_o = \frac{a_{max}}{r} \tag{23}$$

If Equation 23 is substituted into Equation 16, the result may be expressed as

$$S_o = r^2 \frac{I_o}{a_{max}^2} \tag{24}$$

where r is a constant that may be determined from Figures 9 through 16. The average peak factors for rock sites, stiff soil sites, deep cohesionless soil sites, and soft soil sites found in this study were 5.911, 5.422, 6.996, and 5.695, respectively. Evidently, the peak factors are nearly independent of site conditions. Therefore, an average peak factor of 6.0 is an adequate estimate for use with long record lengths such as those used in this report. However, r is dependent on the choice of record duration. Vanmarcke and Lai (1980) found the average peak factor for 140 horizontal earthquake records to be about 2.75 because they used strong-motion durations. Their simplified definition of strong-motion duration is

$$S_o = (2.75)^2 \frac{I_o}{a_{max}^2} = 7.5 \frac{I_o}{a_{max}^2} \tag{25}$$

However, Equation 25 is not employed in this study.

Comparison of Average Acceleration and Peak Ground Acceleration Versus Distance

39. The average acceleration λ_o in Tables 1-3 and the peak

ground acceleration (PGA) or a_{max} of the San Fernando earthquake of 9 February 1971 are compared qualitatively in Figures 19 and 20. The spread of the average acceleration is as wide as that of the PGA, but the attenuation of the average acceleration is slower than that of the PGA. The average acceleration of an accelerogram is inversely proportional to the duration, which in this study was arbitrarily selected. In earthquake engineering design, both strong-motion duration and wave amplitude should be considered. The average power of the PSD function and the average acceleration, the square root of the average power, possess information on both duration and amplitude. The previous sections have shown good correlation between the PGA or a_{max} and the average acceleration λ_o. The average acceleration can provide an alternative earthquake engineering intensity scale, describe the intensity of ground motion for input to structural design, and also serve to compute the scaling factor λ_o^2 of the normalized standard PSD spectra.

Potential Uses of Site-Dependent Standard NPSD Spectral Curves

40. In the previous sections of Part V, the four standard site-dependent PSD spectral curves at the common record length of 163.82 sec have been established, and they were also normalized to a unit area. The relationships between the shape of the spectral density function and the duration of strong ground motion for individual records will be explained in an example. It is very easy to select an actual record in Tables 1-4 and to modify its duration only for consistency with a specified design earthquake. Use the N-S component of the El Centro record, 18 May 1940, as an illustration: Record No. 3 of Table 2 shows that the base PSD intensity λ^2 (average power) for a duration of 163.82 sec is 663.202 cm^2/sec^4. Next, let the specified duration for seismic design be 40 sec, then the new PSD intensity will be

$$\lambda_o^2 = 663.202 \times \frac{163.82}{40} = 2716.1\ cm^2/sec^4$$

This value, 2716.1 cm^2/sec^4, is also the scaling factor.

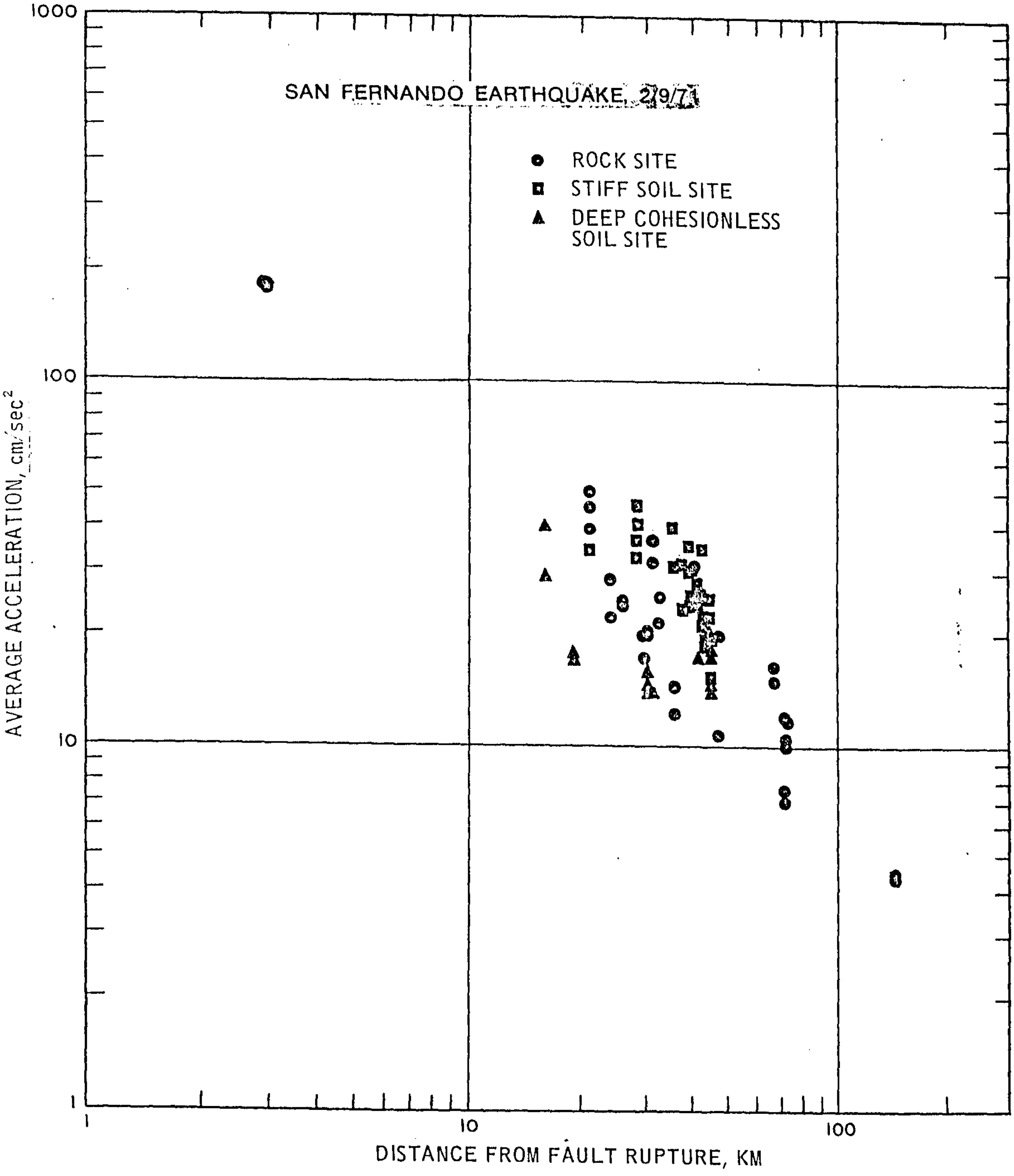

Figure 19. The average acceleration versus distance of San Fernando earthquake, 9 February 1971

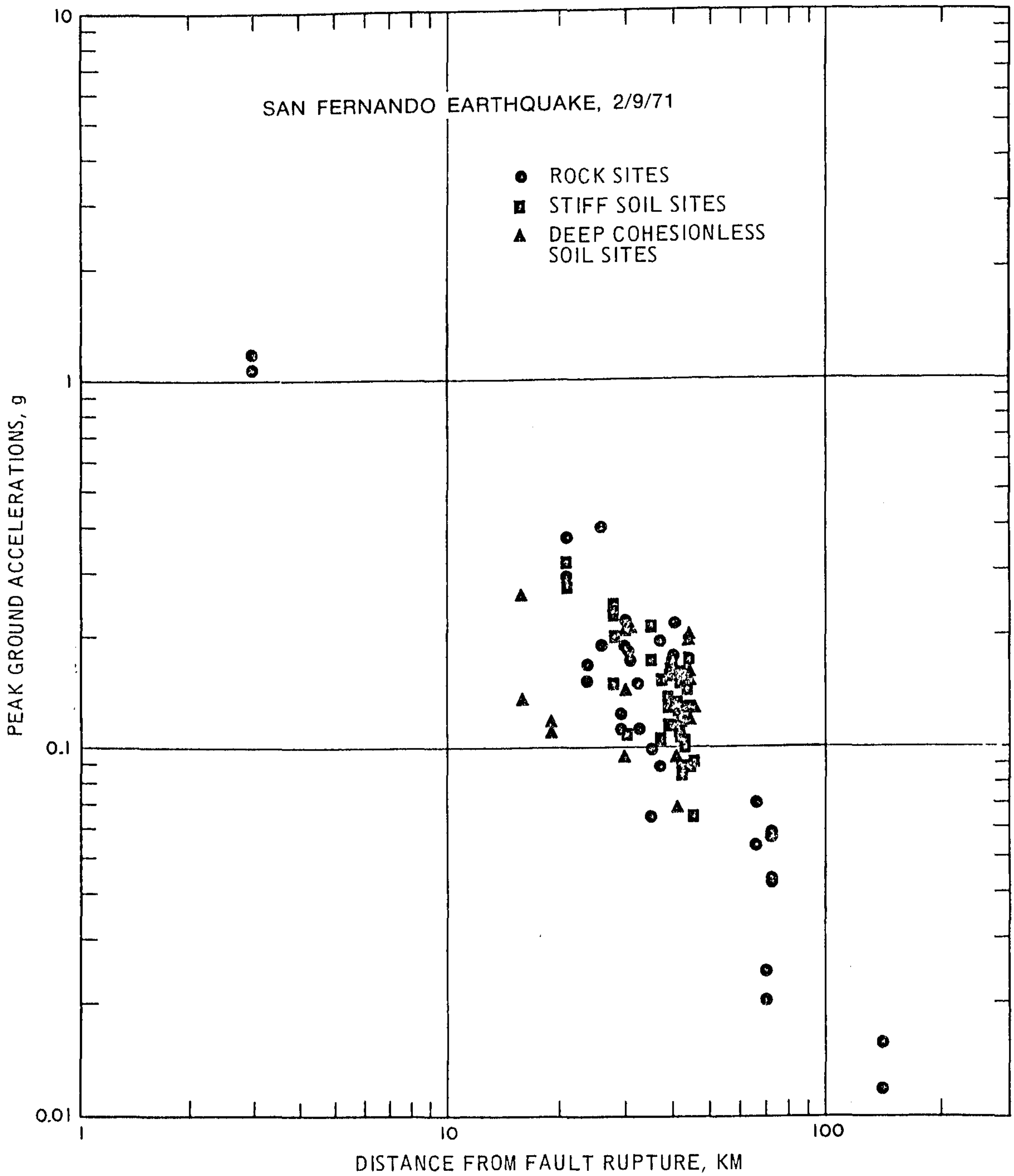

Figure 20. Peak ground acceleration versus distance of San Fernando earthquake, 9 February 1971

41. An alternative way is to emply the approximate linear relationships between a_{max} and λ and between a_{max} and λ_o (for the rock site condition, Figures 9 and 10). If 0.30-g maximum ground acceleration and 15-sec duration are chosen as the design ground motion, what will the scaling factor be for the normalized mean PSD curve for rock sites? In Figure 9, the base average acceleration λ for 0.30 g is 15.5 cm/sec^2, and the conversion factor is 163.82/15 = 10.923; then $(15.5)^2 \times 10.923 = 2624.25\ cm^2/sec^4$ ($\lambda_o = 51.22\ cm/sec^2$). Thus, 2624.25 cm^2/sec^4 is the scaling factor.

Peak Velocity Versus Average Acceleration

42. Figure 21 shows the relationship between the peak velocity and the average acceleration. All 140 average acceleration values in this figure were calculated from the total ground motion intensity I_o listed in the tables of Vanmarcke and Lai (1977) or Vanmarcke (1980), except those of Gazli and Pacoima. All peak velocities are given by Chang (1978). These data points ($4.5 \leq M \leq 6.8$) spread over a wide band; the upper line shown corresponds to magnitude 6.5 and the lower to magnitude 5.5. In the relationship between the peak acceleration and the average acceleration in Figures 17 and 18, this particular feature is not shown, because the velocity is related to the intensity or energy level, and thus magnitude. The largest earthquake represented is the Kern County earthquake of 1952, for which the surface-wave magnitude M_s was estimated as 7.7. Professors Bolt (1978) and Nuttli et al. (1979) found the local magnitude M_L and the body-wave magnitude M_b to be 7.2 and 6.8, respectively. Thus, 6.8 has replaced 7.7 in Figure 21.

43. Vanmarcke and Lai's (1977, 1980) total intensity data were used for calculating average acceleration because they have a unique definition of strong-motion duration. These data were obtained from $I_o = S_o \lambda_o^2$ where S_o is the strong-motion duration and λ_o^2 is the square of average acceleration, or average power.

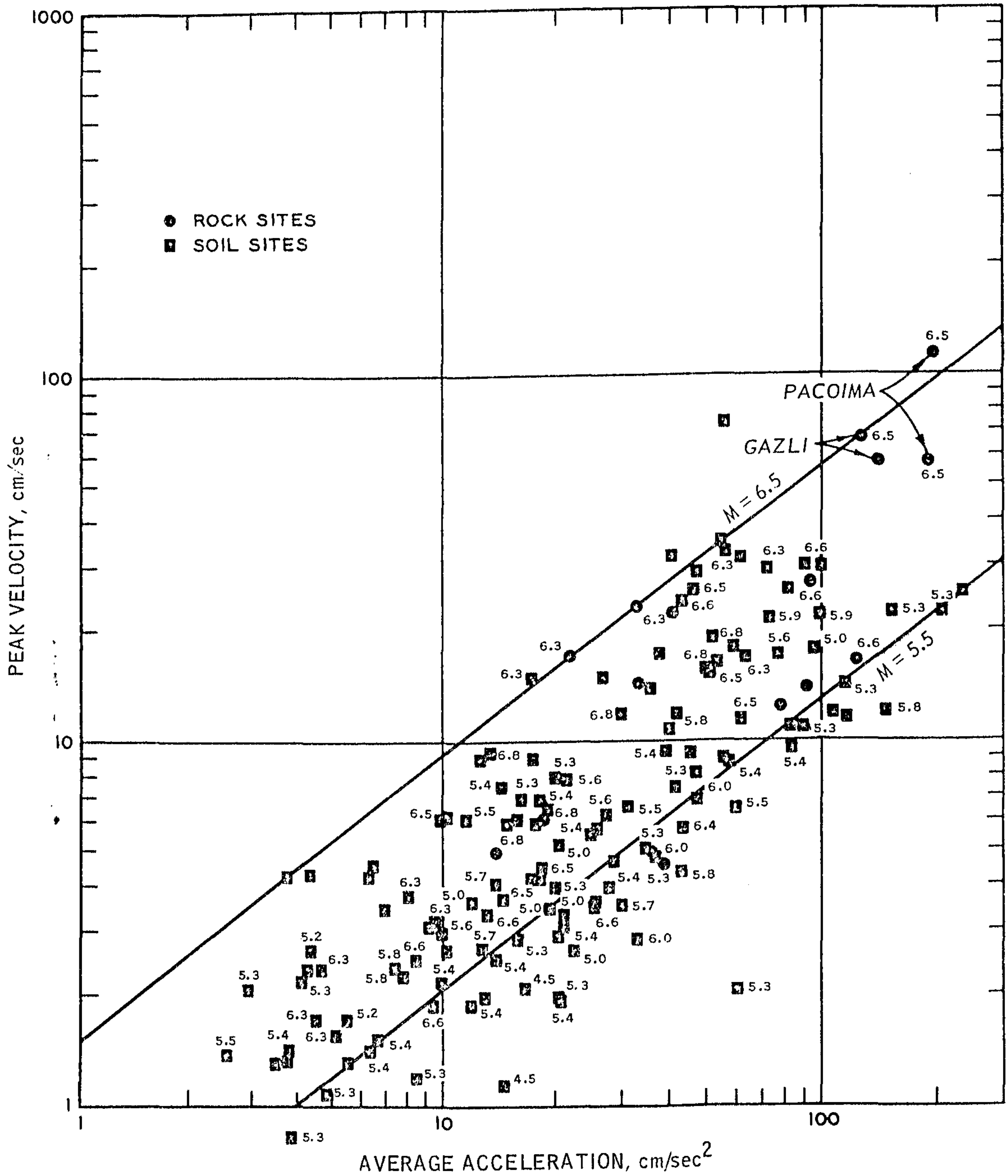

Figure 21. Correlation of peak velocity versus average acceleration

Correlation of Average Acceleration and Modified Mercalli Intensity

44. It will be of much benefit to the engineering community if a quantitative earthquake intensity scale, such as average acceleration intensity, can be correlated with the Modified Mercalli Intensity (MMI) (Figures 22 and 23). Table 8 shows the upper bound of site-dependent rms intensity (square root of the sum of two horizontal average powers) versus the MMI. To obtain these bounds in the table, the rock and stiff soil sites in Figure 22 were combined as hard sites and the deep cohesionless soil and soft soil sites in Figure 23 as soft sites. The Pacoima Dam, Karakyr Point, Koyna Dam, and Lake Hughes Array No. 12 sites were located in the epicentral regions and near the faults ($3km \leq R \leq 20km$). Certainly, they possessed the maximum average acceleration and might be called epicentral average accelerations. It seems from these limited data that the maximum average acceleration at the epicentral region might not be over 550.0 cm/sec^2. However, the power λ_o^2 or the average acceleration λ_o is inversely proportional to the duration, i.e., the smaller the duration, the higher the average acceleration.

Correlation of I_o and MMI

45. The correlations of total intensity I_o with the MMI based on the data of hard sites (Tables 1 and 2) and soft sites (Tables 3 and 4), are plotted in Figures 24 and 25, respectively. The upper bound line of Figure 24 is established by five earthquakes (San Fernando, Gazli, Parkfield, Koyna, and Tokachi Oki). There are four sites located in the epicentral region (see paragraph 44), so the values are named as epicentral intensities. The extrapolation from these values, the probable epicentral seismic intensities versus the MMI, may be listed as follows:

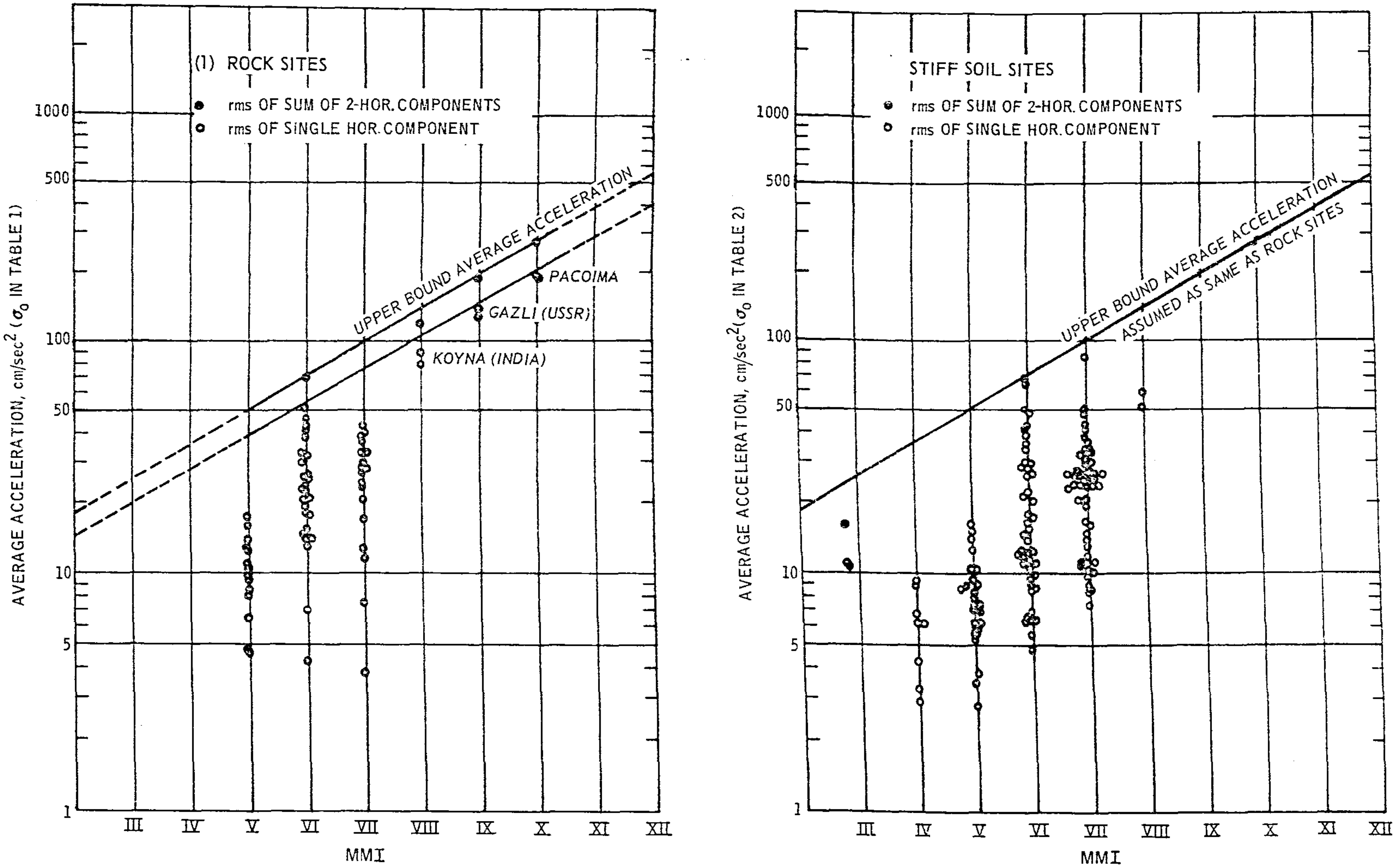

Figure 22. Correlation of upper-bound average acceleration versus MMI - hard sites (rock and stiff soil sites)

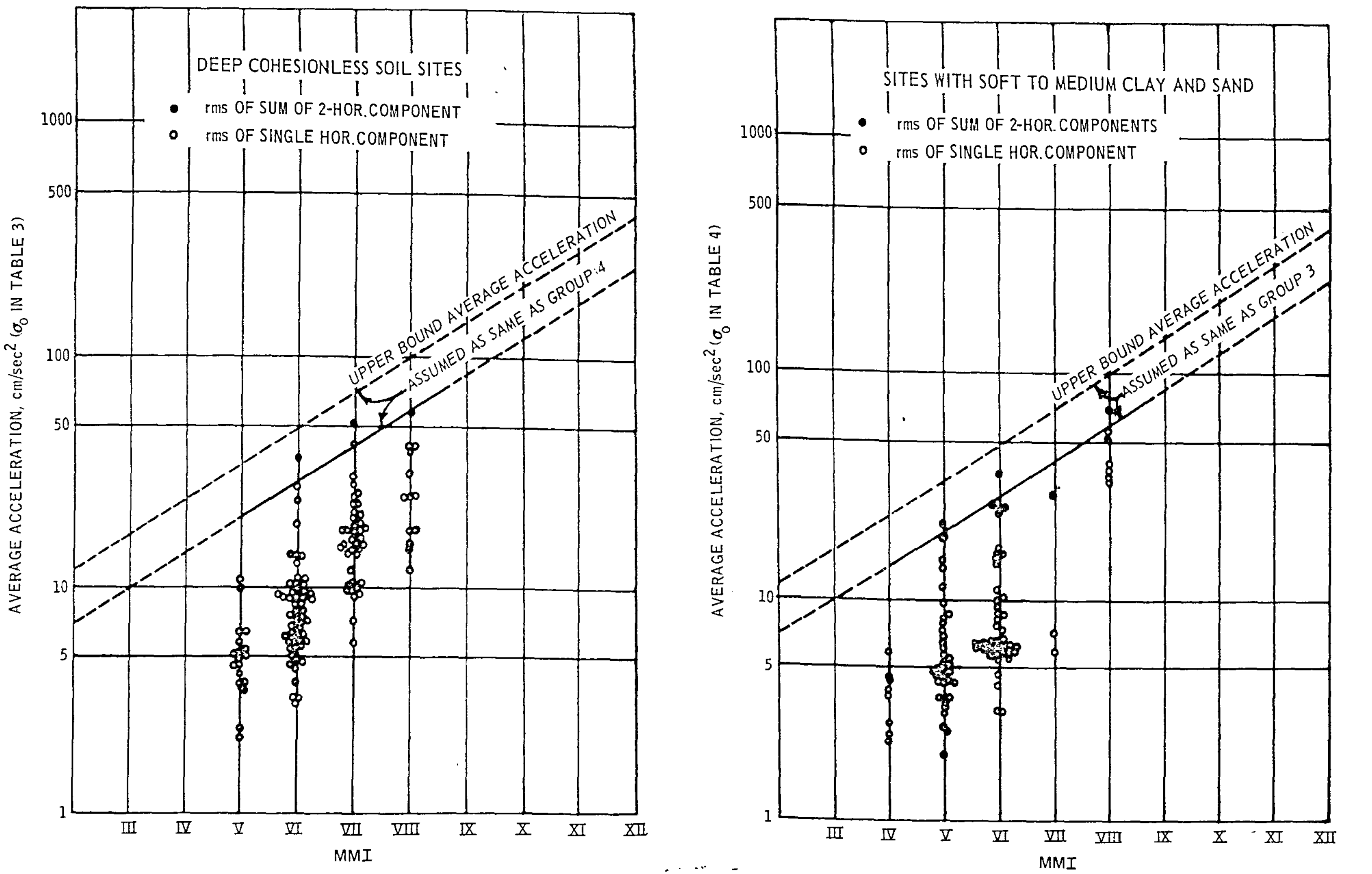

Figure 23. Correlation of upper-bound average acceleration versus MMI - soft sites (deep cohesionless soil and soft to medium clay and sand sites)

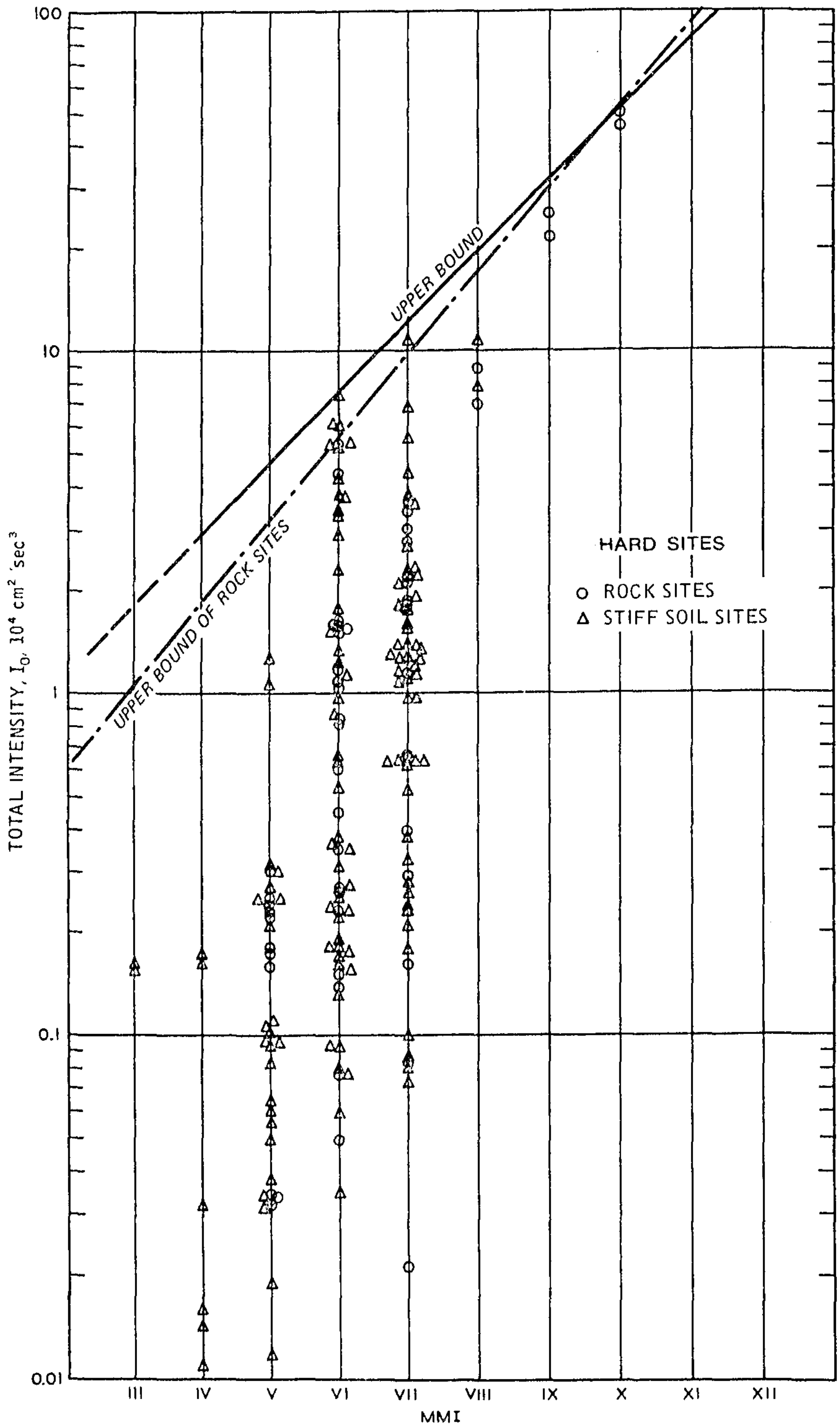

Figure 24. Probable seismic intensity I_o at epicentral region - hard sites

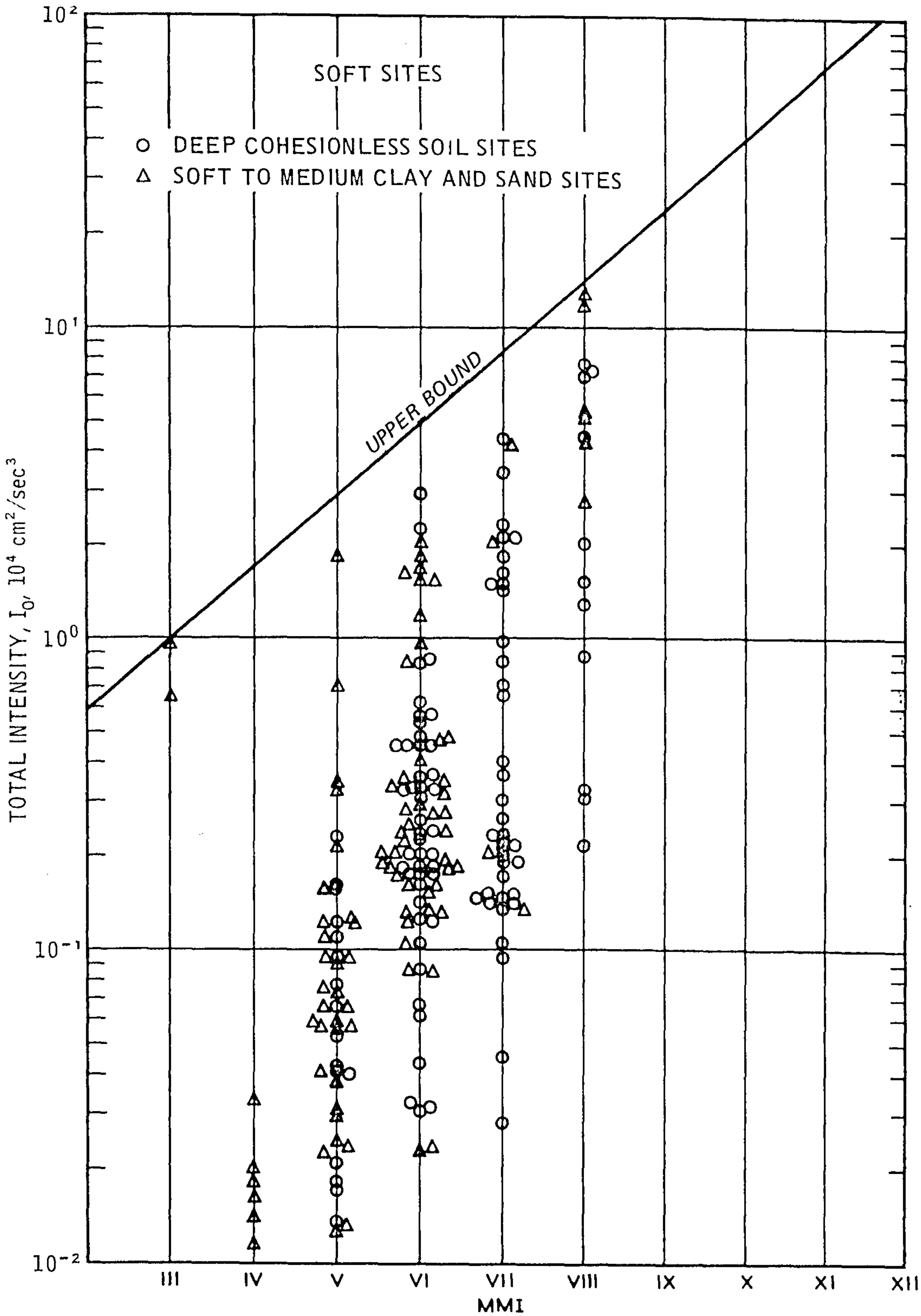

Figure 25. Probable seismic intensity I_o at epicentral region - soft sites

	Probable Seismic Epicentral Intensity	
	Hard Sites	Soft Sites
MMI	$10^4 (cm^2/sec^3)$	$10^4 (cm^2/sec^3)$
XII	135-160	120
XI	82-92	70
X	52-54	40
IX	30-34	24
VIII	17-20	14
VII	10-13	8
VI	6-8	5
V	3-5	3
IV	2-3	2

46. The upper-bound line of Figure 25 indicates that the seismic intensity at soft sites is lower than at hard sites. Also, the rate of attenuation is lower for soft sites than for hard sites. Of course, the upper-bound seismic intensities for the hard sites (Figure 24) and the soft sites (Figure 25) are in the near field. The data under the upper-bound line (both Figures 24 and 25) spread widely because of various earthquake magnitudes and distances.

47. Damage to structures in the epicentral area is generally more severe on soft sites than on hard sites, based on past experience and observations. However, this study showed the seismic total intensity (seismic energy) at soft sites to be lower than at hard sites. Thus, the degree of damage to structures does not correlate with the seismic total intensity in the epicentral region. Furthermore, the predominant frequencies at soft sites are in the range of 0 to 2.5 Hz; the seismic energy in this low-frequency range deserves further investigation as it relates to structural damage.

PART VI: SUMMARY, CONCLUSIONS, AND RECOMMENDATIONS

Summary

48. This study presents the results of a statistical analysis of the spectral shapes of PSD functions of 0 to 10 Hz for 421 ground accelerograms from 89 earthquakes, mostly in the western United States and Japan. The 421 horizontal accelerograms recorded on ground surface level have been divided into groups representing (a) rock sites (56 records), (b) stiff soil sites (131 records), (c) deep cohesionless soil sites (120 records), and (d) soft to medium clays and sands (114 records). The significant earthquake information (earthquake name, recording station, date, distance, magnitude, MMI, and peak acceleration), base average power λ^2 (area under the PSD curve for the extended record of 163.82 sec), base average acceleration λ, conversion factor (ratio of 163.82 sec to the duration of the selected record, or strong-motion duration), raw average power λ_o^2 (spectral intensity, area under the RPSD curve of the actual duration or the selected strong-motion duration), raw average acceleration λ_o, corrected average power λ_s^2 (about 12.5 percent less than λ_o^2), corrected average acceleration λ_s, and total intensity I_o for each record are listed in Tables 1-4. Values of λ_o^2, which were not directly estimated from original (actual) duration, were converted from λ^2. Generally, λ_o^2 was about 12.5 percent higher than λ_s^2.

49. All 421 accelerograms were extended to 163.82 sec at an equal time interval Δt of 0.02 sec by adding a string of zero accelerations. Then, the statistical mean, standard deviation, etc., were calculated for the extended accelerogram and adjusted to a zero mean. Next, the PSD and the area under the PSD curve of the extended, zero-mean accelerogram (up to a frequency of 10 Hz) were estimated. Finally, the PSD curves were normalized to a unit area to contain NPSD curves. The statistical mean and mean plus one standard deviation of the NPSD curves for the four site conditions were established.

50. From the comparison of the four site-dependent NPSD spectra,

it is clear that there are differences in PSD spectral shapes depending on the site conditions. Two major groups are formed in the mean NPSD spectra: soft to medium clays and sands and deep cohesionless soil sites are similar and form one soft group; stiff soil and rock sites form one hard group. The frequency of 2.5 Hz (0.4-sec period) forms a dividing line on the frequency axis; in the frequency range lower than 2.5 Hz, spectral amplifications for the soft sites are much higher than the hard sites; and in the frequency range higher than 2.5 Hz, spectral amplifications for the hard sites are higher. However, in the case of mean plus one standard deviation NPSD spectra, the peak amplitudes in the low frequency range (<2.5 Hz) decrease in the order of soft soil, deep cohesionless soil, stiff soil, and rock sites in accordance with the degree of hardness. This order seems in correlation with the damage.

51. In the soft group, the peak amplitude at about 1 Hz for the soft to medium clays and sands is about 14.3 percent higher than the deep cohesionless soils. Both of them are monotonically attenuated from the sharp peak at 1 to 10 Hz (except one hump at 2.75 Hz for the deep cohesionless soils). In the hard group, the largest peak amplitudes for the rock sites and stiff soil sites are at 2.75 Hz (0.36 sec) and 0.8 Hz (1.25 sec), respectively. Generally speaking, the energy content is spread widely over the frequency range of 0 to 10 Hz. It is possible that there is a connection between the largest peak amplitude at 2.75 Hz for the hard group and the hump at 2.75 Hz for the deep cohesionless soils or the soft group. In other words, it could be said that 2.75 Hz is a common frequency of bedrock under the deep cohesionless soils.

52. A qualitative comparison was made of the spectral shapes of PSD in this study with the Acceleration Response Spectra (ARS) of Seed and Idriss (1971), Seed, Ugas, and Lysmer (1976), and Kiremidjian and Shah (1978). There is general agreement in the spectral shapes of both methods except those for rock sites that the amplitude of the ARS of Seed, Ugas, and Lysmer (1976) was lower than for the PSD in the high frequency range. This discrepancy in amplitudes of spectra between the PSD and the ARS was due principally to the smaller number of records for the latter. The number of rock site records used was 28 for the ARS and

56 for the PSD. Thus, the average spectral amplitude value for the former is less reliable than the latter. Another difference is that the spectral shapes of the PSD function show more peaks than do the ARS.

53. The base average power λ^2 (area) under the PSD curve, which is uniformly distributed on 163.82 sec of the extended record, has been established for each of the 421 records. The raw average power λ_o^2, or any average power of strong-motion duration (see Table 6), which is inversely proportional to the duration, can be easily calculated as λ^2 times the ratio of 163.82 sec to the duration of the selected record.

54. The approximate linear relationships of the maximum ground accelerations a_{max} versus the base average accelerations λ and the average accelerations λ_o provide a set of scaling curves for the four site groups. Since the λ_o^2 is the PSD spectral intensity, or the scaling factor, a PSD spectrum could be generated for any design earthquake based on this set of scaling curves and the four standard mean and mean plus one standard deviation NPSD spectra.

55. In the final analyses, close relationships do exist among the three parameters, duration, average acceleration, and peak ground acceleration. Duration is inversely proportional to the square of the average acceleration (average power). The latter has an approximate linear relation with the peak ground acceleration. It is apparent that duration has a large effect on the average acceleration or PSD spectral intensity λ_o^2, i.e., an engineering intensity scale. It is also the scaling factor for the normalized standard PSD spectrum. However, the average acceleration is a relative value that varies with duration; it is a scaling factor of the NPSD curve. It might be useful to take the Arias intensity I_o as a standard earthquake intensity scale. The Arias value includes the total duration and the average acceleration.

Conclusions

56. The statistical analysis of 421 accelerograms shows clear differences in spectral shapes for different soil and geological conditions. Within the high-frequency range of 2.5 to 10 Hz, the spectrum

for the rock sites contains the highest energy or intensity; the spectrum of the stiff soil sites is slightly lower than for the rock sites; and the spectra of the soft clay and sand sites and the deep cohesionless soil sites are lower still and almost the same. However, in the low-frequency range of 0 to 2.5 Hz, the reverse exists: the soft sites indicate the highest energy, the deep cohesionless soil sites are next, the stiff soil sites are third, and finally, the rock sites. Generally, the spectra of rock sites and stiff soil sites of similar characteristics can be classified together as hard sites; the other two site types can be classified together as soft sites.

57. The site dependence of NPSD spectra have been established by statistical analysis as expected. The most significant finding of the study is the approximate linear correlation of the PGA (a_{max}) and average acceleration (λ_o). Since λ_o^2 is the area under the PSD curve, therefore λ_o^2 can be used as a scaling factor for NPSD spectra. If a_{max} is given, λ_o can be found from the correlation curves of a_{max} and λ_o. The standard NPSD spectrum can be amplified by λ_o^2 to become a design PSD spectrum.

58. The comparison of the attenuation curves of the PGA and the average acceleration versus distance of the San Fernando earthquake of 9 February 1971 showed that the attenuation rate of the average acceleration is less than the PGA and approximately linear on a log scale.

Recommendations

59. Further developments in the following three areas are needed:

- a. Generation of accelerograms based on the design PSD spectrum.
- b. Relationships between the PSD spectrum and the response spectrum.
- c. A new earthquake engineering intensity scale based on average acceleration or average power of strong-motion duration.

REFERENCES

Arnold, P. 1975. "The Influence of Site Azimuth and Local Soil Conditions on Earthquake Ground Motion Spectra," M.S. thesis, Massachusetts Institute of Technology, Cambridge, Mass.

Arnold, P., and Vanmarcke, E. H. 1977. "Ground Motion Spectral Content: The Influence of Local Soil Conditions and Site Azimuth," Proceedings, Sixth World Conference on Earthquake Engineering, New Delhi, India, Vol 2, pp 113-118.

Bendat, J. S., and Piersol, A. G. 1971. Random Data, Analysis and Measurement Procedures, Wiley-Interscience, New York.

Blackman, R. B., and Tukey, J. W. 1958. The Measurement of Power Spectral, Dover Publications, Inc., New York.

Bolt, B. A. 1978. "The Local Magnitude M_L of the Keon County Earthquake of July 21, 1952, Large Creep Events on Imperial Fault, California," Bulletin, Seismological Society of America, Vol 68, No. 2, pp 513-515.

Berrill, J. B. 1977. "Site Effects During the San Fernando, California, Earthquake," Proceedings, Sixth World Conference on Earthquake Engineering, New Delhi, India, Vol 2, pp 101-106.

California Institute of Technology. 1971-1975. "Strong-Motion Earthquake Accelerograms; Corrected Accelerograms and Integrated Ground Velocities and Displacements," Vol 2, Parts A-N, Earthquake Engineering Research Laboratory, Pasadena, Calif.

Chang, F. K. 1978 (Apr). "State-of-the-Art for Assessing Earthquake Hazards in the United States; Catalogue of Strong-Motion Earthquake Records, Volume I, Western United States, 1933-1971," Miscellaneous Paper S-73-1, Report 9, U. S. Army Engineer Waterways Experiment Station, CE, Vicksburg, Miss.

Chang, F. K., and Krinitzsky, E. L. 1977 (Dec). "State-of-the-Art for Assessing Earthquake Hazards in the United States; Duration, Spectral Content, and Predominant Period of Strong Motion Earthquake Records from Western United States," Miscellaneous Paper S-73-1, Report 8, U. S. Army Engineer Waterways Experiment Station, CE, Vicksburg, Miss.

Duke, C. M., and Hradilek, P. J. 1977. "Spectral Analysis of Site Effects in the San Fernando Earthquake," Proceedings, Sixth World Conference on Earthquake Engineering, New Delhi, India, Vol 2, pp 680-690.

Hsu, H. P. 1967. Outline of Fourier Analysis, Simon and Schuster, Inc., New York.

Hudson, D. E. 1972. "Local Distributions of Strong Earthquake Ground Shaking," Bulletin, Seismological Society of America, Vol 62, No. 6, pp 1765-1786.

Hudson, D. E., and Udwadia, F. E. 1974. "Local Distributions of Strong Earthquake Ground Motions," Proceedings, Fifth World Conference on Earthquake Engineering, Rome, Italy, Vol 1, pp 691-700.

Kiremidjian, A. S., and Shah, C. H. 1978. "Probabilistic Site-Dependent Response Spectra," Report No. 29, John A. Blume Earthquake Engineering Center, Department of Civil Engineering, Stanford, University, Stanford, Calif.

McCann, M. W., Jr., and Shah, C. H. 1979. "Determining Strong-Motion Duration of Earthquakes," Bulletin, Seismological Society of America, Vol 69, No. 4, pp 1253-1266.

Nuttli, O. W., Bollinger, G. A., and Griffiths, D. N. 1979. "On the Relation Between Modified Mercalli Intensity and Body-Wave Magnitude," Bulletin, Seismological Society of America, Vol 69, No. 3, pp 893-910.

Pereira, J., Oliverira, C. S., and Duarte, R. T. 1977. "Direct and Indirect Conversion from Power Spectra to Response Spectra," Proceedings, Sixth World Conference on Earthquake Engineering, New Delhi, India, Vol 2, pp 279-284.

Ravana, A. 1965. "Spectral Analysis of Seismic Actions," Proceedings, Third World Conference on Earthquake Engineering, New Zealand, Vol 1, pp 195-204.

Seed, H. B., and Idriss, I. M. 1971. "Influence of Soil Conditions on Building Damage Potential During Earthquakes," Journal, Structural Division, American Society of Civil Engineers, Vol 97, No. ST2, Proceedings Paper 7909, pp 639-663.

Seed, H. B., Ugas, C., and Lysmer, J. 1976. "Site-Dependent Spectra for Earthquake-Resistant Design," Bulletin, Seismological Society of America, Vol 66, pp 221-244.

Shannon and Wilson, Inc., and Agbabian Associates. 1976. "Site-Dependent Effects of Strong-Motion Accelerogram Stations," Progress Report prepared for U. S. Nuclear Regulatory Commission, Office of Nuclear Regulatory Research, Washington, D. C.

Tezcan, S. S. 1971. "Earthquake Design Formula Considering Local Soil Conditions," Journal, Structural Division, American Society of Civil Engineers, Vol 97, No. ST9, Proceedings Paper 8399, pp 2383-2405.

U. S. Nuclear Regulatory Commission, Office of Nuclear Reactor Regulation. "Design Response Spectral for Nuclear Power Plants," Regulatory Guide No. 1.60, Washington, D. C.

Vanmarcke, E. H. 1979 (Aug). "State-of-the-Art for Assessing Earthquake Hazards in the United States; Representation of Earthquake Ground Motion: Scaled Accelerograms and Equivalent Response Spectra," Miscellaneous Paper S-73-1, Report 14, U. S. Army Engineer Waterways Experiment Station, CE, Vicksburg, Miss.

Vanmarcke, E. H., and Cornell, C. A. 1972. "Seismic Risk and Design Response Spectra," American Society of Civil Engineers Specialty Conference on Safety and Reliability of Metal Structures, Pittsburgh, Pa.

Vanmarcke, E. H., and Gasparini, D. A. 1977. "Simulated Earthquake Ground Motions," Transactions, Fourth International Conference on Structural Mechanics in Reactor Technology, Vol K, pp 1-9.

Vanmarcke, E. H., and Lai, S. S. P. 1977. "Strong-Motion Duration of Earthquakes," Evaluation of Seismic Safety of Buildings, Publication No. R77-16, Report No. 10, Massachusetts Institute of Technology, Cambridge, Mass.

__________. 1980. "Strong-Motion Duration and R.M.S. Amplitude of Earthquake Records, Bulletin, Seismological Society of America, Vol 70, No. 4, pp 1293-1307.

Table 1

Rock Sites

Record No.	Earthquake	Date	Mag.	Approx. Source Dist. km	Dir.	Max. Acc. g	Soil Depth ft	Site	Estimated Duration sec	λ^2 cm^2/sec^4*	λ cm/sec^2**	Conversion Factor†	λ_o^2 cm^2/sec^4††	λ_o cm/sec^2‡	λ_s^2 cm^2/sec^4‡‡	λ_s cm/sec^2§	Modified Mercalli Intensity	I_o 10^4 cm^2/sec^3§§
1-1	Helena	10/31/35	6.0	8.0	NS	0.146	Rock	Federal Building, Helena	5.0	24.688	4.97	32.768	808.976	28.44	707.854	26.605	VII	0.4044
1-2	Helena	10/31/35	6.0	8.0	EW	0.145		Federal Building, Helena	5.0	41.132	6.41	32.768	1,347.813	36.71	1,179.336	34.341	VII	0.6738
1-3	Kern County	07/21/52	7.6	56.0	N21E	0.156		Taft	45.0	205.919	14.35	3.64	749.728	27.38	656.012	25.613	VII	3.3733
1-4	Kern County	07/21/52	7.6	56.0	S69E	0.179		Taft	45.0	223.411	14.95	3.64	813.216	28.52	711.564	26.675	VII	3.6599
1-5	San Francisco	03/22/57	5.25	16.0	N10E	0.083		Golden Gate Park--Sn. Fco.	10.0	9.969	3.16	16.384	163.332	12.78	142.916	11.955	VII	0.1633
1-6	San Francisco	03/22/57	5.25	16.0	S80E	0.105		Golden Gate Park--Sn. Fco.	10.0	17.935	4.23	16.384	293.847	17.14	257.116	16.035	VII	0.2938
1-7	Lytle Creek	09/12/70	5.4	16.1	NS	0.197		Wrightwood, Calif.	4.5	49.047	7.00	36.408	1,785.703	42.26	1,562.528	39.529	VI	0.8035
1-8	Lytle Creek	09/12/70	5.4	16.1	EW	0.142		Wrightwood, Calif.	4.5	51.331	7.16	36.408	1,868.859	43.23	1,635.252	40.438	VI	0.8409
1-9	Parkfield	06/27/66	5.6	7.0	N65W	0.269		Tremblor	17.0	115.376	10.74	9.637	1,111.953	33.35	972.959	31.192	VII	1.8901
1-10	Parkfield	06/27/66	5.6	7.0	S25W	0.347		Tremblor	17.0	170.910	13.07	9.637	1,647.059	40.58	1,441.177	37.963	VII	2.7998
1-11	Borrego Mtn.	04/08/68	6.5	135.8	N33E	0.041		SCE Power Plant-San Onofre	23.0	10.678	3.27	7.123	76.064	8.72	66.556	8.158	V	0.1749
1-12	Borrego Mtn.	04/08/68	6.5	135.8	N57W	0.046		SCE Power Plant-San Onofre	23.0	13.520	3.68	7.123	96.303	9.81	84.265	9.179	V	0.2215
1-13	Lytle Creek	09/12/70	5.4	22.6	S85E	0.071		Cedar Springs, Allen Ranch	4.0	9.057	3.01	40.95	370.994	19.26	324.603	18.017	VI	0.1484
1-14	Lytle Creek	09/12/70	5.4	22.6	S05E	0.056		Cedar Springs, Allen Ranch	4.0	4.744	2.18	40.95	194.267	13.94	169.983	13.038	VI	0.0777
1-15	San Fernando	02/09/71	6.6	37.0	NS	0.089		Cal Tech Seismological Lab.	50.0	40.390	6.36	3.277	132.358	11.50	115.806	10.761	VII	0.6617
1-16				37.0	EW	0.192		Cal Tech Seismological Lab.	50.0	128.151	11.32	3.277	419.951	20.49	367.434	19.168	VII	2.0994
1-17				30.0	S08E	0.217		Sante Felicia Dam (Outlet)	35.0	99.257	9.96	4.681	464.622	21.55	406.544	20.163	VI	1.6260
1-18				30.0	S82W	0.202		Santa Felicia Dam (Outlet)	35.0	96.616	9.83	4.681	452.259	21.27	395.726	19.893	VI	1.5828
1-19				29.8	S69E	0.171		Lake Hughes Station No. 4	16.0	66.981	8.18	10.240	685.885	26.19	600.149	24.498	VI	1.0973
1-20				29.8	S21W	0.146		Lake Hughes Station No. 4	16.0	63.398	7.96	10.240	649.195	25.48	568.046	23.834	VI	1.0386
1-21				3.0	S14W	1.170		Pacoima Dam	13.0	3053.318	55.26	12.603	38,480.966	196.17	33,670.846	183.496	X	50.0194
1-22				3.0	N76W	1.075		Pacoima Dam	13.0	2775.606	52.68	12.603	36,082.378	189.95	31,572.518	177.686	X	45.4699
1-23				45.2	N03E	0.140		Santa Anita Dam	15.0	90.942	9.54	10.923	993.359	31.52	869.189	29.482	VI	1.4898
1-24				45.2	N87W	0.169		Santa Anita Dam	15.0	94.671	9.73	10.923	1,034.091	32.16	904.829	30.080	VI	1.5509
1-25				21.0	N21E	0.367		Lake Hughes Station No. 12	20.0	327.267	18.09	8.192	2,680.971	51.78	2,345.849	48.434	VI	5.3613
1-26				21.0	N69W	0.287		Lake Hughes Station No. 12	20.0	269.543	16.42	8.192	2,208.096	46.99	1,932.084	43.955	VI	4.4156
1-27				24.0	N00E	0.167		3838 Lankershim Blvd.	20.0	69.504	8.34	8.192	569.376	23.86	498.205	22.321	VII	1.1386
1-28				24.0	S90W	0.151		3838 Lankershim Blvd.	20.0	110.048	10.49	8.192	901.513	30.03	788.824	28.086	VII	1.8028
1-29				31.0	S00W	0.180		Griffith Park Observatory	20.0	133.335	11.55	8.192	1,092.280	33.05	955.745	30.915	VII	2.1843
1-30				31.0	S90W	0.171		Griffith Park Observatory	20.0	187.356	13.69	8.192	1,534.320	39.18	1,342.968	36.646	VII	3.0693
1-31				32.3	N21E	0.148		Lake Hughes Station No. 1	22.0	97.715	9.89	7.447	727.710	26.98	636.746	25.234	VI	1.6008
1-32				32.3	S69E	0.111		Lake Hughes Station No. 1	22.0	71.916	8.48	7.447	535.558	23.14	468.614	21.647	VI	1.1781
1-33				29.6	S21E	0.122		Lake Hughes Station No. 9	14.0	36.854	6.07	11.703	431.247	20.77	377.385	19.426	VI	0.6037
1-34				29.6	N69W	0.111		Lake Hughes Station No. 9	14.0	27.697	5.26	11.703	324.138	18.00	283.621	16.841	VI	0.4537
1-35				66.3	N55E	0.071		Puddingstone Res., San Dimas	10.0	18.618	4.31	16.384	305.037	17.46	266.907	16.337	V	0.3050
1-36				66.3	N35W	0.054		Puddingstone Res., San Dimas	10.0	15.149	3.89	16.384	248.201	15.75	217.176	14.755	V	0.2482
1-37				35.3	N56E	0.066		Fairmont Reservoir	15.0	15.750	3.97	10.922	172.021	13.12	150.519	12.268	VI	0.2580
1-38				35.3	N34W	0.099		Fairmont Reservoir	15.0	21.873	4.68	10.922	238.897	15.46	209.035	14.458	VI	0.3583
1-39				140.4	N33W	0.012		SCE Power Plant-San Onofre	15.0	1.975	1.41	10.922	21.572	4.64	18.876	4.345	V	0.0324
1-40				140.4	N57W	0.016		SCE Power Plant-San Onofre	15.0	2.153	1.47	10.922	23.515	4.85	20.575	4.536	V	0.0353
1-41				69.7	N00E	0.025		Fort Tejon, Tejon	6.0	2.048	1.43	27.306	55.924	7.48	48.933	6.995	V	0.0336
1-42				69.7	N90E	0.021		Fort Tejon, Tejon	6.0	2.434	1.56	27.306	66.463	8.15	58.155	7.626	V	0.0399
1-43				71.9	N65W	0.043		Wrightwood, Calif.	15.0	9.866	3.14	10.922	107.756	10.38	94.281	9.710	V	0.1616
1-44				71.9	N25E	0.057		Wrightwood, Calif.	15.0	14.234	3.77	10.922	155.464	12.47	136.031	11.663	V	0.2332
1-45				71.9	N65W	0.044		Wrightwood, Calif.	15.0	11.445	3.38	10.922	125.002	11.18	109.377	10.458	V	0.1875
1-46				71.9	N25E	0.058		Wrightwood, Calif.	15.0	15.104	3.89	10.922	164.966	12.84	144.345	12.014	V	0.2474
1-47	Oroville	08/01/75	5.7	14.4	N37E	0.093		Oroville Dam, Seis. Station	12.18	14.440	3.80	1.341	193.629	13.92	169.425	13.016	VI	0.2366
1-48	Oroville	08/01/75	5.7	14.4	N53E	0.083		Oroville Dam, Seis. Station	12.22	16.392	4.05	1.336	219.079	14.80	191.694	13.845	VI	0.2685

(Continued)

* λ^2: base average power = $I_o/163.82$, area under PSD curve for the extended record of 163.82 sec.

** λ: base average acceleration (cm/sec^2) = $(I_o/163.82)^{1/2}$.

† Conversion factor: ratio of 163.82 sec to the arbitrarily selected duration, or record length.

†† λ_o^2: raw average power or spectral intensity, area under the raw PSD curve of the actual/arbitrarily selected duration, cm^2/sec^4.

‡ λ_o: raw average acceleration, cm/sec^2.

‡‡ λ_s^2: corrected average power = $\lambda_o^2 \times 0.875$, cm^2/sec^4.

§ λ_s: corrected average acceleration, cm/sec^2.

§§ I_o: total (Arias) intensity or total energy = $\lambda^2 \times 163.82$ sec, cm^2/sec^3.

Table 1 (Concluded)

Record No.	Earthquake	Date	Mag.	Approx. Source Dist. km	Dir.	Max. Acc. g	Soil Depth ft	Site	Estimated Duration sec	λ^2 cm^2/sec^4*	λ cm/sec^2**	Conversion Factor†	λ_o^2 cm^2/sec^4††	λ_o cm/sec^2‡	λ_s^2 cm^2/sec^4‡‡	λ_s cm/sec^2§	Modified Mercalli Intensity	I_o 10^4 cm^2/sec^3§§
1-49	Gazli, USSR	05/17/76	6.6	22.0	NS	0.574	Rock	Karakyr Point	13.44	1320.975	36.35	12.156	16,057.460	126.72	14,050.278	118.534	IX-X	21.6402
1-50	Gazli, USSR	05/17/76	6.6	22.0	EW	0.689		Karakyr Point	13.02	1552.056	39.40	12.546	19,473.154	139.55	17,039.010	130.533	IX-X	25.4258
1-51	Koyna, India	12/10/67	6.5	5.0	T	0.457		Koyna Dam	11.10	424.199	20.60	14.760	6,261.330	79.13	5,478.664	74.018	VIII	6.9492
1-52	Koyna, India	12/10/67	6.5	5.0	L	0.632		Koyna Dam	10.66	546.646	23.38	15.369	8,401.402	91.66	7,351.227	85.739	VIII	8.9551
1-53	Japan	09/14/70	6.2	25.6	NS	0.025		Ofunado Bochi-S	15.00	1.314	1.15	10.909	14.339	3.79	12.547	3.542	VII	0.0215
1-54	Japan	09/14/70	6.2	25.6	EW	0.067		Ofunado Bochi-S	15.00	5.153	2.27	10.909	56.216	7.49	49.189	7.013	VII	0.0844
1-55	Japan	11/19/73	6.4	46.1	NS	0.037		Ofunado Bochi-S	28.00	3.084	1.76	5.848	18.034	4.25	15.780	3.972	VI	0.0505
1-56	Japan	11/19/73	6.4	46.1	EW	0.062		Ofunado Bochi-S	28.00	8.391	2.90	5.848	49.070	7.00	42.936	6.552	VI	0.1374
				Mean		0.196							Mean	33.47	Mean	31.308		
				S.D.		0.234							S. D.	40.77	S. D.	38.138		
				VAR.		0.054							VAR.	1632.67	VAR.	1428.541		

Table 2

Stiff Soil Sites

Record No.	Earthquake	Date	Mag.	Approx. Source Dist. km	Dir.	Max. Acc. g	Soil Depth ft	Site	Estimated Duration sec	λ^2 cm^2/sec^4*	λ cm/sec^2**	Conversion Factor†	λ_o^2 cm^2/sec^4††	λ_o cm/sec^2‡	λ_s^2 cm^2/sec^4‡‡	λ_s cm/sec^2§	Modified Mercalli Intensity	I_o 10^4 cm^2/sec^3§§
2-1	Lower Calif.	12/30/34	6.5	62.8	NS	0.160	100	El Centro	25.00	199.782	14.13	6.554	1309.291	36.184	1145.630	33.847	VI	3.2728
2-2	Lower Calif.	12/30/34	6.5	62.8	EW	0.182	100	El Centro	25.00	229.230	15.14	6.554	1502.373	38.760	1314.577	36.257	VI	3.7552
2-3	El Centro	05/18/40	6.6	18.5	NS	0.348	100	El Centro	30.00	663.202	25.75	5.461	3621.967	60.183	3169.221	56.296	VIII	10.8646
2-4	El Centro	05/18/40	6.6	18.5	EW	0.214	100	El Centro	30.00	482.990	21.98	5.461	2637.608	51.358	2307.907	48.041	VIII	7.9123
2-5	San Francisco	03/22/57	5.25	18.7	N09W	0.043	140	Alexander Bldg.-S.F.	15.00	6.096	2.47	10.923	66.584	8.160	58.261	7.633	VII	0.0999
2-6	San Francisco	03/22/57	5.25	18.7	N81E	0.046	140	Alexander Bldg.-S.F.	15.00	5.287	2.30	10.923	54.419	7.377	47.617	6.900	VII	0.0866
2-7	San Francisco	03/22/57	5.25	18.3	S09E	0.085	200	State Bldg.-S. F.	15.00	19.941	4.46	10.923	217.815	14.758	190.588	13.805	VII	0.3267
2-8	San Francisco	03/22/57	5.25	18.3	S81W	0.056	200	State Bldg.-S. F.	15.00	12.730	3.57	10.923	139.049	11.792	121.668	11.030	VII	0.2085
2-9	Sendai	04/30/62	6.0	55.0	NS	0.059	15	Tohoku Daigaku Kogakubu	13.98	14.153	3.76	1.168	165.411	12.861	144.735	12.030	↓	0.2319
2-10	Sendai	04/30/62	6.0	55.0	EW	0.048	15	Tohoku Daigaku Kogakubu	14.18	10.919	3.30	1.152	125.819	11.217	110.092	10.492	↓	0.1789
2-11	Kanto	05/08/63	Ukn.	66.4	NS	0.056	70	Genken Pr. Hall - Kanto	13.98	17.046	4.13	1.168	199.225	14.115	174.322	13.203	↓	0.2792
2-12	Kanto	05/08/63	Ukn.	66.4	EW	0.059	70	Genken Pr. Hall - Kanto	13.98	23.349	4.83	1.168	272.898	16.519	238.786	15.453	↓	0.3825
2-13	Kanto	02/05/64	Ukn.	66.4	NS	0.046	50	Genken Jrr-3 - Kanto	9.98	4.949	2.22	1.635	80.937	8.996	70.820	8.415	↓	0.0811
2-14	Kanto	02/05/64	Ukn.	66.4	EW	0.036	50	Genken Jrr-3 - Kanto	9.98	4.445	2.11	1.635	72.708	8.527	63.619	7.976	↓	0.0728
2-15	Parkfield	06/27/66	5.6	0.1	N65E	0.489	150	Cholame Shandon No. 2	15.00	668.831	26.25	10.923	7523.871	86.740	6583.387	81.138	VII	10.9486
2-16	Parkfield	06/27/66	5.6	5.0	N05W	0.354	100	Cholame Shandon No. 5	20.00	229.100	15.14	8.192	1876.787	43.322	1642.189	40.524	VI	3.7531
2-17	Parkfield	06/27/66	5.6	5.0	N85E	0.434	100	Cholame Shandon No. 5	20.00	317.697	17.82	8.192	2602.574	51.015	2277.252	47.720	VI	5.2045
2-18	San Fernando	02/09/71	6.6	31.4	N21E	0.315	60	Castaic Old Ridge Route	25.00	260.038	16.13	6.554	1704.185	41.282	1491.162	33.615	VI	4.2599
2-19	↓	↓	↓	31.4	N69W	0.270	60	Castaic Old Ridge Route	25.00	370.783	19.26	6.554	2430.124	49.296	2126.359	46.112	VI	6.0742
2-20	↓	↓	↓	39.3	S00W	0.170	200	Hollywood Storage P.E. Lot-L	22.00	141.203	11.88	7.447	1051.538	32.427	920.096	30.333	VII	2.3132
2-21	↓	↓	↓	39.3	N90E	0.211	200	Hollywood Storage P.E. Lot-L	22.00	234.751	15.32	7.447	1748.191	41.811	1529.667	39.111	↓	3.8457
2-22	↓	↓	↓	42.1	N00E	0.136	45	3470 Wilshire Blvd. - LA	23.00	132.601	11.52	7.123	944.580	30.734	826.507	28.749	↓	2.1723
2-23	↓	↓	↓	42.1	S90W	0.114	45	3470 Wilshire Blvd. - LA	23.00	94.703	9.73	7.123	674.569	25.972	590.248	24.295	↓	1.5514
2-24	↓	↓	↓	42.0	North	0.153	100	3550 Wilshire Blvd. - LA	26.00	116.043	10.77	6.301	731.249	27.042	639.843	25.295	↓	1.9010
2-25	↓	↓	↓	42.0	West	0.129	100	3550 Wilshire Blvd. - LA	26.00	107.931	10.39	6.301	680.073	26.078	595.064	24.394	↓	1.7681
2-26	↓	↓	↓	32.0	N11E	0.225	70	15250 Ventura Blvd. - LA	30.00	340.701	18.46	5.461	1860.568	43.134	1627.997	40.348	↓	5.5814
2-27	↓	↓	↓	32.0	N79W	0.149	70	15250 Ventura Blvd. - LA	30.00	219.440	14.81	5.461	1198.362	34.167	1048.567	32.381	↓	3.5949
2-28	↓	↓	↓	32.0	S12W	0.243	70	14724 Ventura Blvd. - LA	30.00	424.402	20.60	5.461	2317.659	48.142	2027.952	45.033	↓	6.9526
2-29	↓	↓	↓	32.0	N78W	0.197	70	14724 Ventura Blvd. - LA	30.00	268.214	16.38	5.461	1464.716	38.272	1281.627	35.800	↓	4.3939
2-30	↓	↓	↓	42.0	S00W	0.161	40	3407 Sixth Street - LA	20.00	169.569	13.02	8.192	1389.109	34.271	1215.470	34.863	↓	2.7779
2-31	↓	↓	↓	42.0	N90E	0.165	40	3407 Sixth Street - LA	20.00	129.431	11.38	8.192	1060.298	32.562	927.761	30.459	↓	2.1203
2-32	↓	↓	↓	37.3	S00W	0.106		Hollywood Storage, basement	22.00	86.212	9.29	7.447	642.021	25.338	561.768	23.702	↓	1.4123
2-33	↓	↓	↓	37.3	N90E	0.151		Hollywood Storage, basement	22.00	144.000	12.00	7.447	1072.368	32.747	938.322	30.632	↓	2.3590
2-34	↓	↓	↓	41.0	N08E	0.125		6200 Wilshire Blvd. - LA	21.00	109.937	10.49	7.802	857.718	29.287	750.503	27.395	↓	1.8010
2-35	↓	↓	↓	41.0	N82W	0.131		6200 Wilshire Blvd. - LA	21.00	84.990	9.22	7.802	663.092	25.751	580.205	24.087	↓	1.3923
2-36	↓	↓	↓	41.6	S75W	0.083		4680 Wilshire Blvd. - LA	20.00	66.554	8.16	8.192	545.210	23.350	477.059	21.842	↓	1.0903
2-37	↓	↓	↓	41.6	N15E	0.117		4680 Wilshire Blvd. - LA	20.00	85.701	9.26	8.192	702.062	26.496	614.305	24.785	↓	1.4039
2-38	↓	↓	↓	42.0	S00W	0.149		3710 Wilshire Blvd. - LA	20.00	77.957	8.83	8.192	638.624	25.271	558.796	23.639	↓	1.2771
2-39	↓	↓	↓	42.0	S90W	0.159		3710 Wilshire Blvd. - LA	17.00	137.775	11.74	9.637	1327.827	36.439	1161.848	34.086	↓	1.3515
2-40	↓	↓	↓	41.9	N00E	0.109		616 S. Normandie Ave. - LA	18.58	82.502	9.08	8.800	726.034	26.945	635.280	25.205	↓	1.6178
2-41	↓	↓	↓	41.9	S90W	0.114		616 S. Normandie Ave. - LA	18.58	98.754	9.94	8.800	869.055	29.479	760.423	27.576	↓	1.1344
2-42	↓	↓	↓	41.9	South	0.106		3435 Wilshire Blvd. - LA	20.84	69.247	8.32	7.848	543.43	23.311	475.501	21.806	↓	1.1603
2-43	↓	↓	↓	41.9	West	0.127		3435 Wilshire Blvd. - LA	20.84	70.830	8.42	7.848	555.853	23.576	486.371	22.054	↓	0.9609
2-44	↓	↓	↓	42.7	N29E	0.098		2500 Wilshire Blvd. - LA	25.36	58.655	7.66	6.451	378.394	19.452	331.095	18.196	↓	1.0837
2-45	↓	↓	↓	42.7	N61W	0.101		2500 Wilshire Blvd. - LA	25.34	66.152	8.13	6.456	427.095	20.666	373.708	19.331	↓	1.3778
2-46	↓	↓	↓	43.8	N37E	0.088		800 W. First St. - LA	25.00	84.106	9.17	6.554	551.197	23.477	482.297	21.961	↓	1.2805
2-47	↓	↓	↓	43.8	N53W	0.141		800 W. First St. - LA	23.00	78.163	8.84	7.123	556.792	23.596	487.193	22.072	↓	1.1973
2-48	↓	↓	↓	44.4	N50W	0.129		Water and Power Bldg. - LA	18.00	73.089	8.55	9.102	665.272	25.793	582.113	24.127	↓	1.2891
2-49	↓	↓	↓	44.4	S40W	0.173		Water and Power Bldg. - LA	18.00	78.690	8.87	9.102	716.236	26.763	626.707	25.034	↓	

(Continued)

(Sheet 1 of 3)

* λ^2: base average power = $I_o/163.82$, area under PSD curve for the extended record of 163.82 sec.

** λ: base average acceleration (cm/sec^2) = $(I_o/163.82)^{1/2}$.

† Conversion factor: ratio of 163.82 sec to the arbitrarily selected duration, or record length.

†† λ_o^2: raw average power or spectral intensity, area under the raw PSD curve of the actual/arbitrarily selected duration, cm^2/sec^4.

‡ λ_o: raw average acceleration, cm/sec^2.

‡‡ λ_s^2: corrected average power = $\lambda_o^2 \times 0.875$, cm^2/sec^4.

§ λ_s: corrected average acceleration, cm/sec^2.

§§ I_o: total (Arias) intensity or total energy = $\lambda^2 \times 163.82$ sec, cm^2/sec^3.

Table 2 (Continued)

Record No.	Earthquake	Date	Mag.	Approx. Source Dist. km	Dir.	Max. Acc. g	Soil Depth ft	Site	Estimated Duration sec	λ^2 cm^2/sec^4*	λ cm/sec^2**	Conversion Factor†	λ_o^2 cm^2/sec^4††	λ_o cm/sec^2‡	λ_s^2 cm^2/sec^4‡‡	λ_s cm/sec^2§	Modified Mercalli Intensity	I_o 10^4 cm^2/sec^3§§
2-50	San Fernando	02/09/71	6.6	45.0	S62E	0.065		2011 Zonal Ave. - LA	20.00	31.744	5.63	8.192	260.047	16.126	227.541	15.084	VII	0.5200
2-51	San Fernando	02/09/71	6.6	45.0	S28W	0.081		2011 Zonal Ave. - LA	15.00	38.888	6.24	10.923	424.774	20.610	371.677	19.279	↓	0.6371
2-52	San Fernando	02/09/71	6.6	42.0	S00W	0.110		3345 Wilshire Blvd. - LA	18.00	77.428	8.80	9.102	704.767	26.547	616.671	24.833	↓	1.2684
2-53	San Fernando	02/09/71	6.6	42.0	N90E	0.089		3345 Wilshire Blvd. - LA	18.00	59.016	7.68	9.102	537.164	23.177	470.018	21.680	↓	0.9668
2-54	Kern County	07/21/52	7.6	128.0	S00W	0.055	200	Hollywood Storage, Basmt - LA	55.00	37.759	6.14	2.979	112.480	10.606	98.420	9.921	↓	0.6186
2-55	Kern County	07/21/52	7.6	128.0	N90E	0.044	200	Hollywood Storage, Basmt - LA	55.00	39.473	6.28	2.979	117.590	10.844	102.891	10.144	↓	0.6466
2-56	Kern County	07/21/52	7.6	128.0	S00W	0.059	200	Hollywood Storage, P.E. Lot - LA	50.00	38.526	6.21	3.277	126.242	11.236	110.462	10.510	↓	0.6311
2-57	Kern County	07/21/52	7.6	128.0	N90E	0.042	200	Hollywood Storage, P.E. Lot - LA	50.00	38.741	6.22	3.277	126.954	11.267	111.085	10.540	↓	0.6347
2-58	El Alamo	02/09/56	6.8	126.0	S00W	0.033	100	El Centro	50.00	21.421	4.63	3.277	70.192	8.378	61.418	7.837	VI	0.3509
2-59	El Alamo	02/09/56	6.8	126.0	S90W	0.051	100	El Centro	50.00	38.936	6.24	3.277	127.593	11.296	111.644	10.566	VI	0.6378
2-60	San Francisco	03/22/57	5.25	26.7	N26E	0.040		Oakland City Hall, Basmt	15.00	3.626	1.90	10.923	39.605	6.293	34.655	5.880	VI	0.0594
2-61	San Francisco	03/22/57	5.25	26.7	S64E	0.024		Oakland City Hall, Basmt	15.00	2.144	1.46	10.923	23.419	4.839	20.491	4.527	VI	0.0351
2-62	Borrego Mt.	04/08/68	6.5	72.6	S00W	0.130	100	El Centro	37.00	92.149	9.60	4.428	408.046	20.200	357.040	18.895	VI	1.5096
2-63	Borrego Mt.	04/08/68	6.5	72.6	S90W	0.057	100	El Centro	65.00	58.463	7.65	2.521	147.363	12.139	128.942	11.355	VI	0.9577
2-64	Borrego Mt.	04/08/68	6.5	111.7	S00W	0.030		San Diego Light & Power Bldg	46.00	8.369	2.89	3.562	29.808	5.469	26.082	5.107	VI	0.1371
2-65	Borrego Mt.	04/08/68	6.5	111.7	N90E	0.029		San Diego Light & Power Bldg	46.00	11.078	3.33	3.562	39.459	6.282	34.527	5.876	VI	0.1815
2-66	Long Beach	03/10/33	6.3	48.8	N08E	0.133		Vernon CMD Bldg	27.00	82.285	9.07	6.068	499.317	22.345	436.903	20.902	VI	1.3480
2-67	Long Beach	03/10/33	6.3	48.8	S82E	0.154		Vernon CMD Bldg	27.00	68.753	8.29	6.068	417.193	20.425	365.044	19.106	VI	1.1263
2-68	Southern Calif.	10/02/33	5.4	39.5	S00E	0.033	200	Hollywood Storage, Basmt	40.00	3.724	1.93	4.096	15.253	3.906	13.347	3.653	V	0.0610
2-69	Southern Calif.	10/02/33	5.4	39.5	S90E	0.027	200	Hollywood Storage, Basmt	45.00	3.938	1.98	3.641	14.338	3.786	12.545	3.542	V	0.0645
2-70	Wheeler Ridge	01/12/54	5.9	43.0	N21E	0.065		Taft Lincoln School	25.00	14.745	3.84	6.554	96.633	9.830	84.554	9.195	VII	0.2416
2-71	Wheeler Ridge	01/12/54	5.9	43.0	S69E	0.068		Taft Lincoln School	25.00	16.008	4.00	6.554	104.916	10.243	91.802	9.581	VII	0.2622
2-72	Parkfield	06/27/66	5.6	9.1	N50E	0.237		Cholame, Shandon Array No. 8	20.00	107.571	10.37	8.192	881.222	29.685	771.069	27.768	VI	1.7622
2-73	Parkfield	06/27/66	5.6	9.1	N40W	0.275		Cholame, Shandon Array No. 8	14.00	139.979	11.83	8.192	1146.708	33.8631	1003.369	31.676	VI	2.2931
2-74	Parkfield	06/27/66	5.6	37.5	N50E	0.053		Cholame, Shandon Array No. 12	35.00	19.098	4.37	4.681	89.400	9.455	78.225	8.844	VI	0.3129
2-75	Parkfield	06/27/66	5.6	37.5	N40W	0.064		Cholame, Shandon Array No. 12	32.00	22.537	4.75	5.120	115.389	10.742	100.966	10.048	VI	0.3692
2-76	Parkfield	06/27/66	5.6	76.6	N36W	0.014		San Luis Oblispo Rec. Bldg.	16.00	1.168	1.08	10.240	11.960	3.458	10.465	3.335	V	0.0191
2-77	Parkfield	06/27/66	5.6	76.6	S54W	0.012		San Luis Oblispo Rec. Bldg.	15.00	3.422	1.85	10.923	7.821	2.797	6.843	2.616	V	0.0117
2-78	Tokachi Oki	05/16/68	7.9	290.0	NS	0.208	50	Muroran-S (PHRI)#	70.00	375.297	19.37	2.341	878.400	29.638	768.608	27.723	VI	6.1481
2-79	Tokachi Oki	05/16/68	7.9	290.0	EW	0.138	50	Muroran-S (PHRI)	70.00	325.587	18.04	2.341	762.199	27.608	666.924	25.825	VI	5.3338
2-80	Tokachi Oki	05/16/68	7.9	189.1	NS	0.114	35	Miyako-S (PHRI)	113.78	452.629	21.27	1.439	651.737	25.529	570.270	23.880	VI	7.4150
2-81	Tokachi Oki	05/16/68	7.9	189.1	EW	0.098	35	Miyako-S (PHRI)	114.00	322.349	17.95	1.437	463.253	21.523	405.347	20.133	VI	5.2807
2-82	Tokachi Oki	05/16/68	7.4	218.4	NS	0.094	50	Muroran-S (PHRI)	49.00	77.272	8.79	3.344	258.372	16.085	226.076	15.036	V	1.2659
2-83	Tokachi Oki	05/16/68	7.4	218.4	EW	0.074	50	Muroran-S (PHRI)	49.00	64.811	8.05	3.344	216.728	14.722	189.632	13.771	V	1.0617
2-84	Tokachi Oki Yoshin	05/17/68	5.9	156.7	NS	0.037	35	Miyako-S (PHRI)	13.00	6.201	2.55	12.603	78.152	8.840	63.383	8.269	V	0.1016
2-85	Tokachi Oki Yoshin	05/17/68	5.9	156.7	EW	0.041	35	Miyako-S (PHRI)	13.00	6.496	2.55	12.603	81.869	9.048	71.635	8.464	V	0.1064
2-86	Tokachi Oki Yoshin	05/23/68	6.3	77.8	NS	0.051	35	Miyako-S (PHRI)	13.00	15.203	3.90	12.603	191.604	13.842	167.654	12.948	V	0.2491
2-87	Tokachi Oki Yoshin	05/23/68	6.3	77.8	EW	0.052	35	Miyako-S (PHRI)	13.00	12.651	3.56	12.603	159.440	12.627	139.510	11.811	V	0.2072
2-88	Tokachi Oki	06/12/68	7.3	116.9	NS	0.112	35	Miyako-S (PHRI)	41.50	208.991	14.46	3.948	825.086	28.724	727.950	26.869	VI	3.4237
2-89	Tokachi Oki	06/12/68	7.3	116.9	EW	0.099	35	Miyako-S (PHRI)	41.50	177.293	13.32	3.948	699.953	26.457	612.458	24.748	VI	2.9044
2-90		06/13/68	5.7	128.6	NS	0.047	35	Miyako-S (PHRI)	13.00	9.769	3.13	12.603	123.118	11.096	107.729	10.379	II-III	0.1600
2-91		06/13/68	5.7	128.6	EW	0.035	35	Miyako-S (PHRI)	13.00	9.188	3.03	12.603	115.796	10.761	101.322	10.066	II-III	0.1505
2-92	Saitamaken Chubu	07/01/68	6.1	116.4	NS	0.031	80	Kashima-S (PHRI)	20.00	9.956	3.16	8.192	81.559	9.031	71.365	8.447	(IV)	0.1631
2-93	Saitamaken Chubu	07/01/68	6.1	116.4	EW	0.045	80	Kashima-S (PHRI)	20.00	10.738	3.28	8.192	86.966	9.326	76.970	8.773	IV	0.1759
2-94	Tokachi Oki	09/21/68	6.9	158.0	NS	0.047	50	Muroran-S (PHRI)	28.00	18.587	4.31	5.851	108.760	10.429	95.165	9.755	V	0.3045
2-95	Toakchi Oki	09/21/68	6.9	158.0	EW	0.041	50	Muroran-S (PHRI)	28.00	15.206	3.90	5.851	88.970	9.432	77.849	8.823	V	0.2491

(Continued)

PHRI = Port and Harbour Research Institute, Japan, contributed these data.

Table 2 (Concluded)

Record No.	Earthquake	Date	Mag.	Approx. Source Dist. km	Dir.	Max. Acc. g	Soil Depth ft	Site	Estimated Duration sec	λ^2 cm^2/sec^4*	λ cm/sec^2**	Conversion Factor†	λ_o^2 cm^2/sec^4††	λ_o cm/sec^2‡	λ_s^2 cm^2/sec^4‡‡	λ_s cm/sec^2§	Modified Mercalli Intensity	I_o 10^4 cm^2/sec^3§§
2-96	Tokachi Oki Yoshin	11/14/68	6.0	77.8	NS	0.053	35	Miyako-S (PHRI)♯	15.00	5.112	2.26	21.845	111.673	10.567	97.714	9.885	V	0.0837
2-97	Tokachi Oki Yoshin	11/14/68	6.0	77.8	EW	0.033	35	Miyako-S (PHRI)	15.00	3.028	1.74	21.845	66.147	8.133	57.878	7.608	V	0.0496
2-98	Kashimanada	05/13/69	5.2	53.4	NS	0.016	80	Kashima-S (PHRI)	13.00	0.681	0.83	12.603	8.583	2.930	7.509	2.740	(IV)	0.0111
2-99	Kashimanada	05/13/69	5.2	53.4	EW	0.024	80	Kashima-S (PHRI)	13.00	0.869	0.93	12.603	10.952	3.309	9.583	3.096	(IV)	0.0142
2-100	Gihuken Chubu	09/09/69	6.6	105.9	NS	0.023	>100	Kanazawa-S (PHRI)	20.00	4.767	2.18	8.192	39.051	6.249	34.169	5.845	(VI)	0.0781
2-101	Gihuken Chubu	09/09/69	6.6	105.9	EW	0.021	>100	Kanazawa-S (PHRI)	20.00	5.652	2.38	8.192	46.301	6.804	40.513	6.365	(VI)	0.0926
2-102		01/21/70	6.7	191.6	NS	0.034	50	Muroran-S (PHRI)	35.00	16.781	4.10	4.681	78.552	8.863	68.733	8.290	VI	0.2749
2-103		01/21/70	6.7	191.6	EW	0.033	50	Muroran-S (PHRI)	35.00	10.271	3.20	4.681	48.070	6.934	42.069	6.486	VI	0.1683
2-104		04/01/70	5.8	32.0	NS	0.117	35	Miyako-S (PHRI)	20.00	39.757	6.31	8.192	325.689	18.047	284.978	16.881	VI	0.6513
2-105		04/01/70	5.8	32.0	EW	0.091	35	Miyako-S (PHRI)	20.00	32.875	5.73	8.192	269.372	16.413	235.648	15.351	VI	0.5386
2-106		09/14/70	6.2	81.2	NS	0.040	35	Miyako-S (PHRI)	15.00	14.246	3.77	10.923	155.609	12.474	136.158	11.668	VI	0.2334
2-107		09/14/70	6.2	81.2	EW	0.038	35	Miyako-S (PHRI)	15.00	10.997	3.32	10.923	120.120	10.960	105.105	10.252	VI	0.1802
2-108		06/13/71	5.3	41.8	NS	0.042	80	Kashima-S (PHRI)	16.50	5.689	2.39	9.929	56.490	7.516	49.428	7.030	(V)	0.0932
2-109		06/13/71	5.3	41.8	EW	0.055	80	Kashima-S (PHRI)	16.00	5.868	2.42	10.240	60.088	7.577	52.577	7.251	(V)	0.0961
2-110		08/02/71	7.0	253.1	NS	0.025	50	Muroran-S (PHRI)	21.00	5.615	2.37	7.802	43.808	6.618	38.332	6.191	VI	0.0920
2-111		08/02/71	7.0	253.1	EW	0.026	50	Muroran-S (PHRI)	21.00	9.651	3.11	7.802	75.297	8.677	65.885	8.117	VI	0.1581
2-112		10/11/71	5.2	17.3	NS	0.035	80	Kashima-S (PHRI)	20.00	4.935	2.22	8.192	40.427	6.362	35.374	5.947	VI	0.0808
2-113		10/11/71	5.2	17.3	EW	0.130	80	Kashima-S (PHRI)	20.00	15.189	3.90	8.192	124.428	11.155	108.875	10.434	VI	0.2488
2-114		02/29/72	7.0	258.2	NS	0.023		Koken-S (PHRI)	12.00	3.453	1.86	13.653	47.145	6.866	41.252	6.423	(V)	0.0566
2-115		02/29/72	7.0	258.2	EW	0.015		Koken-S (PHRI)	12.00	2.053	1.43	13.653	28.029	5.294	24.526	4.952	(V)	0.0336
2-116		03/20/72	6.4	153.0	NS	0.046	35	Miyako-S (PHRI)	39.00	19.156	4.38	4.201	80.475	8.971	70.415	8.391	V	0.3138
2-117		03/20/72	6.4	153.0	EW	0.048	35	Miyako-S (PHRI)	39.00	16.692	4.08	4.201	70.123	8.374	61.358	7.833	V	0.2734
2-118		03/20/72	6.4	162.1	NS	0.024	50	Muroran-S (PHRI)	8.50	1.978	1.41	19.275	38.126	6.175	33.361	5.776	IV	0.0324
2-119		03/20/72	6.4	162.1	EW	0.019	50	Muroran-S (PHRI)	8.50	0.952	0.98	19.275	18.349	4.283	16.056	4.007	IV	0.0156
2-120		06/17/73	7.4	416.6	NS	0.019	50	Muroran-S (PHRI)	30.00	5.739	2.40	5.458	31.326	5.597	27.411	5.235	V	0.0940
2-121		06/17/73	7.4	416.6	EW	0.023	50	Muroran-S (PHRI)	30.00	6.719	2.59	5.458	36.676	6.056	32.091	5.665	V	0.1101
2-122		11/09/74	5.8	74.9	NS	0.039	50	Muroran-S (PHRI)	24.00	11.691	2.42	6.827	79.810	9.934	69.834	8.356	(VI)	0.1915
2-123		11/09/74	5.8	74.9	EW	0.045	50	Muroran-S (PHRI)	24.00	22.998	4.79	6.827	157.007	12.530	137.381	11.721	(VI)	0.3767
2-124		01/23/75	6.1	64.0	NS	0.018	66	Oita-S (PHRI)	8.00	2.333	1.53	20.480	47.780	6.912	41.807	6.466	(V)	0.0382
2-125		01/23/75	6.1	64.0	EW	0.022	66	Oita-S (PHRI)	8.00	1.932	1.39	20.480	39.567	6.290	34.621	5.884	(V)	0.0316
2-126		04/21/75	6.4	42.5	NS	0.044	66	Oita-S (PHRI)	9.00	10.731	3.28	18.204	195.352	13.977	170.933	13.074	(VI)	0.1758
2-127		04/21/75	6.4	42.4	EW	0.072	66	Oita-S (PHRI)	9.00	13.351	3.65	18.204	243.042	15.589	212.661	14.583	(VI)	0.2187
2-128	Ibaragiken	11/19/70	6.0	56.0	NS	0.083	80	Kashima-S (PHRI)	16.00	14.518	3.81	10.240	145.592	12.066	127.393	11.286	(VI)	0.2378
2-129	Oki	11/19/70	6.0	56.0	EW	0.056	80	Kashima-S (PHRI)	16.00	9.493	3.08	10.240	97.208	9.859	85.057	9.222	(VI)	0.1555
2-130	Takachi Oki	05/16/68	7.4	226.6	NS	0.091	35	Miyako-S (PHRI)	40.00	74.747	8.65	4.096	306.164	17.498	267.893	16.368	VI	1.2245
2-131	Takachi Oki	05/16/68	7.4	226.6	EW	0.076	35	Miyako-S (PHRI)	40.00	52.620	7.25	4.096	215.531	14.681	188.590	13.733	VI	0.8620
					Mean	0.049							Mean	18.651	Mean	17.446		
					S. D.	0.369							S. D.	13.777	S. D.	12.791		
					VAR.	0.137							VAR.	188.352	VAR.	162.369		

♯ PHRI = Port and Harbour Research Institute, Japan, contributed these data.

Table 3

Deep Cohesionless Soil Sites

Record No.	Earthquake	Date	Mag.	Approx. Source Dist. km	Dir.	Max. Acc. g	Soil Depth ft	Site	Estimated Duration sec	λ^2 cm^2/sec^4*	λ cm/sec^2**	Conversion Factor†	λ_o^2 cm^2/sec^4††	λ_o cm/sec^2‡	λ_s^2 cm^2/sec^4‡‡	λ_s cm/sec^2§	Modified Mercalli Intensity	I_o 10^4 cm^2/sec^3§§
3-1	Western Wash.	04/13/49	7.1	72.0	S04E	0.165	420	Hwy. Test Lab. - Olympia	45.00	279.368	16.71	3.641	1017.148	31.893	890.004	29.83	VIII	4.5766
3-2	Western Wash.	04/13/49	7.1	72.0	S86W	0.280	420	Hwy. Test Lab. - Olympia	45.00	422.246	20.55	3.641	1537.398	39.209	1345.223	36.68	VIII	6.9172
3-3	Kern County	07/21/52	7.6	127.0	NS	0.047	350	Cal Tech Athenaeum - Pasadena	77.26	24.803	4.98	2.120	52.577	7.251	46.005	6.78	VII	0.4063
3-4	Kern County	07/21/52	7.6	127.0	EW	0.053	350	Cal Tech Athenaeum - Pasadena	77.26	43.516	6.60	2.117	92.126	9.598	80.610	8.98	VII	0.7129
3-5	Eureka	12/21/54	6.5	28.8	N11W	0.168	250	Federal Bldg. - Eureka	77.96	128.513	11.34	2.101	269.977	16.431	236.229	15.37	VII	2.1053
3-6	Eureka	12/21/54	6.5	28.8	N79E	0.257	250	Federal Bldg. - Eureka	79.56	269.136	16.40	2.058	554.028	23.538	484.774	22.02	VII	4.4090
3-7	Eureka	12/21/54	6.5	43.4	N44E	0.159	500	City Hall - Ferndale	42.30	208.100	14.43	3.870	805.369	28.379	704.698	26.55	VII	3.4091
3-8	Eureka	12/21/54	6.5	43.4	N46W	0.201	500	City Hall - Ferndale	42.38	143.470	11.98	3.863	554.197	23.541	484.922	22.02	VII	2.3503
3-9	Tokyo	09/30/56	6.7	53.0	NS	0.049	1000	Tetsudo Kaikan - Tokyo 103	14.58	3.046	1.75	11.208	34.135	5.843	29.868	5.46	VII	0.0287
3-10	Tokyo	09/30/56	6.7	53.0	EW	0.046	1000	Tetsudo Kaikan - Tokyo 103	14.18	7.397	2.72	11.523	85.234	9.232	74.579	8.64	VII	0.0446
3-11	Puget-Sound	04/29/65	6.5	85.6	S04E	0.137	420	Hwy. Test Lab. - Olympia	81.94	107.355	10.36	2.001	214.840	14.657	187.985	13.71	VII	0.1697
3-12	Puget-Sound	04/29/65	6.5	85.6	S86W	0.198	420	Hwy. Test Lab. - Olympia	81.94	160.184	12.66	1.999	320.173	17.893	280.151	16.74	VII	0.2074
3-13	Ferndale	12/10/67	5.6	34.5	N46W	0.105	500	City Hall - Ferndale	92.96	27.830	5.28	1.762	49.036	7.003	42.906	6.55	VI	0.0865
3-14	Ferndale	12/10/67	5.6	34.5	S44W	0.237	500	City Hall - Ferndale	93.04	39.611	6.29	1.760	69.732	8.351	61.015	7.81	VI	0.1030
3-15	Tokachi Oki	05/16/68	7.9	188.0	NS	0.229	1250	Hachinohe Harbor	35.98	343.111	18.52	4.549	1560.859	39.508	1365.752	36.96	VIII	0.3034
3-16	Tokachi Oki	05/16/68	7.9	188.0	EW	0.186	1250	Hachinohe Harbor	35.98	394.004	19.85	4.549	1792.379	42.336	1568.332	39.60	VIII	0.3252
3-17	San Fernando	02/09/71	6.6	25.9	NS	0.255	550	8244 Orion Blvd. - Los Angeles	45.00	484.058	22.00	3.641	1762.401	41.981	1542.101	39.27	VII	0.3604
3-18				25.9	EW	0.134	550	8244 Orion Blvd. - Los Angeles	45.00	255.708	15.99	3.641	931.033	30.513	814.654	28.54	VII	0.2619
3-19				37.2	NS	0.117	550	Van Owen St. - Los Angeles	98.62	209.692	14.48	1.661	348.269	18.662	304.735	17.46	VII	0.2372
3-20				37.2	EW	0.110	550	Van Owen St. - Los Angeles	98.64	196.584	14.02	1.661	326.432	18.067	285.628	16.90	VII	0.2297
3-21				41.8	NS	0.095	350	Cal Tech Athenaeum - Pasadena	28.56	47.485	6.89	5.729	272.059	16.494	238.052	15.43	VII	0.1129
3-22				41.8	EW	0.109	350	Cal Tech Athenaeum - Pasadena	28.58	80.255	8.96	5.725	459.492	21.436	402.055	20.05	VII	0.1468
3-23				41.8	NS	0.202	350	CIT Millikan Lib. - Pasadena	98.98	142.341	11.93	1.655	235.548	15.347	206.104	14.36	VII	0.1954
3-24				41.8	EW	0.185	350	CIT Millikan Lib. - Pasadena	98.98	132.856	11.53	1.655	219.853	14.827	192.371	13.87	VII	0.1889
3-25				34.1	NS	0.141	450	CIT Jet Prop. Lab. - Pasadena	97.56	130.713	11.43	1.679	219.454	14.814	192.022	13.86	VII	0.1872
3-26				34.1	EW	0.212	450	CIT Jet Prop. Lab. - Pasadena	97.62	66.463	8.15	1.678	111.515	10.560	97.576	9.88	VII	0.1335
3-27	Nemuro Pen.	06/17/73	7.4	132.2	NS	0.169	250	Kushiro S-733 - Japan	87.00	337.793	18.38	1.883	636.069	25.220	556.561	23.59	VII	0.3011
3-28	Nemuro Pen.	06/17/73	7.4	132.2	EW	0.122	250	Kushiro S-733 - Japan	87.00	173.302	13.16	1.883	326.330	18.065	285.538	16.89	VII	0.2156
3-29	Nemuro Pen.	06/24/73	7.1	172.8	EW	0.051	250	Kushiro S-741 - Japan	60.00	33.408	5.78	2.730	91.208	9.550	79.807	8.93	VII	0.0947
3-30	Numero Pen.	06/24/73	7.1	172.8	NS	0.058	250	Kushiro S-741 - Japan	60.00	41.373	6.43	2.730	112.951	10.628	98.832	9.94	VII	0.1053
3-31	Northwestern Calif.	10/07/51	5.8	58.5	S44W	0.104	500	City Hall - Ferndale	55.88	33.818	5.82	2.930	99.095	9.955	86.708	9.31	V	0.0953
3-32	Northwestern Calif.	10/07/51	5.8	58.5	N46W	0.112	500	City Hall - Ferndale	55.88	42.639	6.53	2.930	124.945	11.178	109.327	10.46	V	0.1070
3-33	San Fernando	02/09/71	6.6	41.1	N83W	0.069	260	5900 Wilshire Blvd. L. A.	36.06	71.156	8.44	4.539	322.982	17.972	282.609	16.81	VII	0.1383
3-34	San Fernando	02/09/71	6.6	41.1	S07W	0.095	260	5900 Wilshire Blvd. L. A.	36.10	72.580	8.52	4.534	329.081	18.141	287.946	16.97	VII	0.1396
3-35	San Fernando	02/09/71	6.6	43.8	N52W	0.150		445 Figueroa St.	57.26	83.221	9.12	2.859	237.986	15.427	208.238	14.43	VII	0.1494
3-36	San Fernando	02/09/71		43.8	N38W	0.119		445 Figueroa St.	47.06	78.036	8.83	2.858	223.081	14.936	195.196	13.97	VII	0.1446
3-37	San Fernando	02/09/71	6.6	43.7	N37E	0.199		234 S. Figueroa St.	47.06	194.221	13.94	3.479	675.693	25.994	591.231	24.32	VII	0.2284

(Continued)

* λ^2: base average power = I_o/163.82, area under PSD curve for the extended record of 163.82 sec.

** λ: base average acceleration (cm/sec^2) = $(I_o/163.82)^{1/2}$.

† Conversion factor: ratio of 163.82 sec to the arbitrarily selected duration, or record length.

†† λ_o^2: raw average power or spectral intensity, area under the raw PSD curve of the actual/arbitrarily selected duration, cm^2/sec^4.

‡ λ_o: raw average acceleration, cm/sec^2.

‡‡ λ_s^2: corrected average power = $\lambda_o^2 \times 0.875$, cm^2/sec^4.

§ λ_s: corrected average acceleration, cm/sec^2.

§§ I_o: total (Arias) intensity or total energy = $\lambda^2 \times 163.82$ sec, cm^2/sec^3.

Table 3 (Continued)

Record No.	Earthquake	Date	Mag.	Approx. Source Dist. km	Dir.	Max. Acc. g	Soil Depth ft	Site	Estimated Duration sec	λ^2 cm^2/sec^4*	λ cm/sec^2**	Conversion Factor †	λ_o^2 cm^2/sec^4††	λ_o cm/sec^2‡	λ_s^2 cm^2/sec^4‡‡	λ_s cm/sec^2§	Modified Mercalli Intensity	I_o 10^4 cm^2/sec^3§§
3-38	San Fernando	02/09/71	6.6	43.7	N53E	0.192		234 S. Figueroa St.	47.12	128.713	11.35	3.475	447.222	21.148	391.319	19.78	VII	2.1086
3-39	San Fernando	02/09/71	6.6	43.8	N53W	0.152		222 Figueroa St.	41.86	87.541	9.36	3.911	342.349	18.503	299.555	17.31	VII	1.4341
3-40	San Fernando	02/09/71	6.6	43.8	S37W	0.128		222 Figueroa St.	41.86	92.893	9.64	3.911	363.282	19.060	317.872	17.83	VII	1.5218
3-41	Kern County	07/21/52	7.6	90.9	N42E	0.089	320	Santa Barbara Courthouse	75.48	90.657	9.52	2.930	196.704	14.025	172.116	13.12	VII	1.4851
3-42	Kern County	07/21/52	7.6	90.9	S48E	0.131	320	Santa Barbara Courthouse	75.46	110.654	10.52	2.930	238.878	15.457	209.018	14.46	VII	1.8127
3-43	Holister	04/08/61	5.6	41.5	S01W	0.076		City Hall - Hollister	40.46	50.870	7.13	4.046	205.817	14.346	180.089	13.42	VII	0.8334
3-44	Holister	04/08/61	5.6	41.5	N89W	0.179		City Hall - Hollister	40.48	99.570	9.98	4.044	402.655	20.066	352.323	18.77	VII	1.6312
3-45	1st N-W Calif.	09/11/38	5.5	57.5	S45W	0.144	500	City Hall - Ferndale	71.36	37.888	6.16	2.295	86.953	9.325	76.084	8.72	VI	0.6207
3-46	1st N-W Calif.	09/11/38	5.5	57.5	N45W	0.089	500	City Hall - Ferndale	71.36	27.857	5.28	2.295	63.930	7.996	55.939	7.48	VI	0.4564
3-47	2nd N-W Calif.	02/09/41	6.6	99.7	S45W	0.062	500	City Hall - Ferndale	67.26	15.596	3.95	2.435	37.974	6.162	33.227	5.76	VI	0.2555
3-48	2nd N-W Calif.	02/09/41	6.6	99.7	N45W	0.039	500	City Hall - Ferndale	67.24	12.114	3.48	2.435	29.504	5.432	25.816	5.08	VI	0.1985
3-49	Northern Calif.	10/03/41	6.4	33.8	N45W	0.120	500	City Hall - Ferndale	67.92	39.663	6.30	2.411	95.632	9.779	83.678	9.15	VII	0.6498
3-50	Northern Calif.	10/03/41	6.4	33.8	S45W	0.115	500	City Hall - Ferndale	67.88	59.563	7.72	2.412	95.448	9.769	83.517	9.14	VII	0.9758
3-51	Northern Calif.	06/05/60	5.7	62.4	N46W	0.058	500	City Hall - Ferndale	82.26	12.214	3.49	1.991	24.318	4.931	21.278	4.61	VI	0.2001
3-52	Northern Calif.	06/05/60	5.7	62.4	S44W	0.075	500	City Hall - Ferndale	82.28	14.148	3.76	1.991	28.161	5.307	24.641	4.96	VI	0.2318
3-53	Northern Calif.	09/22/52	5.5	46.0	S44W	0.054	500	City Hall - Ferndale	57.86	19.784	4.45	2.830	55.992	7.483	48.993	6.99	VI	0.3241
3-54	Northern Calif.	09/22/52	5.5	46.0	N46W	0.076	500	City Hall - Ferndale	57.98	20.034	4.48	2.824	56.580	7.522	49.507	7.04	VI	0.3282
3-55	Western Wash.	04/13/49	7.1	90.7	S02W	0.068	420	District Engineers Office	59.00	78.117	8.84	2.777	216.927	14.872	189.811	13.78	VIII	1.2797
3-56	Western Wash.	04/13/49	7.1	90.7	N88W	0.067	420	District Engineers Office	59.00	53.428	7.31	2.777	148.369	12.181	129.823	11.39	VIII	0.8753
3-57	Santa Barbara	06/30/41	5.9	39.3	N45E	0.238	320	Santa Barbara Courthouse	61.82	120.229	10.96	2.649	318.474	17.846	278.665	16.69	VIII	1.9696
3-58	Santa Barbara	06/30/41	5.9	39.3	S45E	0.175	320	Santa Barbara Courthouse	61.80	92.289	9.61	2.649	244.544	15.638	213.976	14.63	VIII	1.5119
3-59	2nd North Calif.	12/10/67	5.8	53.0	S11E	0.021	250	Eureka Federal Bldg.	29.98	1.825	1.35	5.458	9.962	3.156	8.717	2.95	VI	0.0299
3-60	2nd North Calif.	12/10/67	5.8	53.0	N79E	0.020	250	Eureka Federal Bldg.	29.84	1.905	1.38	5.484	10.449	3.232	9.143	3.02	VI	0.0312
3-61	Niigata, Japan	06/16/64	7.5	69.6	NS	0.135		Kawagishicho Apts. Bldg.	37.52	178.983	13.38	4.365	781.249	27.951	683.593	26.15	VI	2.9321
3-62	Niigata, Japan	06/16/64	7.5	69.6	EW	0.159		Kawagishicho Apts. Bldg.	38.20	136.785	11.69	4.287	586.436	24.216	513.131	22.65	VI	2.2408
3-63		10/26/65	7.1	163.8	NS	0.073	250	Kushiro-S (PHRI)ƒ	19.00	21.715	4.66	8.615	187.077	13.678	163.692	12.79	VI	0.3557
3-64		10/26/65	7.1	163.8	EW	0.058	250	Kushiro-S (PHRI)	19.00	11.223	3.35	8.615	96.688	9.833	84.602	9.19	VI	0.1839
3-65	Takachi Oki	05/16/68	7.9	188.1	NS	0.237	1250	Hachinohe-S (PHRI)	119.00	466.866	21.61	1.377	642.754	25.353	562.410	23.72	VIII	7.6482
3-66	Takachi Oki	05/16/68	7.9	188.1	EW	0.183	1250	Hachinohe-S (PHRI)	119.00	446.322	21.13	1.377	614.472	24.788	537.663	23.19	VIII	7.3116
3-67	Takachi Oki	05/16/68	7.9	259.7	NS	0.040	250	Kushiro-S (PHRI)	112.50	50.225	7.09	1.456	73.142	8.552	63.999	7.99	VI	0.8228
3-68	Takachi Oki	05/16/68	7.9	259.7	EW	0.048	250	Kushiro-S (PHRI)	113.00	52.015	7.21	1.499	75.413	8.684	65.986	8.12	VI	0.8521
3-69	Takachi Oki	06/12/68	7.3	201.0	EW	0.032	1250	Hachinohe-S (PHRI)	89.50	18.482	4.30	1.830	33.831	5.816	29.602	5.44	VI	0.3028
3-70	Takachi Oki	06/12/68	7.3	201.0	NS	0.038	1250	Hachinohe-S (PHRI)	90.00	21.226	4.61	1.820	38.637	6.216	33.807	5.81	VI	0.3477
3-71	Kushiro Oki	09/03/68	5.2	60.0	NS	0.018	250	Kushiro-S (PHRI)	28.98	0.817	0.90	5.650	4.615	2.148	4.038	2.01	V	0.0134
3-72	Kushiro Oki	09/03/68	5.2	60.0	EW	0.030	250	Kushiro-S (PHRI)	29.98	2.594	1.61	5.462	14.170	3.764	12.399	3.52	V	0.0425
3-73	Takachi Oki	09/21/68	6.9	186.3	NS	0.036	1250	Hachinohe-S (PHRI)	60.00	10.547	3.25	2.730	28.793	5.366	25.194	5.02	VI	0.1728
3-74	Takachi Oki	09/21/68	6.9	186.3	EW	0.029	1250	Hachinohe-S (PHRI)	60.00	12.168	3.49	2.730	33.221	5.764	29.069	5.39	VI	0.1993
3-75		01/19/69	?	182.7	NS	0.026	250	Kushiro-S (PHRI)	25.00	5.718	2.39	6.549	37.446	6.119	32.766	5.72		0.0937
3-76		01/19/69	?	182.7	EW	0.031	250	Kushiro-S (PHRI)	25.00	9.776	3.13	6.549	64.026	8.002	56.022	7.48		0.1602
3-77	Aomorikento-hooki	06/21/69	5.6	66.8	NS	0.031	1250	Hachinohe-S (PHRI)	30.00	2.833	1.68	5.458	15.461	3.932	13.529	3.68		0.0464
3-78	Aomorikento-hooki	06/21/69	5.6	66.8	EW	0.025	1250	Hachinohe-S (PHRI)	29.50	2.165	1.47	5.551	12.016	3.466	10.514	3.24		0.0354

(Continued)

ƒ PHRI = Port and Harbour Research Institute, Japan, contributed these data.

Table 3 (Concluded)

Record No.	Earthquake	Date	Mag.	Approx. Source Dist. km	Dir.	Max. Acc. g	Soil Depth ft	Site	Estimated Duration sec	λ^2 cm^2/sec^4*	λ cm/sec^2**	Con-version Factor†	λ_o^2 cm^2/sec^4††	λ_o cm/sec^2‡	λ_s^2 cm^2/sec^4‡‡	λ_s cm/sec^2§	Modified Mercalli Intensity	I_o 10^4 cm^2/sec^3§§
3-79	Hokkaido Tohooki	08/12/69	7.8	416.4	NS	0.041	250	Kushiro-S (PHRI)#	90.00	33.917	5.82	1.820	61.737	7.857	54.020	7.35	VI	0.5556
3-80	Hokkaido Tohooki	08/12/69	7.8	416.4	EW	0.038	250	Kushiro-S (PHRI)	90.00	26.843	5.18	1.820	48.870	6.991	-2.762	6.54		0.4398
3-81	Yakushima Kinaki	09/18/69	5.9	130.7	NS	0.025	>82	Kagoshima-S (PHRI)	40.50	9.486	3.08	4.044	38.362	6.194	33.567	5.79		0.1554
3-82		09/18/69	5.9	130.7	EW	0.028	>82	Kagoshima-S (PHRI)	40.50	7.546	2.75	4.044	30.517	5.524	26.703	5.17		0.1236
3-83		01/21/70	6.7	246.7	NS	0.020	1250	Hachinohe-S (PHRI)	30.00	4.038	2.01	5.458	22.042	4.695	19.287	4.39	VI	0.0662
3-84		01/21/70	6.7	246.7	EW	0.012	1250	Hachinohe-S (PHRI)	30.00	2.000	1.41	5.458	10.921	3.305	9.555	3.09	VI	0.0328
3-85		01/21/70	6.7	116.3	NS	0.042	250	Kushiro-S (PHRI)	45.00	12.603	3.55	3.639	45.872	5.773	40.138	6.34	V	0.2065
3-86	Yakushima Kinaki	01/21/70	6.7	116.3	EW	0.032	250	Kushiro-S (PHRI)	45.00	11.201	3.35	3.639	40.769	6.385	35.673	5.97	V	0.1835
3-87		04/01/70		89.4	NS	0.032	1250	Hachinohe-S (PHRI)	30.00	3.175	1.78	5.458	17.333	4.163	15.166	3.89	V	0.0520
3-88		04/01/70		89.4	EW	0.024	1250	Hachinohe-S (PHRI)	30.00	3.918	1.98	5.458	21.385	4.624	18.712	4.33	V	0.0642
3-89		07/26/70	6.7	147.4	NS	0.019	>82	Kagoshima-S (PHRI)	55.50	9.971	3.16	2.951	29.427	5.425	25.784	5.07	V	0.1633
3-90		07/26/70	6.7	147.4	EW	0.024	>82	Kagoshima-S (PHRI)	59.00	7.725	2.78	2.776	21.447	4.631	18.766	4.33	V	0.1266
3-91		08/02/71	7.0	183.3	NS	0.069	250	Kushiro-S (PHRI)	60.00	34.836	5.90	2.730	95.105	9.752	83.217	9.12	VI	0.5707
3-92		08/02/71	7.0	183.3	EW	0.066	250	Kushiro-S (PHRI)	60.00	32.866	5.73	2.730	89.726	9.472	78.510	8.86	VI	0.5384
3-93		03/20/72	6.4	56.8	NS	0.055	1250	Hachinohe-S (PHRI)	30.00	14.524	3.81	5.458	79.277	8.904	69.367	8.33	VI	0.2379
3-94		03/20/72	6.4	56.8	EW	0.046	1250	Hachinohe-S (PHRI)	30.00	10.473	3.24	5.458	57.165	7.561	50.019	7.07	VI	0.1716
3-95		05/11/72	5.8	73.6	NS	0.095	250	Kushiro-S (PHRI)	28.00	28.041	5.29	5.848	163.981	12.806	143.483	11.98	VI	0.4594
3-96		05/11/72	5.8	73.6	EW	0.067	250	Kushiro-S (PHRI)	27.98	13.718	3.70	5.852	80.281	8.960	70.245	8.38	VI	0.2247
3-97		08/20/72	5.3	39.0	NS	0.030	>66	Sakata-S (PHRI)	28.00	2.490	1.58	5.848	14.564	3.816	12.743	3.57	V	0.0408
3-98		08/20/72	5.3	39.0	EW	0.047	>66	Sakata-S (PHRI)	28.00	4.688	2.16	5.848	27.417	5.236	23.989	4.89	V	0.0768
3-99		06/17/73	7.4	358.7	NS	0.027	>100	Tomakomai-S (PHRI)	90.00	13.904	3.73	1.820	25.309	5.031	22.146	4.71	V	0.2278
3-100		06/17/73	7.4	358.7	EW	0.018	>100	Tomakomai-S (PHRI)	90.00	9.542	3.09	1.820	17.369	4.168	15.198	3.90	V	0.1563
3-101		09/04/74	5.6	53.4	NS	0.062	1250	Hachinohe-S (PHRI)	30.00	10.932	3.31	5.458	59.672	7.725	52.213	7.23	VI	0.1791
3-102		09/04/74	5.6	53.4	EW	0.050	1250	Hachinohe-S (PHRI)	30.00	9.762	3.12	5.458	53.283	7.299	46.623	6.83	VI	0.1599
3-103		09/20/74	?	59.4	NS	0.021	250	Kushiro-S (PHRI)	30.00	1.065	1.03	5.458	5.811	2.411	5.085	2.25	V	0.0174
3-104		09/20/74	?	59.4	EW	0.030	250	Kushiro-S (PHRI)	29.98	2.385	1.54	5.462	13.026	3.609	11.398	3.38	V	0.0391
3-105		11/09/74	6.5	15.1	NS	0.064	>100	Tomakomai-S (PHRI)	40.00	11.928	3.45	4.094	48.838	6.988	42.733	6.54		0.1954
3-106		11/09/74	6.5	15.1	EW	0.054	>100	Tomakomai-S (PHRI)	40.00	10.260	3.20	4.094	42.011	6.481	36.760	6.06		0.1681
3-107		11/09/74	6.5	214.7	NS	0.021	250	Kushiro-S (PHRI)	50.00	3.721	1.93	3.276	12.190	3.491	10.667	3.27		0.0609
3-108		11/09/74	6.5	214.7	EW	0.020	250	Kushiro-S (PHRI)	50.00	3.349	1.83	3.276	10.974	3.313	9.602	3.10		0.0549
3-109		03/03/74	6.1	37.8	NS	0.036	100	Kashima-Ji-S (PHRI)	40.00	11.577	3.40	4.094	47.401	6.885	41.476	6.44	(VI)	0.1897
3-110		03/03/74	6.1	37.8	EW	0.100			40.00	29.349	5.42	4.094	120.168	10.962	105.147	10.25	(VI)	0.4808
3-111		07/08/74	6.3	81.7	NS	0.049			30.00	7.537	2.74	5.458	41.138	6.414	35.995	6.00	VI	0.1235
3-112		07/08/74	6.3	81.7	EW	0.032			30.00	7.508	2.74	5.458	40.983	6.402	35.860	5.99	VI	0.1230
3-113		11/16/74	6.1	47.3	NS	0.069			30.00	21.994	4.69	5.458	120.052	10.957	105.045	10.25	VI	0.3603
3-114		11/16/74	6.1	47.3	EW	0.077			30.00	20.056	4.48	5.458	109.473	10.463	95.789	9.79	VI	0.3286
3-115		09/30/73	5.9	25.6	NS	0.037			50.00	10.610	3.26	3.276	34.757	5.895	30.413	5.51	(VI)	0.1738
3-116		09/30/73	5.9	25.6	EW	0.071			50.00	27.643	5.26	3.276	90.571	9.517	79.249	8.90	(VI)	0.4529
3-117		07/20/73	5.9	68.9	NS	0.034			29.00	3.363	1.83	5.646	18.992	4.358	16.618	4.08		0.0551
3-118		07/20/73	5.9	68.9	EW	0.020			29.00	2.588	1.61	5.646	14.616	3.823	12.789	3.58		0.0424
3-119		10/01/73	5.8	25.6	NS	0.024			30.00	3.731	1.93	5.458	20.364	4.513	17.218	4.15	(VI)	0.0611
3-120		10/01/73	5.8	25.6	EW	0.039			30.00	8.629	2.94	5.458	47.105	6.836	41.217	6.42	(VI)	0.1414
					Mean	0.063							Mean	12.039	Mean	11.160		
					S. D.	0.272							S. D.	8.749	S. D.	8.154		
					VAR.	0.074							VAR.	75.902	VAR.	65.938		

PHRI = Port and Harbour Research Institute, Japan, contributed these data.

Table 4

Sites With Soft to Medium Clay and Sand

Record No.	Earthquake	Date	Mag.	Approx. Source Dist. km	Dir.	Max. Acc. g	Soil Depth ft	Site	Estimated Duration sec	λ^2 cm^2/sec^4*	λ cm/sec^2**	Conversion Factor†	λ_o^2 cm^2/sec^4††	λ_o cm/sec^2‡	λ_s^2 cm^2/sec^4‡‡	λ_s cm/sec^2§	Modified Mercalli Intensity	I_o 10^4 cm^2/sec^3§§
4-1	San Francisco	03/22/57	5.25	18	N45E	0.047	285	Sthrn. Pacific Bldg. - S. F.	38.94	8.276	2.88	4.204	34.788	5.898	30.439	5.517	VII	0.1356
4-2	San Francisco	03/22/57	5.25	18	N45W	0.046	285	Sthrn. Pacific Bldg. - S. F.	39.02	12.386	3.52	4.195	51.960	7.208	45.465	6.743	VII	0.2029
4-3	Higashi-Matsuyame	07/01/68	6.4	45	NS	0.050	700	Koto Denwa Kyoku - Tokyo 119	11.38	13.576	3.68	14.348	194.796	13.597	170.446	13.055		0.2224
4-4	↓	↓	↓	↓	EW	0.034	700	Koto Denwa Kyoku - Tokyo 119	11.20	9.461	3.08	14.578	137.921	11.744	120.681	10.985		0.1550
4-5	↓	↓	↓	↓	NS	0.047	500	Bokuto Hospital - Tokyo 121	13.62	23.750	4.87	11.995	284.899	16.879	249.287	15.789		0.3891
4-6	↓	↓	↓	↓	EW	0.049	500	Bokuto Hospital - Tokyo 121	12.82	14.632	3.83	12.742	164.442	12.823	143.887	11.995		0.2397
4-7	↓	↓	↓	↓	NS	0.040	500	Ueno Matsuzakaya - Tokyo 112	7.42	5.712	2.39	21.965	125.474	11.202	109.789	10.478		0.0936
4-8	↓	↓	↓	↓	EW	0.030	500	Ueno Matsuzakaya - Tokyo 112	7.68	4.559	2.14	21.225	96.767	9.837	84.671	9.202		0.0747
4-9	↓	↓	↓	↓	NS	0.044	500	Ikebukuro Marubutsu - Tokyo 113	7.78	6.922	2.63	20.954	145.043	12.043	126.913	11.265		0.1134
4-10	↓	↓	↓	↓	EW	0.058	500	Ikebukuro Marubutsu - Tokyo 113	8.36	10.203	3.19	19.507	199.028	14.108	174.149	13.196		0.1671
4-11	Bucharest	03/04/77	7.2	189	NS	0.178	Deep	Bldg. Research Institute, Basmt	16.20	310.568	17.62	10.127	3145.220	56.082	2752.067	52.460	VIII	5.0877
4-12	Bucharest	03/04/77	7.2	189	EW	0.109	Deep	Bldg. Research Institute, Basmt	16.14	168.525	12.98	10.090	1700.404	41.236	1487.854	38.573	VIII	2.7608
4-13	(Japan)	03/27/63	6.9	125	NS	0.031	>100	Nagoya-Zokan-S (PHRI)#	50.00	12.056	3.47	3.276	39.496	6.284	34.559	5.878	VI	0.1975
4-14	↓	03/27/63	6.9	125	EW	0.024	>100	Nagoya-Zokan-S (PHRI)	50.00	12.217	3.50	3.276	40.023	6.326	35.019	5.917	VI	0.2010
4-15	↓	09/17/63	4.1	20.4	NS	0.029	>100	Nagoya-Zokan-S (PHRI)	18.00	0.697	0.84	9.093	6.344	2.517	5.551	2.356	IV	0.0114
4-16	↓	09/17/63	4.1	20.4	EW	0.019	>100	Nagoya-Zokan-S (PHRI)	18.00	0.850	0.92	9.093	7.732	2.781	6.766	2.601	IV	0.0139
4-17	↓	04/20/65	6.1	20.8	NS	0.096	>100	Shimizu-Kojyo-S (PHRI)	25.00	94.705	9.73	6.554	620.696	24.914	543.109	23.305	VI	1.5515
4-18	↓	04/20/65	6.1	20.8	EW	0.109	>100	Shimizu-Kojyo-S (PHRI)	25.00	104.693	10.23	6.554	1686.116	26.194	600.351	24.502	VI	1.7151
4-19	↓	01/20/66	5.3	74.6	NS	0.020	>66	Niigata-S (PHRI)	10.00	0.817	0.91	16.353	13.355	3.654	11.685	3.418	V	0.0134
4-20	↓	01/20/66	5.3	74.6	EW	0.018	>60	Niigata-S (PHRI)	9.94	0.769	0.88	16.452	12.665	3.559	11.081	3.329	V	0.0126
4-21	↓	04/03/66	5.8	76.4	NS	0.057	>135	Onahama-S (PHRI)	29.50	10.807	3.29	5.551	59.991	7.745	52.492	7.245	VI	0.1770
4-22	↓	04/03/66	5.8	76.4	EW	0.086	>135	Onahama-S (PHRI)	29.50	19.123	4.37	5.551	106.151	10.303	92.882	9.637	VI	0.3133
4-23	↓	01/17/67	6.3	100.4	NS	0.047	92	Shiogama-S (PHRI)	40.00	15.003	3.87	4.094	61.429	7.838	53.750	7.331		0.2458
4-24	↓	01/17/67	6.3	100.4	EW	0.032	92	Shiogama-S (PHRI)	40.00	8.538	2.97	4.094	34.957	5.912	30.588	5.530		0.1399
4-25	↓	01/17/67	6.3	94.8	NS	0.026	>62	Ofunado-S (PHRI)	44.00	8.065	2.84	3.722	30.019	5.479	26.267	5.125	VI	0.1321
4-26	↓	01/17/67	6.3	94.8	EW	0.048	>62	Ofunado-S (PHRI)	45.00	21.299	4.62	3.639	77.522	8.805	67.832	8.236	VI	0.3489
4-27	↓	06/23/67	4.1	16.5	NS	0.029	>100	Yokkaichi-Ji-S (PHRI)	10.00	0.362	0.93	16.353	14.097	3.755	12.335	3.512	IV	0.0059
4-28	↓	06/23/67	4.1	16.5	EW	0.022	>100	Yokkaichi-Ji-S (PHRI)	9.90	0.327	0.57	16.518	5.404	2.325	4.728	2.174	IV	0.0054
4-29	↓	09/29/67	4.2	5.2	NS	0.055	>70	Wakayama-Ji-S (PHRI)	10.00	2.814	1.68	16.353	46.021	6.784	40.268	6.346		0.0461
4-30	↓	09/29/67	4.2	5.2	EW	0.089	>70	Wakayama-Ji-S (PHRI)	10.00	3.383	1.84	16.353	55.329	7.438	48.413	6.958		0.0554
4-31	↓	11/10/67	?	54.7	NS	0.021	160	Shinagawa-S (PHRI)	14.00	0.355	0.596	11.687	4.154	2.038	3.635	1.906	V	0.0058
4-32	↓	11/10/67	?	54.7	EW	0.024	160	Shinagawa-S (PHRI)	30.00	3.355	1.83	5.458	18.316	4.279	16.027	4.003	V	0.0550
4-33	↓	04/01/68	7.5	164.4	NS	0.066	>100	Kochi-S (PHRI)	89.50	71.623	8.46	1.830	131.101	11.450	141.713	10.710	VI	1.1733
4-34	↓	04/01/68	7.5	164.4	EW	0.098	>100	Kochi-S (PHRI)	90.00	122.147	11.05	1.820	222.339	14.907	194.547	13.948	VI	2.0010
4-35	↓	04/01/68	7.5	121.1	NS	0.186	160	Hososhima-S (PHRI)	45.00	259.212	16.10	3.641	943.762	30.721	825.792	28.736	VIII	4.2464
4-36	↓	04/01/68	7.5	121.1	EW	0.247	160	Hososhima-S (PHRI)	45.00	323.628	17.99	3.641	1178.320	34.327	1031.038	32.109	VIII	5.3017
4-37	↓	05/16/68	7.9	242.9	NS	0.211	>100	Aomori-S (PHRI)	87.00	776.443	27.86	1.883	1462.212	38.239	1279.435	35.769	VIII	12.7197
4-38	↓	05/16/68	7.9	242.9	EW	0.183	>100	Aomori-S (PHRI)	87.00	719.027	26.81	1.883	1354.085	36.798	1184.824	34.421	VIII	11.7791
4-39	Tokachioki	05/16/68	7.4	217.5	NS	0.055	>100	Aomori-S (PHRI)	57.00	93.314	9.66	2.874	268.220	16.377	234.693	15.319	VI	1.5287
4-40	Tokachioki	05/16/68	7.4	217.5	EW	0.088	>100	Aomori-S (PHRI)	57.00	101.681	10.08	2.874	292.231	17.095	255.702	15.991	VI	1.6657
4-41	Wakayama Fukin	03/30/68	5.0	5.2	NS	0.176	>70	Wakayama-Ji-S (PHRI)	15.00	39.485	6.28	10.909	430.755	20.755	376.910	19.414	VI	0.6468

(Continued)

* λ^2: base average power = $I_o/163.82$, area under PSD curve for the extended record of 163.82 sec.

** λ: base average acceleration (cm/sec^2) = $(I_o/163.82)^{1/2}$.

† Conversion factor: ratio of 163.82 sec to the arbitrarily selected duration, or record length.

†† λ_o^2: raw average power or spectral intensity, area under the raw PSD curve of the actual/arbitrarily selected duration, cm^2/sec^4.

‡ λ_o: raw average acceleration, cm/sec^2.

‡‡ λ_s^2: corrected average power = $\lambda_o^2 \times 0.875$, cm^2/sec^4.

§ λ_s: corrected average acceleration, cm/sec^2.

§§ I_o: total (Arias) intensity or total energy = $\lambda^2 \times 163.82$ sec, cm^2/sec^3.

Table 4 (Continued)

Record No.	Earthquake	Date	Mag.	Approx. Source Dist. km	Dir.	Max. Acc. g	Soil Depth ft	Site	Estimated Duration sec	λ^2 cm^2/sec^4*	λ cm/sec^2**	Conversion Factor†	λ_o^2 cm^2/sec^4††	λ_o cm/sec^2‡	λ_s^2 cm^2/sec^4‡‡	λ_s cm/sec^2§	Modified Mercalli Intensity	I_o 10^4 cm^2/sec^3§§
4-42	Wakayama Fukin	03/30/68	5.0	5.2	EW	0.258	>70	Wakayama-Ji-S (PHRI)#	15.44	58.421	7.64	10.599	619.198	24.884	541.798	23.276	VI	0.9571
4-43	Hyuganada	04/01/68	7.5	319.0	NS	0.047	>70	Wakayama-Ji-S (PHRI)	9.50	0.959	0.98	17.212	16.507	4.063	14.444	3.800	IV	0.0157
4-44	Hyuganada	04/01/68	7.5	319.0	EW	0.077	>70	Wakayama-Ji-S (PHRI)	9.48	1.995	1.41	17.248	34.411	5.866	30.110	5.487	IV	0.0327
4-45	Tokachioki-Yoshin	05/18/68	5.1	171.3	NS	0.080	>62	Ofunado-S (PHRI)	52.50	111.537	10.56	3.121	348.080	18.657	304.570	17.452	V	1.8272
4-46	Tokachioki Yoshin	05/18/68	5.1	171.3	EW	0.050	>62	Ofunado-S (PHRI)	52.50	43.553	6.60	3.121	135.929	11.659	118.938	10.906	V	0.7135
4-47	Tokachioki	06/12/68	7.3	263.4	NS	0.020	>100	Aomori-S (PHRI)	47.50	9.642	3.11	3.448	33.248	5.766	29.092	5.394	VI	0.1583
4-48	Tokachioki	06/12/68	7.3	263.4	EW	0.022	>100	Aomori-S (PHRI)	47.50	13.316	3.65	3.448	45.917	6.776	40.177	6.338	VI	0.2181
4-49	Saitamaken Chubu	07/01/68	6.1	65.8	NS	0.051	160	Yamashita-Hen-S	55.00	15.085	3.88	2.978	44.927	6.703	39.312	6.270	VI	0.2471
4-50	Saitamaken Chubu	07/01/68	6.1	65.8	EW	0.045	160	Yamashita-Hen-S (PHRI)	55.00	11.021	3.32	2.978	32.823	5.729	28.720	5.359	VI	0.1805
4-51	Saitamaken Chubu	07/01/68	6.1	53.3	NS	0.069	160	Shinagawa-S (PHRI)	35.00	50.876	7.13	4.681	238.151	15.432	208.382	14.435	VI	0.8335
4-52	Saitamaker Chubu	07/01/68	6.1	53.3	EW	0.115	160	Shinagawa-S (PHRI)	35.00	57.376	7.57	4.681	268.585	16.388	235.012	15.330	VI	0.9399
4-53	Bosohanton-antobu	07/04/68	?	107.7	NS	0.027	160	Yamashita-Hen-S (PHRI)	34.00	1.479	1.22	4.816	7.122	2.669	6.232	2.496	V	0.0242
4-54	Bosohanton-antobu	07/04/68	?	107.7	EW	0.011	160	Yamashita-Hen-S (PHRI)	34.00	1.397	1.18	4.816	6.731	2.594	5.889	2.427	V	0.0229
4-55	Miyazakiken Oki	07/05/68	6.4	84.9	NS	0.030	>62	Ofunado-S (PHRI)	59.42	13.746	3.71	2.757	37.896	6.156	33.159	5.758	VI	0.2252
4-56	Miyazakiken Oki	07/05/68	6.4	84.9	EW	0.052	>62	Ofunado-S (PHRI)	60.00	13.963	3.74	2.730	38.122	6.174	33.356	5.775	VI	0.2287
4-57	Bungosuido	08/06/68	6.6	117.0	NS	0.062	160	Hiroshima-S (PHRI)	16.00	19.273	4.39	10.240	197.355	14.048	172.686	13.141	V	0.3157
4-58	↓	↓	↓	117.0	EW	0.049	160	Hiroshima-S (PHRI)	16.00	22.896	4.78	10.240	234.455	15.312	205.148	14.323	V	0.3751
4-59				139.7	NS	0.045	171	Hososhima-S (PHRI)	48.50	28.362	3.377	3.377	95.784	9.787	83.811	9.158	VI	0.4646
4-60				139.7	EW	0.039	171	Hososhima-S (PHRI)	48.50	20.779	4.56	3.377	70.176	8.377	61.404	7.836	VI	0.3404
4-61				110.9	NS	0.043	>100	Kochi-S (PHRI)	69.30	20.976	4.58	2.364	49.584	7.042	43.386	6.587	V	0.3436
4-62				110.9	EW	0.044	>100	Kochi-S (PHRI)	70.00	19.751	4.44	2.340	46.221	6.798	40.443	6.359	V	0.3236
4-63	Saitamaken Chubu	07/01/68	6.1	170.7	NS	0.038	>135	Onahama-S (PHRI)	39.50	6.603	2.57	4.146	27.378	5.232	23.956	4.894	V	0.1082
4-64	Saitamaken Chubu	07/01/68	6.1	170.7	EW	0.033	>135	Onahama-S (PHRI)	39.48	7.659	2.77	4.148	31.773	5.637	27.801	5.273	V	0.1255
4-65	Kyotoshihukin	08/27/68	4.9	51.0	NS	0.021	>100	Kobe-Ji-S (PHRI)	9.50	1.200	1.09	17.212	20.664	4.546	18.081	4.252	IV	0.0197
4-66	Kyotoshihukin	08/27/68	4.9	51.0	EW	0.024	>100	Kobe-Ji-S (PHRI)	9.50	1.103	1.05	17.212	18.984	4.357	16.611	4.076	IV	0.0181
4-67	Tokachioki	09/21/68	6.9	204.2	NS	0.026	>100	Aomori-S (PHRI)	58.96	11.402	3.38	2.778	31.677	5.682	27.718	5.265	VI	0.1868
4-68	Tokachioki	09/21/68	6.9	204.2	EW	0.023	>100	Aomori-S (PHRI)	59.50	14.418	3.80	2.753	39.695	6.300	34.733	5.893	VI	0.2362
4-69	Chibaken Chubu	10/08/68	5.3	39.4	ES	0.064	160	Yamashita-Hen-S (PHRI)	30.98	7.216	2.69	5.286	38.142	6.176	33.374	5.777	V	0.1182
4-70	Chibaken Chubu	10/08/68	5.3	39.4	EW	0.028	160	Yamashita-Hen-S (PHRI)	31.00	3.926	1.98	5.282	20.737	4.554	18.145	4.259	V	0.0643
4-71	Tokushima Seibu	12/11/68	6.0	53.1	NS	0.018	>100	Kochi-S (PHRI)	29.50	1.768	1.33	5.551	9.814	3.133	8.588	2.930	V	0.0290
4-72	Tokushima Seibu	12/11/68	6.0	53.1	EW	0.024	>100	Kochi-S (PHRI)	29.48	2.472	1.56	5.554	13.483	3.672	11.797	3.435	V	0.0405
4-73	Chibaken Chubu	10/08/68	5.3	39.3	NS	0.030	160	Shinagawa-S (PHRI)	31.00	3.551	1.88	5.282	18.756	4.331	16.411	4.051	V	0.0582
4-74	Chibaken Chubu	10/08/68	5.3	39.3	EW	0.036	160	Shinagawa-S (PHRI)	31.00	4.374	2.09	5.282	23.103	4.806	20.215	4.496	V	0.0717
4-75	Hyuganada	04/21/69	6.5	90.5	NS	0.064	171	Hososhima-S (PHRI)	61.00	30.042	5.48	2.685	80.673	8.982	70.589	8.402		0.4921
4-76	Hyuganada	04/21/69	6.5	90.5	EW	0.100	171	Hososhima-S (PHRI)	60.00	42.029	6.48	2.730	114.745	10.712	100.402	10.020		0.6885
4-77	Gifuken	09/09/69	6.6	101.3	NS	0.040	>60	Kinuura-S (PHRI)	40.00	13.801	3.71	4.094	56.508	7.517	49.445	7.032		0.2261
4-78	Gifuken (Japan)	09/09/69	6.6	101.3	EW	0.062	>60	Kinuura-S (PHRI)	40.50	22.408	4.73	4.044	90.617	9.519	79.290	8.904		0.3671
4-79	Gifuken (Japan)	07/26/70	6.7	73.7	NS	0.090	171	Hososhima-S (PHRI)	22.50	92.875	9.64	7.282	676.295	26.006	591.758	24.326	VI	1.5215

(Continued)

PHRI = Port and Harbour Research Institute, Japan, contributed these data.

Table 4 (Concluded)

Record No.	Earthquake	Date	Mag.	Approx. Source Dist. km	Dir.	Max. Acc. g	Soil Depth ft	Site	Estimated Duration sec	λ^2 cm^2/sec^4*	λ cm/sec^2**	Conversion Factor †	λ_o^2 cm^2/sec^4††	λ_o cm/sec^2‡	λ_s^2 cm^2/sec^4‡‡	λ_s cm/sec^2§	Modified Mercalli Intensity	I_o 10^4 cm^2/sec^3§§
4-80	(Japan)	07/26/70	6.7	73.7	EW	0.124	171	Hososhima-S (PHRI)#	22.50	97.544	9.88	7.282	710.315	26.652	621.526	24.930	VI	1.5980
4-81		07/26/70	6.1	82.0	NS	0.049	171	Hososhima-S (PHRI)	29.00	7.529	2.74	5.646	42.516	6.520	37.202	6.099	V	0.1233
4-82		07/26/70	6.1	82.0	EW	0.049	171	Hososhima-S (PHRI)	29.00	9.588	3.10	5.646	54.138	7.358	47.371	6.883	V	0.1571
4-83		02/29/72	7.0	258.2	NS	0.023		Koken-S (PHRI)	15.00	3.453	1.86	10.909	37.668	6.137	32.959	5.741		0.0566
4-84				258.2	EW	0.015		Koken-S (PHRI)	15.00	2.053	1.43	10.909	22.395	4.732	19.595	4.427		0.0336
4-85				283.9	NS	0.030	160	Keihin-Ji-S (PHRI)	69.00	17.681	4.20	2.374	41.976	6.479	36.729	6.060	VI	0.2897
4-86				283.9	EW	0.031	160	Keihin-Ji-S (PHRI)	69.00	16.903	4.11	2.374	40.129	6.335	35.113	5.926	VI	0.2769
4-87				282.0	NS	0.054	160	Yamashita-Hen-S (PHRI)	45.00	24.360	4.94	3.641	88.692	9.418	77.605	8.809	VI	0.3991
4-88				282.0	EW	0.048	160	Yamashita-Hen-S (PHRI)	45.00	28.861	5.37	3.641	105.083	10.251	91.947	9.589	VI	0.4728
4-89				278.3	NS	0.023	>100	Chiba-S (PHRI)	59.00	6.283	2.51	2.776	17.443	4.176	15.263	3.906	VI	0.1029
4-90				278.3	EW	0.022	>100	Chiba-S (PHRI)	59.00	8.059	2.84	2.776	22.375	4.730	4.730	4.425	VI	0.1320
4-91				285.8	NS	0.019	>66	Tagonoura-S (PHRI)	70.00	5.845	2.42	2.340	13.679	3.698	11.969	3.459	(V)	0.0958
4-92				285.8	EW	0.033	>60	Tagonoura-S (PHRI)	70.00	12.932	3.60	2.340	30.264	5.501	26.481	5.146	(V)	0.2119
4-93		02/29/72	7.0	294.0	NS	0.029	160	Shinagawa-S (PHRI)	49.0	12.191	3.49	3.343	40.750	6.383	35.656	5.971	VI	0.1997
4-94		02/29/72	7.0	294.0	EW	0.032	160	Shinagawa-S (PHRI)	49.0	11.168	3.34	3.343	37.333	6.110	32.667	5.715	VI	0.1830
4-95		03/20/72	6.4	84.7	NS	0.050	>100	Aomori-S (PHRI)	59.0	16.780	4.10	2.776	46.587	8.825	40.764	6.385	VI	0.2749
4-96		03/20/72	6.4	84.7	EW	0.057	>100	Aomori-S (PHRI)	59.0	20.355	4.51	2.776	56.511	7.517	49.447	7.032	VI	0.3335
4-97		12/04/72	7.3	292.1	NS	0.026	160	Shinagawa-S (PHRI)	50.0	10.335	3.31	3.276	33.856	5.818	29.624	5.443	VI	0.1693
4-98		12/04/72	7.3	292.1	EW	0.022	160	Shinagawa-S (PHRI)	50.0	9.126	3.02	3.276	29.894	5.467	26.157	5.114	VI	0.1495
4-99		12/04/72	7.3	278.4	NS	0.029	160	Yamashita-Hen-S (PHRI)	65.0	14.851	3.85	2.520	37.426	6.118	32.748	5.722	VI	0.2433
4-100		12/04/72	7.3	278.4	EW	0.039	160	Yamashita-Hen-S (PHRI)	65.0	16.519	4.06	2.520	41.629	6.452	36.426	6.035	VI	0.2706
4-101		12/04/72	7.3	417.0	NS	0.015	>135	Onahama-S (PHRI)	70.0	4.402	2.10	2.340	10.302	3.210	9.014	3.002	VI	0.0721
4-102		12/04/72	7.3	417.0	EW	0.026	>135	Onahama-S (PHRI)	70.0	4.430	2.10	2.340	10.367	3.220	9.071	3.012	VI	0.0726
4-103		07/20/73	5.9	50.8	NS	0.023	>135	Onahama-S (PHRI)	30.0	3.978	1.99	5.458	21.714	4.660	18.999	4.358	V	0.0652
4-104		07/20/73	5.9	50.8	EW	0.024	>135	Onahama-S (PHRI)	30.0	3.455	1.86	5.458	18.856	4.342	16.499	4.062	V	0.0566
4-105		09/30/73	5.9	63.1	NS	0.022	>100	Chiba-S (PHRI)	39.0	5.456	8.33	4.199	22.912	4.787	20.048	4.477	(V)	0.0894
4-106		09/30/73	5.9	63.1	EW	0.017	>100	Chiba-S (PHRI)	39.0	5.569	2.36	4.199	23.388	4.836	20.464	4.524	(V)	0.0912
4-107		11/19/73	6.4	113.3	NS	0.047	92	Shiogama-Kojyo-S (PHRI)	15.0	19.264	4.39	3.343	64.394	8.024	56.345	7.506		0.3156
4-108		11/19/73	6.4	113.3	EW	0.057	92	Shiogama-Kojyo-S (PHRI)	15.0	23.328	4.83	3.343	77.979	8.831	68.232	8.260		0.3822
4-109		11/25/73	5.8	42.4	NS	0.056	>70	Wakayama-Ji-S (PHRI)	30.0	7.211	2.68	5.458	39.362	6.274	34.441	5.868	VI	0.1181
4-110		11/25/73	5.8	42.4	EW	0.056	>70	Wakayama-Ji-S (PHRI)	30.0	8.074	2.84	5.458	44.073	6.638	38.564	6.210	VI	0.1323
4-111		11/25/73	5.9	80.6	NS	0.024	>100	Komatusujima-S (PHRI)	30.0	3.406	1.85	5.458	18.592	4.312	16.268	4.033	V	0.0558
4-112		11/25/73	5.9	80.6	EW	0.031	>100	Komatusujima-S (PHRI)	30.0	4.591	2.14	5.458	25.059	5.006	21.927	4.683	V	0.0752
4-113		02/10/74	?	13.8	NS	0.030	>60	Kinuura-S (PHRI)	20.0	1.373	1.17	8.185	11.234	3.352	9.829	3.135	(V)	0.0225
4-114		02/10/74	?	13.8	EW	0.050	>60	Kinuura-S (PHRI)	20.0	3.304	1.82	8.185	27.044	5.200	23.663	4.864	(V)	0.0541
					Mean	0.054							Mean	9.912	Mean	9.272		
					S.D.	0.046							S.D.	9.015	S.D.	8.434		
					VAR.	0.002							VAR.	80.555	VAR.	70.508		

PHRI = Port and Harbour Research Institute, Japan, contributed these data.

(Sheet 3 of 3)

Table 5

Comparison of Average Powers Estimated From Uncorrected, Corrected, and Extended 163.82-sec Duration Records

Row	Records and Duration	El Centro 1940 N-S 30 sec	El Centro 1940 E-W 30 sec	El Centro 1934 N-S 25 sec	El Centro 1934 E-W 25 sec	Taft 1952 N-S 30 sec	Taft 1952 E-W 30 sec	Olympia 1949 N-S 30 sec	Olympia 1949 E-W 30 sec
		Average Power, $cm^2 sec^{-4}$							
(1)	Ravara* uncorrected	3820	2690	1900	2305	1360	1775	2930	2190
	Error (%) relative to (2)	19.6	17.6	57.3	65.9	39.0	65.9	38.5	59.3
(2)	CIT corrected (standard value)	3193	2288	1208	1389	978	1070	2116	1375
(3)	Extended 163.82 sec	3621	2637	1309	1502	1124	1219	2305	1525
	Error (%) relative to (2)	13.4	15.3	8.4	8.1	14.9	13.9	8.9	10.9
(4)	Final correction (3) × 0.875	3168	2307	1145	1314	983	1067	2017	1334
	Accuracy of this study (%) relative to (2)	0.8	0.8	5.2	5.4	0.51	0.3	4.7	3.0

* From Ravara (1965).

Example: Conversion Factor $= \dfrac{\text{Extended record length (sec)}}{\text{Actual or selected length (sec)}}$

$= \dfrac{163.82}{30.0}$

= 5.46 for El Centro, 1940

Average power for N-S component at duration 30 sec = Base average power for 163.82 sec duration (Column 10) × conversion factor

= 663.2 (from Table 2) × 5.46

= 3621 $cm^2 sec^{-4}$ (in 3rd column of Row 3)

Final corrected average power due to adding zeros = 3621 × 0.875

= 3168 $cm^2 sec^{-4}$ (in 3rd column of Row 4)

Table 6

Comparison of Variances Estimated in Same Duration by Vanmarcke and Lai and This Study

Record* No.	CIT No.	Earthquake	Instr. Comp.	Richter Magnitude	Max. Acc. g	Base Avg Power at Extended 163.82 sec cm^2/sec^4	Strong-Motion Duration S_o ** sec	Converting Factor $163.82/S_o$	Variance (σ_o^2) and rms Acc: This Study σ_o^2 cm^2/sec^4	This Study σ_o cm/sec^2	Vanmarcke and Lai† σ_o^2 cm^2/sec^4	Vanmarcke and Lai† σ_o cm/sec^2
3-31	A002-1	Northwest Calif.	S 44 W	6.0	0.104	33.818	3.78	43.3386	1,465.6	38.3	1,485.7	38.5
3-32	A002-2	10/7/51	N 46 W		0.112	42.639	4.19	39.0978	1,667.1	40.8	1,681.8	41.0
1-3	A004-1	Kern County	N 21 E	7.7	0.156	205.919	10.28	15.9358	3,281.5	57.3	3,309.3	57.5
1-4	A004-2	7/21/52 (Taft)	S 69 E		0.179	223.411	8.34	19.6427	4,388.4	66.2	4,422.9	66.5
1-9	B037-1	Parkfield 6/27/66	N 65 W	5.6	0.269	115.376	1.89	86.6770	10,000.5	100.0	10,084.1	100.4
1-10	B037-2	(Temblor)	S 25 W		0.347	170.910	1.65	99.2848	16,968.8	130.3	17,054.5	130.6
3-17	C048-1	San Fernando 2/9/71 (8244	NS	6.6	0.255	484.058	8.99	18.2224	8,820.7	93.9	8,876.9	94.2
3-18	C048-2	Onion Blvd)	EW		0.134	255.708	16.99	9.6421	2,465.6	49.6	2,479.6	49.8

* This is the record number in this study; i.e., Tables 1-4.

** The values of strong-motion duration were calculated from $I_o = S_o\sigma_o^2$ by Vanmarcke and Lai (1977), where $\sigma_o^2 = \int_o^\infty G(\omega)\, d\omega$.

† This was calculated from the values of I_o of Vanmarcke and Lai (1977).

Table 7

Statistical Characteristics of Earthquake Ground Motion

Condition	Maximum Ground Acceleration, g			Frequencies of Selected Peaks, PSD	Nor. Max. PSD		Average Acceleration, cm/sec^2		
	Mean	S.D.	Var.	Hz	Mean	Mean + σ	Mean	S.D.	Var.
Rock	0.196	0.234	0.054				30.84	38.35	1444.8
				1.06	0.146	0.369			
				2.75	0.184	0.412			
				3.80	0.160	0.353			
				5.17	0.133	0.321			
Stiff soil	0.050	0.369	0.137				17.5	12.8	162.4
				0.80	0.192	0.547			
				2.45	0.180	0.412			
				5.20	0.127	0.327			
Deep cohesion-less soil	0.063	0.272	0.074				11.2	8.3	68.5
				1.00	0.350	0.827			
				2.80	0.190	0.445			
Soft to medium clay and sand	0.054	0.046	0.002				9.3	8.4	70.5
				1.05	0.405	1.315			
				4.58	0.089	0.266			

Table 8

Correlation of rms Intensity Versus MMI

Upper bound of the site-dependent rms intensity, cm/sec^2 (square root of the sum of 2-horizontal variances)

	Site Conditions	
MMI	Hard Sites	Soft Sites
XII	400-550	250-400
XI	285-395	170-280
X	205-275	120-200
IX	145-190	84-140
VIII	105-140	59-100
VII	75-99	41-70
VI	54-70	29-50
V	37-50	20-35

In accordance with letter from DAEN-RDC, DAEN-ASI dated 22 July 1977, Subject: Facsimile Catalog Cards for Laboratory Technical Publications, a facsimile catalog card in Library of Congress MARC format is reproduced below.

Chang, Frank K.

Site effects on power spectral densities and scaling factors : final report / by Frank K. Chang (Geotechnical Laboratory, U.S. Army Engineer Waterways Experiment Station). -- Vicksburg, Miss. : The Station ; Springfield, Va. : available from NTIS, [1981].

57, [15] p. : ill. ; 27 cm. -- (Miscellaneous paper / U.S. Army Engineer Waterways Experiment Station ; GL-81-2)

Cover title.

"July 1981."

"Prepared for Office, Chief of Engineers, U.S. Army, under Project 4A161102AT22, Work Unit 00296."

Bibliography: p. 55-57.

1. Earthquakes. 2. Power spectra. 3. Spectrum analysis. I. United States. Army. Corps of Engineers. Office of the Chief of Engineers. II. U.S. Army Engineer Waterways Experiment Station. Geotechnical Laboratory. III. Title IV. Series: Miscellaneous paper (U.S. Army Engineer Waterways Experiment Station) ; GL-81-2.

TA7.W34m no.GL-81-2